

**Structural and functional characterisation of
mutant calreticulin in chronic
myeloproliferative neoplasms**

Jeanne Florence Chan Rivera

Submitted in accordance with the requirements for the degree of
Doctor of Philosophy

The University of Leeds

School of Molecular and Cellular Biology
Faculty of Biological Sciences

October 2019

The candidate confirms that the work submitted is his/her own, except where work which has formed part of jointly-authored publications has been included. The contribution of the candidate and the other authors to this work has been explicitly indicated below. The candidate confirms that appropriate credit has been given within the thesis where reference has been made to the work of others.

Co-authored, used in this thesis:

Chapter 4: Elf S, Abdelfattah NS, Baral AJ, Beeson D, Rivera JF, Ko A, Florescu N, Birrane G, Chen E, Mullally A. (2018) **Defining the requirements for the pathogenic interaction between mutant calreticulin and MPL in MPN.** Blood 131:782-6.

I generated the results in Figure 1G-I of this publication.

This copy has been supplied on the understanding that it is copyright material and that no quotation from the thesis may be published without proper acknowledgement.

The right of Jeanne Florence Chan Rivera to be identified as Author of this work has been asserted by her in accordance with the Copyright, Designs and Patents Act 1988.

© 2019 The University of Leeds and Jeanne Florence Chan Rivera

Acknowledgements

First and foremost, I would like to thank my supervisor Dr. Edwin Chen for the opportunity to do my research project in his lab and his unending support and guidance for the last few years. I would also like to thank all of the members of the group, current and former, for their help and favours.

An extended thank you to all of the facility managers for all the help with my project, in particular, Dr. Sally Boxall for her outstanding knowledge of confocal microscopy and flow cytometry, to Dr. Iain Manfield for his thoughts on SPR and to Dr. Brian Jackson for his expertise in protein production and other resources.

A big thank you to University of Leeds who funded my PhD studentship. To all of my colleagues at FBS, who I have had some great times with, and to those who had always lifted my spirits. In particular, April and Fatima, to whom this experience would not be the same without. April, you have been such an amazing friend. Thank you for listening to my rants, feeding me Filipino food, introducing me to hazelnut coffee mate and for making my first two years of this research project enjoyable. To Fatima, thank you for being patient with me especially throughout the protein production ordeal. Thank you for all the professional and personal advice, you made my last year manageable. To the both of you, an unending gratitude for all the coffee breaks that gave me that break I needed.

To my family and friends back in Wales, diolch yn fawr iawn. Sa panginoong maykapal, utang ko po ang buhay ko sa inyo, walang hanggang pasasalamat sa biyayang ipinagkaloob niyo sa akin. To my parents, I would not be here if it was not for your guidance, sacrifices, emotional and financial support and for always believing in me, daghang salamat sa pagpadako sa amoa Papa Rey and Mama Mae. A special mention to my sisters; Elaine, Savannah, Uriel and Sealtiel, who always had my back. To Julie, Garry and Abi, thank you for the support for the last few years and the delicious regular Sunday roast. Last but not the very least, to my little family; to Brad, Thor and Arya, who has been there for me throughout this journey. Babs, thank you for always feeding me and making sure that I don't work too hard, I wouldn't have survived this if it wasn't for you.

Abstract

Calreticulin (CALR) is an endoplasmic reticulum (ER)-resident chaperone that is mutated in ~40% of patients with myeloproliferative neoplasms (MPNs). Mutant CALR exerts its effects by binding to and activating the thrombopoietin receptor MPL to instigate hyperactive JAK-STAT signalling and the MPN phenotype. However, several aspects of the mechanism by which mutant CALR interacts with MPL to promote aberrant MPL activation remains unclear. In this work, I present work that identifies critical domains within mutant CALR and within MPL which are essential for malignant transformation.

In Chapter 3, I describe experiments that implicate two motifs critical for mutant CALR oncogenic activity: (i) the glycan-binding lectin motif, and (ii) the zinc-binding domain. Further analysis demonstrated that the zinc-binding domain was required for facilitating mutant CALR homomultimerisation which was a co-requisite for MPL binding, and that depletion of intracellular zinc levels led to decreased CALR-MPL heteromeric complexes. These data implicate zinc as an essential cofactor for mutant CALR oncogenic activity.

In Chapter 4, I describe experiments that identify essential signalling motifs within MPL that are required to transmit mutant CALR-induced signalling. Specifically, I identified that mutant CALR does not exert its oncogenic effects by binding to the thrombopoietin binding site on the extracellular domain nor the thrombopoietin binding site in the transmembrane domain. Moreover, my data show that a single residue, Tyr626, within the intracellular domain of MPL is critical for mediating mutant CALR signalling.

Finally, in Chapter 5, I optimised conditions for purification of wild-type and mutant CALR and undertook preliminary structural analysis and initial protein modelling of purified proteins using electron microscopy to reveal structural differences between wild-type and mutant CALR. These data indicate that mutant CALR is unstable and prone to aggregation, which make their purification challenging.

Altogether, these findings reveal new biological insights into the molecular mechanism of action of mutant CALR, which could have therapeutic implications for treatment of CALR-mutated MPN.

Table of Contents

Acknowledgements	iii
Abstract	iv
Table of Contents	v
List of Tables	viii
List of Figures	ix
Abbreviations	xii
Buffer Recipes	xiv
Chapter 1:Literature Review	1
1.1 Overview of haematopoiesis	1
1.2 JAK-STAT signalling	4
1.3 Role of JAK-STAT signalling in myelopoiesis	9
1.3.1 Role of JAK2 signalling in erythropoiesis	9
1.3.2 Role of JAK2 signalling in megakaryopoiesis.....	10
1.3.3 Role of JAK2 signalling in granulopoiesis.....	12
1.4 Myeloproliferative neoplasms	13
1.4.1 History of Myeloproliferative neoplasms	13
1.4.2 Role of cytokine signalling in pathophysiology of MPN	17
1.4.3 Mutational landscape of MPN	19
1.4.3.1 JAK2V617F	19
1.4.3.2 JAK2 Exon 12 mutations	22
1.4.3.3 Thrombopoietin receptor (MPL) mutations	23
1.4.3.4 Calreticulin (CALR) mutations	24
1.5 Calreticulin	25
1.5.1 Cellular functions of calreticulin	25
1.5.2 Structural Analysis of CALR protein	29
1.5.2.1 Overview of CALR and CANX Structure	29
1.5.2.2 CALR N-domain	32
1.5.2.3 CALR P-domain	33
1.5.2.4 CALR C-domain	34
1.5.3 Pathophysiology of calreticulin mutations in MPN	35
1.6 Overview of Thesis	39
Chapter 2:Materials and Methods	41
2.1 Cell Lines and Tissue Culture.....	41
2.2 Drug Treatments	42

2.3 Freezing and Thawing cells.....	42
2.4 Lentiviral Infection of Ba/F3 and Ba/F3-MPL cells	43
2.5 Cytokine Withdrawal Assays	44
2.6 Cell Counting	44
2.7 Co-immunoprecipitation assays	46
2.8 Western Immunoblotting	47
2.9 Intracellular phosphoprotein flow cytometry analysis	49
2.10 Annexin and propidium iodide staining	51
2.11 Site Directed Mutagenesis	51
2.12 Confocal Microscopy	52
2.13 Zinc binding assay	54
2.14 Cloning of CALR cDNA into pOPIN vector	54
2.15 Small scale expression screening	55
2.16 Large scale expression	56
2.17 Affinity chromatography	57
2.18 Ion exchange chromatography	58
2.19 Size exclusion chromatography	59
2.20 GST cleavage	59
2.21 Negative EM staining	60
2.22 Negative EM staining image analysis	61
2.23 Biological replicates and statistical analysis	61
Chapter 3: Zinc dependent homomultimerisation of mutant calreticulin is required for MPN pathogenesis	65
3.1 Introduction	65
3.2 Aims and Hypothesis	68
3.3 Results	69
3.3.1 Alanine mutagenesis screen identified residues in the CALR ^{del52} N-domain essential for oncogenic activity.....	69
3.3.2 A triad of histidine residues in the N-domain regulates CALR ^{del52} oncogenic activity	75
3.3.3 Histidine-mutated CALR ^{del52} variants lose the capacity to homomultimerise, an essential property for MPL binding activation	84
3.3.4 Zinc chelation impairs CALR ^{del52} homomultimers and CALR ^{del52} -MPL complexes	88
3.4 Discussion	96

Chapter 4: Mutant calreticulin requires Tyr-626 of the thrombopoietin receptor, MPL, for oncogenic transformation	101
4.1 Introduction	101
4.1.1 Extracellular domain	103
4.1.2 Transmembrane domain	104
4.1.3 Cytoplasmic domain	105
4.2 Aims and Hypothesis	108
4.3 Results	109
4.3.1 Tyrosine residue 626 (Tyr626) of the intracellular domain of MPL is critical for CALR ^{del52} mediated transformation	109
4.3.2 Loss of TPO- and eltrombopag-binding sites does not affect the ability of MPL to support CALR ^{del52} mediated transformation	115
4.4 Discussion	119
Chapter 5: Expression, purification and structural analysis of wildtype CALR and CALR^{del52} purified from <i>E. coli</i>	124
5.1 Introduction	124
5.2 Aims and Hypothesis	126
5.3 Results	127
5.3.1 Cloning	127
5.3.2 Expression and Small Scale Purification	129
5.3.3 Large Scale Purification of recombinant CALR ^{WT} and CALR ^{del52}	131
5.3.4 Cleavage of GST tag from purified CALR ^{WT} and CALR ^{del52}	138
5.3.5 Structural and Functional Analysis	148
5.4 Discussion	153
Chapter 6: General Discussion	156
Bibliography	161

List of Tables

Table 1.1 Variations of mutant specific C-terminal domain of CALR^{del52} performed in the study	38
Table 2.1 Antibody table	49
Table 2.2 Summary of negative stain EM analysis work flow	63

List of Figures

Figure 1.1 Schematic overview of haematopoietic lineage	3
Figure 1.2 Mechanisms of JAK-STAT pathway	7
Figure 1.3 Mutational frequencies of MPN	20
Figure 1.4 Calnexin/calreticulin cycle	27
Figure 1.5 Structural model of calnexin and calreticulin	31
Figure 1.6 Possible mechanism of mutant CALR mediated MPL activation and JAK-STAT signalling	36
Figure 2.1 Gating strategy for FACS acquisition and downstream analysis of cell counts	46
Figure 2.2 Gating strategy for FACS acquisition and downstream analysis of intracellular phosphoflow STAT3 and STAT5 signalling	51
Figure 2.3 Gating strategy for FACS acquisition and downstream analysis of cell cycle	54
Figure 3.1 Domain structure of calreticulin	66
Figure 3.2 Alanine screening mutagenesis identified essential CALR ^{del52} residues involved in the ability to confer cytokine independent growth	71
Figure 3.3 Growth curves of cells expressing CALR ^{del52} lectin variants	72
Figure 3.4 Non-transforming CALR ^{del52} lectin variants lead to impaired STAT3 and STAT5 phosphorylation	73
Figure 3.5 Non-transforming CALR ^{del52} lectin variants do not bind to MPL	74
Figure 3.6 Loss of two or more histidine residues within the zinc binding domain of CALR ^{del52} leads to impaired ability to confer cytokine independent growth	77
Figure 3.7 Loss of two or more histidine residues within the zinc binding domain of CALR ^{del52} leads to impaired ability to confer cytokine independent growth	78
Figure 3.8 Loss of two or more histidine residues lead to diminished STAT3 and STAT5 phosphorylation	79
Figure 3.9 Loss of His42 does not affect CALR ^{del52} activity	80
Figure 3.10 Loss of two or more histidine residues in CALR ^{del52} lead to impaired capacity to bind to MPL	82
Figures 3.11 Assessment of colocalisation of histidine-deficient CALR ^{del52} variants and MPL by FRET	83
Figure 3.12 CALR ^{del52} is capable of homomultimerisation	85

Figure 3.13 Lectin-deficient CALR ^{del52} retained their ability to homomultimerise	86
Figure 3.14 Loss of two or more histidine residues lead to impaired homomultimerisation	87
Figure 3.15 Loss of two or more histidine residues leads to an impairment of zinc binding	89
Figure 3.16 Zinc chloride enhances CALR ^{del52} homomultimerisation and MPL binding	90
Figure 3.17 TPEN chelation diminishes CALR ^{del52} homomultimerisation and MPL binding	91
Figure 3.18 TPEN chelation in Ba/F3-MPL cells stably expressing CALR ^{del52} decreases MPL binding in a dose dependent manner	93
Figure 3.19 Effect of TPEN chelation on JAK-STAT signalling is specific to CALR ^{del52}	94
Figure 3.20 Zinc chelation abrogates CALR ^{del52} -induced JAK-STAT signalling	95
Figure 3.21 Schematic representation of the predicted mechanisms of CALR ^{del52} and variants in MPL binding	99
Figure 4.1 Mechanisms of MPL activation	102
Figure 4.2 Predicted MPL structure using Phyre2 analysis	107
Figure 4.3 Tyr591/626/631 of MPL are required to support CALR ^{del52} - induced cytokine independence	110
Figure 4.4 MPL tyrosine variants can bind to CALR ^{del52}	112
Figure 4.5 Loss of Tyr626 abolishes MPL ability to support cytokine independent growth of CALR ^{del52}	113
Figure 4.6 Loss of Tyr626 leads to attenuation of pSTAT5 levels...	114
Figure 4.7 MPL variants associated with loss of TPO- and eltrombopag- binding sites does not affect MPL binding capacity to CALR ^{del52}	116
Figure 4.8 MPL variants associated with loss of TPO- and eltrombopag- binding sites does not affect capacity to support CALR ^{del52} cellular transformation	117
Figure 4.9 MPL variants associated with loss of TPO- and eltrombopag- binding sites does not affect capacity to activate JAK-STAT signalling.....	118
Figure 4.10 Schematic representation of mutant CALR binding to MPL on the cell surface	122
Figure 5.1 Successful cloning of CALR ^{wt} and CALR ^{del52} genes into pOPINJ vector	128
Figure 5.2 Small scale expression and purification of CALR ^{WT} and CALR ^{del52} in various <i>E. coli</i>	130

Figure 5.3 Large scale purification of CALR^{WT}	132
Figure 5.4 Further purification of recombinant CALR^{WT} by size exclusion chromatography (SEC)	133
Figure 5.5 Large scale purification of CALR^{del52}	135
Figure 5.6 Confirmation of presence of CALR^{del52} in large scale purification.....	136
Figure 5.7 Mass spectrometry analysis confirms the identity of as CALR	137
Figure 5.8 The GST tag disrupts binding capacity of CALR^{del52} to MPL	139
Figure 5.9 Tag cleavage of CALR^{WT}	142
Figure 5.10 Successful cleavage of CALR^{del52} following manual overnight cleavage	143
Figure 5.11 Size exclusion chromatography was unable to separate GST-tagged and untagged CALR^{del52}	144
Figure 5.12 Western immunoblotting analysis of preparations of cleaved and uncleaved CALR^{WT} and CALR^{del52} samples	146
Figure 5.13 Cleaved CALR^{del52} proteins retain MPL binding capacity	147
Figure 5.14 Negative staining EM staining images of CALR recombinant proteins	150
Figure 5.17 Structural analysis of CALR^{WT}.....	151
Figure 5.18 Structural analysis of CALR^{del52}	152

Abbreviations

AKT	protein kinase B
CALR	calreticulin
CAMT	congenital amegakaryocytic thrombocytopaenia
CANX	calnexin
CFU-Mk	colony-forming unit megakaryocytes
CLP	common lymphoid progenitor cells
CMP	common myeloid progenitor cells
ECD	extracellular domain
ECM	extracellular matrix
EEC	endogenous erythroid colony
EPO	erythropoietin
EPOR	erythropoietin receptor
ER	endoplasmic reticulum
ERK	extracellular signal-regulated kinase
ET	essential thrombocythaemia
FAK	focal adhesion kinase
FRET	fluorescence resonance energy transfer
G-CSFR	granulocyte colony-stimulating factor receptor
GM-CSF	granulocyte-macrophage colony-stimulating factor
GMP	granulocyte-macrophage progenitor cells
HSC	haematopoietic stem cells
IFN	interferons
IGF1	insulin-like factor 1
IL	interleukin
JAK	Janus kinase
JAK2V617F	Janus kinase 2 Valine-617-Phenylalanine
KDEL	Lys-Asp-Glu-Leu ER retrieval signal
LT-HSC	long-term haematopoietic stem cells

MAPK	mitogen-activated protein kinase
MEP	megakaryocyte-erythrocyte progenitor cells
MFI	mean fluorescence intensity
MHC	major histocompatibility complex
MK	megakaryocytes
MPL	thrombopoietin receptor
MPN	myeloproliferative neoplasms
MPP	multipotent progenitor cells
NMR	nuclear magnetic resonance
PI3K	phosphoinositide-3-kinase
PMF	primary myelofibrosis
PV	polycythaemia vera
SCF	stem cell factor
STAT	signal transducers and activators of transcription
ST-HSC	short-term haematopoietic stem cells
TM	transmembrane domain
TPEN	N, N,N',N'-Tetrakis(2-pyridylmethyl)ethylenediamine
TPO	thrombopoietin
ECD	extracellular domain
NMR	nuclear magnetic resonance
EEC	endogenous erythroid colony
MHC	major histocompatibility complex
ECM	extracellular matrix
ER	endoplasmic reticulum

Buffer Recipes

FACS Buffer

- PBS
- 2% Foetal bovine serum

Luria Bertani (LB) Broth –

- 1% w/v Tryptone
- 1% w/v NaCl
- 0.5% w/v Yeast extract
- Make up in dH₂O
- Autoclave to sterilise

NuPAGE MOPS SDS running buffer 20x

- 1M MOPS
- 1M Tris
- 2% SDS
- 20mM EDTA

Protein loading buffer (also referred to as 2X Laemmli Buffer)

- 125 mM Tris pH 6.8
- 4% w/v SDS
- 40% v/v glycerol
- 0.2% w/v bromophenol blue
- 10 mM β -mercaptoethanol

TBS (Tris buffered saline) 1x

- 50mM Tris
- 150mM NaCl
- Adjust pH to 7.5 with HCl

Chapter 1

Literature Review

Chapter 1

Literature Review

1.1 Overview of haematopoiesis

Haematopoiesis refers to the continual process of blood cell formation and replenishment throughout the life of an organism. This hierarchical process begins with multipotential haematopoietic stem cells (HSCs) (Lorenz et al., 1951; Ng and Alexander, 2017). HSCs have the ability to self-renewal to give rise to more HSCs, or undergo differentiation in which these cells lose self-renewal potential and ultimately generate a spectrum of terminally differentiated, specialised blood cells of a specific haematopoietic lineage (**Figure 1.1**) (Orkin and Zon, 2008).

HSCs give rise to two main haematopoietic lineages, namely, the myeloid and the lymphoid lineages (Traver and Akashi, 2004; Jagannathan-Bogdan and Zon, 2013; Ivanovs et al., 2017) (**Figure 1.1**). The terminal myeloid lineage includes erythrocytes, megakaryocytes, neutrophils, macrophages, eosinophils and mast cells. The lymphoid lineage includes the T-lymphocytes, natural killer (NK) cells and B lymphocytes. Mature, terminally differentiated haematopoietic cell types are highly divergent and participate in distinct processes and perform different physiological functions.

Under homeostatic conditions, HSCs maintain a quiescent state in the G0 phase of the cell cycle (Rossi et al., 2007). Stress stimuli such as bleeding or infection

triggers the activation of transcriptional systems that stimulate HSCs to differentiate to cope with the elevated demand for blood cells; when the demand of these blood cells subsides, these HSCs return to their quiescent form (Wilson et al., 2008; Nakamura-Ishizu et al., 2014). Dysregulation of steady-state haematopoiesis is associated with accumulation of intermediate or terminally differentiated cells in the blood, bone marrow or peripheral lymphoid system and the development of haematopoietic malignancies (Warr et al., 2011).

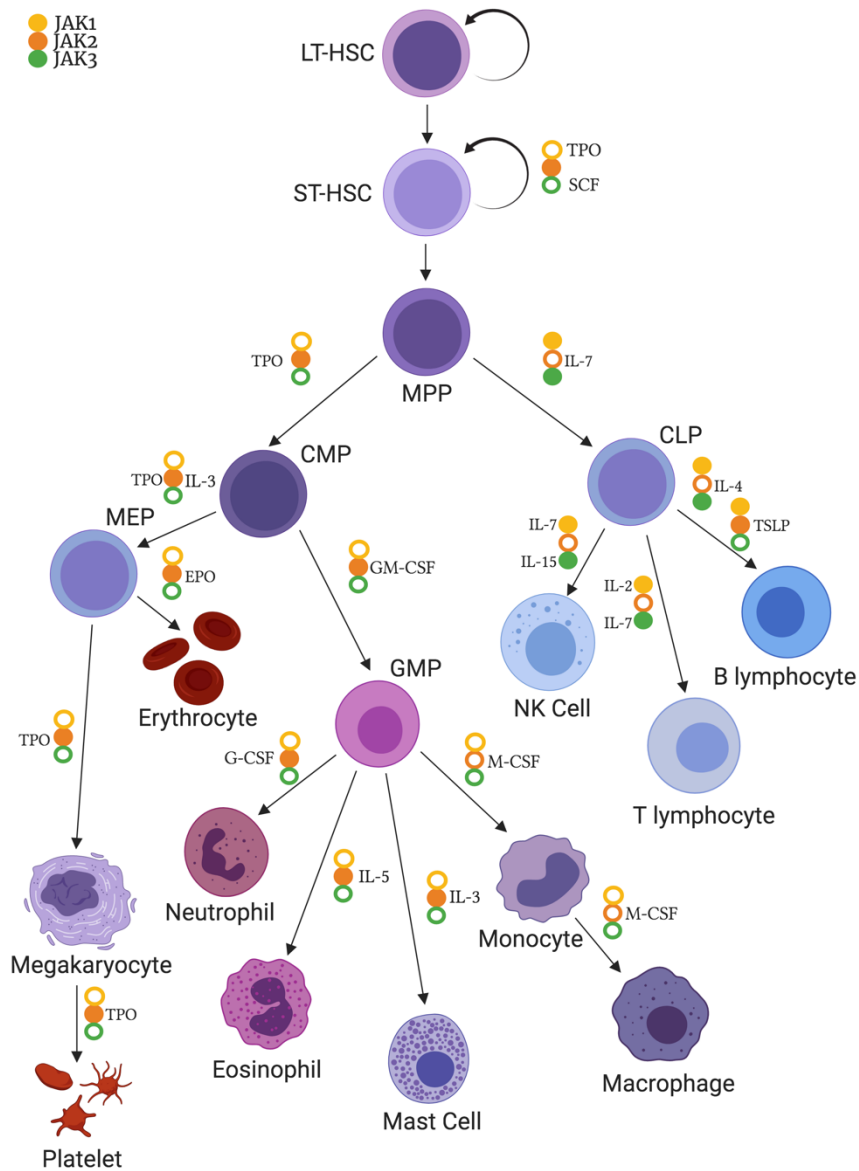


Figure 1.1 Schematic overview of haematopoietic lineage. Classical model of haematopoietic hierarchy with a major bifurcation between the myeloid and lymphoid branches as an important step in the lineage commitment. Cytokines and their associated receptors are responsible in the recruit specific JAK kinases necessary for cell maturation. LT-HSC: long term-haematopoietic stem cell; ST-HSC: short term- haematopoietic stem cell; MPP: multipotent progenitor cells; CMP: common myeloid progenitor; CLP: common lymphoid progenitor; MEP: megakaryocyte-erythrocyte progenitor; GMP: granulocyte-macrophage progenitor. Closed circles represent JAK associated activation, JAK1 (yellow), JAK2 (orange) and JAK3 (green).

1.2 JAK-STAT signalling

Cytokines play a crucial role during haematopoiesis and are responsible for initiating various responses that drive proliferation, survival, differentiation and maturation of HSCs (Metcalf, 2008; Brown and Ceredig, 2019). Since the discovery of specific cytokines, it is now known that some cytokines have specific lineage specification activity whereas others have broader functions in combination with multiple cytokines to stimulate proliferative responses.

To exert their function, cytokines bind to their cognate transmembrane cytokine receptors on the extracellular domain to transmit signals intracellularly. Generally, there are two types of receptor families that are structurally related which are heavily involved in haematopoiesis, host defence and immunoregulation. Type I receptors are known to bind to cytokines such erythropoietin (Epo) and thrombopoietin (Tpo), most interleukins (IL) and colony-stimulating factors; type II receptors bind to interferons (IFN) and IL-10 family cytokines (Gadina et al., 2001; Prigge et al., 2015; Brown and Ceredig, 2019). Most type I and type II cytokine receptors lack functional tyrosine kinase activity and therefore requires cytoplasmic tyrosine kinases, such as Janus Kinases (JAKs), to drive signalling. Activation of type I and type II receptors is triggered following cytokine binding to the ligand-binding domains on the extracellular domain of the receptor, which results in either receptor homodimerisation, oligomerisation or induction of conformational change in preformed receptor dimers/multimers depending on the type of receptor that is being activated (Robb, 2007). Receptor activation leads to activation of receptor-associated JAKs, as described in detail below (Staerk and Constantinescu, 2012).

There are four mammalian JAKs that are essential for transmitting receptor signals, namely, JAK1, JAK2, JAK3 and TYK2 (Yamaoka et al., 2004; Staerk and Constantinescu, 2012). There is significant pleiotropy with respect to the utilisation of various JAKs by various cytokine receptors, with both types of cytokine receptors having been demonstrated to activate various JAKs, either individually or in combination, to affect a wide range of physiological processes. The JAK family of proteins are characterised by the presence of four common domains: (i) a JH1 kinase domain, (ii) a JH2 pseudokinase domain, (iii) JH3-7 domains in the N-terminal of the protein of undetermined function, and (iv) the four-point-one, ezrin, radixin, moesin (FERM) domain within the N-terminus (Ihle, 1995). JAK proteins are usually constitutively bound to the intracellular domain of cytokine receptor signalling chains *via* the FERM domain, and upon ligand-mediated receptor multimerisation, are brought in close proximity to one another, leading to transphosphorylation of adjacent JAK molecules which leads to JAK activation (Rawlings et al., 2004).

Intramolecularly, the individual JAK domains mediate the process of JAK activation in three events. Firstly, JAKs are phosphorylated within the activation loop in the JH1 domain (Ihle and Gilliland, 2007). Secondly, this causes the phosphorylated activation loop to exhibit diminished capacity to interact with the JH2 pseudokinase domain. The JH2 pseudokinase domain is primarily involved in inhibition of kinase activity, and thus, phosphorylation within the JH1 activation loop relieves JH2-induced repression and promotes JAK activation. Thirdly, a further level of regulation involves phosphorylation within in the FERM domain

of JAK2 proteins that can also modulate JAK2 kinase activity (Funakoshi-Tago et al., 2006).

Activated JAK kinases at the receptor are then responsible for phosphorylating key tyrosine residues within the cytokine receptor intracellular domain. These phosphorylated tyrosines then act as docking sites for STAT transcription factors. In humans, seven STAT members exist (STAT1, STAT2, STAT3, STAT4, STAT5A, STAT5B and STAT6). Receptor-recruited STATs are in turn phosphorylated on a single tyrosine residue by receptor-associated JAKs within their C-terminal transactivation domain (TAD) (Benekli et al., 2003). STAT phosphorylation then triggers homo- and heterodimerisation of STAT proteins which facilitates their translocation from the cytoplasm into the nucleus to act as transcription factors and activate or represses transcription of target genes (**Figure 1.2**). Unique combinations of cytokine receptors, JAKs and STATs are critical in specifying distinct haematopoietic lineages. In general, STAT3 and STAT5a/b governs signal transduction in growth factor-regulated control of myelopoiesis, whereas STAT1, STAT4 and STAT6 are essential for immune cells. Of note, STAT serine phosphorylation also occurs and modulates STAT activity, however, the role of this mechanism in instructing haematopoiesis remains unclear (Decker and Kovarik, 2000; Kiu and Nicholson, 2012). Regardless of the combination, activated STAT dimers are translocated into the cell nucleus where they serve as transcription factors to activate transcription of target genes (Mao et al., 2005).

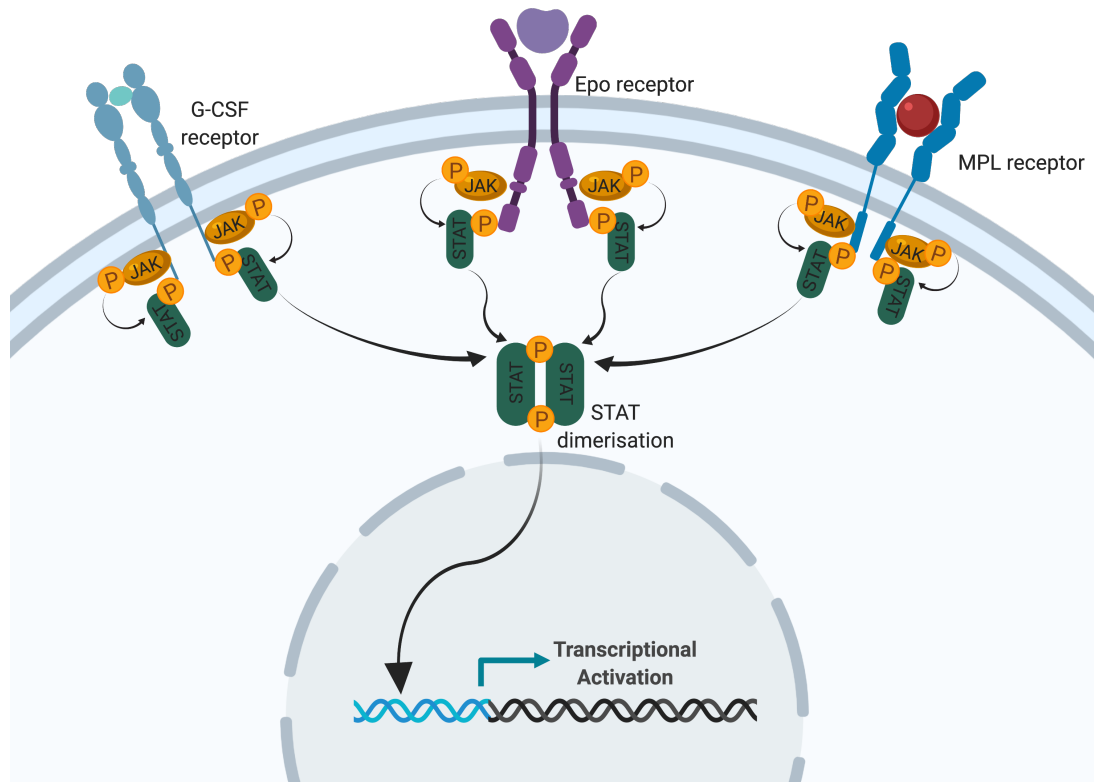


Figure 1.2 Mechanisms of JAK-STAT pathway. Signalling receptors directly associated with JAK-STAT signalling cascade include EpoR, G-CSFR and MPL. Upon ligand binding, these receptors recruit JAK kinase and becomes phosphorylated resulting in STAT activation and dimerisation that lead to the translocation of STAT dimers into the nucleus and drive transcription of genes associated with survival, proliferation and differentiation.

The JAK/STAT signalling pathway is highly regulated through the balance of cytokines that activate the signalling cascade and various mechanisms that antagonise these signals. Cytokine signalling is attenuated by negative regulation that dephosphorylate JAKs and inhibit STAT activation. In addition to the intrinsic inhibitory activity of JH2 domain of JAK in attenuating signalling, several additional mechanisms have evolved to regulate the duration and intensity of JAK-STAT signalling. These are mainly mediated by three classes: (i) protein phosphatases; (ii) the protein inhibitors of activated STAT (PIAS) family; and (iii) the suppressor of cytokine signalling (SOCS) family (Starr et al., 1997; Naka et al., 1997; Seif et al., 2017). Protein phosphatases modulate signalling by dephosphorylating tyrosine residues to down-regulate JAK kinase activity. Several phosphatases that have been previously identified include SH2 domain-containing tyrosine phosphatases (SHPs), T-cell protein tyrosine phosphatase (TC-PTP), protein tyrosine phosphatase 1B (PTP1B) and transmembrane protein CD45 (Murphy et al., 2010). PIAS proteins attenuate signalling through sumoylation, where a SUMO is attached to a lysine residue analogous to ubiquitination, and targets client proteins for degradation (Ungureanu et al., 2003). Finally, SOCS proteins can attenuate signalling directly by binding to activated JAKs and binding to phosphorylated receptors to outcompete STAT binding to the receptor (Starr and Hilton, 1999). Collectively, this illustrates that regulation of JAK-STAT signalling can be mediated through inhibition of the receptors, JAKs and STATs. The exact nature of the crosstalk between these regulatory processes remains a topic of active investigation, and it is likely that additional negative regulators also remain to be identified.

1.3 Role of JAK-STAT signalling in myelopoiesis

As previously stated, cytokines are soluble peptide factors that instruct HSCs and immature progenitors to undergo cellular proliferation and differentiation. This is achieved by receptor-mediated activation of various JAKs and STATs to activate various transcriptional networks to enforce myeloid lineage fate decision. In this section, I will discuss the role of the JAK2-STAT5 signalling axis and its essential role downstream of various cytokine receptors in directing differentiation down various myeloid lineages. The significance of JAK2 in driving commitment of progenitor cells from the myeloid lineage is outlined in **Figure 1.1** through its direct participation in the signal transduction of various cytokine-mediated cell differentiation (Radosevic et al., 2004).

1.3.1 Role of JAK2 signalling in erythropoiesis

Erythropoiesis is a complex, highly-regulated process that produces mature enucleated erythrocytes (red blood cells) from a multipotent progenitor cell (MPP) in the bone marrow (Orkin, 2000; Zivot et al., 2018). This process is primarily driven by the cytokine erythropoietin (Epo), a glycoprotein that acts as a ligand specifically for Epo receptor (EpoR) that is found on erythroid progenitors (Spivak, 2005). Epo is produced primarily in the kidney and is released in the blood upon physiological response to hypoxia and anaemia (Chateauvieux et al., 2011). Direct physical interaction between Epo with pre-formed EpoR homodimers triggers conformational changes of the extracellular and intracellular domains of EpoR and consequently autophosphorylation and activation of JAK2 (**Figure 1.2**) (Witthuhn et al., 1993; Hubbard, 2018). JAK2 activation leads to phosphorylation of eight specific tyrosine residues localised

on the cytoplasmic region of EpoR that serve as docking sites to recruit various SH2-domain containing proteins to initiate four main signalling pathways that are associated with EpoR activation: (i) JAK2/STAT5, (ii) mitogen-activated protein kinase (MAPK)/ extracellular signal-regulated kinase (ERK), (iii) protein kinase C (PKC) and (iv) phosphoinositide 3-kinase (PI3K)/AKT (Hedley et al., 2011; Lacombe and Mayeux, 1999; Frank, 2002; Bao et al., 1999; Kuhrt and Wojchowski, 2015). Collectively, these signalling pathways regulate erythroid cell survival, promote cellular proliferation and erythroid differentiation, and suppress pro-apoptotic signals.

1.3.2. Role of JAK2 signalling in megakaryopoiesis

Thrombopoietin (Tpo) is the principle regulator of proliferation and maturation of megakaryocytes (MK), the process known as thrombopoiesis (Eaton and de Sauvage, 1997; Kaushansky, 1997; Bianchi et al., 2016). Mice lacking either *Tpo* or *Mpl* (the receptor for Tpo) exhibit severe thrombocytopaenia with a deficiency in megakaryocytes and their progenitor cells (Ng et al., 2014), suggesting that Tpo is indispensable for maintaining the megakaryocyte population *in vivo*. Tpo is only critically required in early progenitor cells (Ng et al., 2014). Once the haematopoietic progenitor is committed to the MK lineage, Tpo also mediates the expression of particular cell surface proteins that are involved in platelet function and aggregation, namely, glycoprotein (gp) IIb/IIIa and gpIb (Doubekovski et al., 1997; French and Seligsohn, 2000).

In addition to directing MK maturation, there is also significant evidence

suggesting that Tpo function is not restricted to megakaryopoiesis but rather also has pleiotropic functions (Nakamura-Ishizu and Suda, 2019). For example, studies have also shown that Tpo accelerates red blood cell recovery in myelosuppressed mice and that Tpo supports proliferation of haematopoietic regulators either alone or in combination with other early acting cytokines (Kaushansky et al., 1996; Solar et al., 1998; de Graaf and Metcalf, 2011). Furthermore, Tpo has also been demonstrated to synergise with Epo to stimulate proliferation of erythroid cells *in vitro* (Kaushansky et al., 1995; Kobayashi et al., 1995). Finally, Tpo has also been shown to maintain HSC quiescence (Yoshihara et al., 2007).

The biochemical mechanism of Tpo activity is by binding directly to its cell surface receptor Mpl. Tpo-Mpl binding induces receptor dimerisation and subsequent JAK2 activation (**Figure 1.2**) (Hitchcock and Kaushansky, 2014), that leads to phosphorylation of tyrosine residues Tyr626 and Tyr 631 within the cytoplasmic domain of the receptor itself. This phosphorylation allows recruitment of STAT1, 3 and 5 proteins that lead to the intracellular signal transduction cascade that gives rise to mature megakaryocytes and subsequent platelet production (Fishley and Alexander, 2004). STAT activation leads to expression of genes heavily involved in mediating cell proliferation and cell survival, such as Cyclin D1, p21 and Bcl-X_L (Geddis et al., 2002). Additionally, these tyrosine residues can also stimulate PI3K/AKT and MAPKs signalling cascades (Geddis et al., 2002; Tefferi, 2008). Furthermore, an adapter protein that is known to inhibit JAK2, Lnk, also showed increase activity upon Tpo stimulation, and can act as a negative regulator constraining Tpo-Mpl signalling

in HSCs (Bersenev et al., 2008; Gery and Koeffler, 2013).

1.3.3 Role of JAK2 signalling in granulopoiesis

Granulopoiesis is the process of granulocyte formation that gives rise to neutrophils and macrophages (Bainton, 2004). It is estimated that over 60% of leucocytes in the bone marrow are granulocytes or granulocyte precursors (Kennedy and Deleo, 2009). Neutrophils and macrophages play a critical role in the immune response against bacterial viral and fungal infections. Following HSC differentiation into granulocyte/macrophage-restricted lineages, progenitors engage numerous transcription factors and growth factors that stimulate maturation (Lawrence et al., 2018). The cytokines that govern granulopoiesis are mainly colony-stimulating factors such as stem cell factor (SCF), interleukin-3 (IL3), granulocyte colony-stimulating factor (G-CSF) and granulocyte-macrophage colony-stimulating factor (GM-CSF) (Kawahara, 2011). Both GM-CSF and G-CSF play overlapping roles in granulopoiesis and are dependent on signalling pathways via its specific receptors, GM-CSFR and G-CSFR, respectively. However, knockdown of G-CSF but not GM-CSF results in perturbation of haematopoiesis, thereby indicating that G-CSF play a more prominent role in driving granulopoiesis (Lieschke et al., 1994). It has also been shown that during neutrophil maturation, G-CSF induces changes in the shape and appearance of granulocytic cells and undergo nuclear condensation (Mehta et al., 2015).

Studies in the molecular mechanisms of GM-CSF and G-CSF activity revealed

that (similar to Epo and Tpo) these cytokines also activate JAK/STAT, PI3K/AKT, Ras/ERK and MAPK pathways downstream of their cognate receptors (Shi et al., 2006; Marino and Roguin, 2008). Binding of these cytokines initiates receptor conformational changes that lead to autophosphorylation of JAK2 and activation of STAT5, PI3K and MAPK (**Figure 1.2**) (Dijkers et al., 1999; Jenkins et al., 1998). These signalling pathways drive cell proliferation, cell growth, differentiation and resistance to apoptosis (Shimoda et al., 1994; Schuettpelz et al., 2014).

Collectively, these studies highlight the critical role of JAK2 signalling downstream of various receptors that are essential for maintaining survival and growth during HSC differentiation and for directing myeloid differentiation. Unsurprisingly, dysregulation of these pathways is frequently associated with malignancies of the myeloid lineages, as discussed in the next section.

1.4 Myeloproliferative neoplasms

1.4.1 History of Myeloproliferative neoplasms

The 'humoral theory' was based on the early work of Hippocrates and Galen who believed that illness was due to the imbalance of one of the four 'humors', where blood dominated the others (Cruse, 1999; Falagas et al., 2006; Christie, 1987). Humoral theory suggests that clotted blood is comprised of 4 components that form distinct layers in a test tube: the serum that disassociate from the blood (yellow bile), the white blood cells (phlegm), the oxygenated red blood cells (blood) and the deoxygenated red blood cells (black bile) (Fahreus, 1921). The

scientific application of microscopes in the late seventeenth century led to the first visualisation of red and white blood cells in 1668 and 1749, respectively (Hooke and Allestry, 1665; van Leeuwenhoek, 1674; Cobb, 2000; Lieutaud, 1749). Platelets were recognised in the early nineteenth century and were further demonstrated to play a role in haemostasis (Brewer, 2006). The use of chemical dyes as selective biological stains allowed thorough morphological evaluation of blood cell components. This technique enabled scientists to determine key features that distinguished lymphocytes from granulocytes (Ehrlich, 1877; Drews, 2004). This supported the concept that an 'ancestral cell' gave rise to cellular components of the bone marrow and gave rise to circulating red blood cells (Neumann, 1869; Cooper, 2011).

From the mid nineteenth and early twentieth century, various cases reported individuals suffering from hyperactivity of haematopoietic organs such as the spleen and increased viscosity of the blood (Bennett, 1845; Virchow, 1845; Craigie, 1845; Vaquez, 1895; Osler, 1903; Heuek and Assistenzarzt, 1879; Epstein and Goedel, 1934; Cerquozzi and Tefferi, 2015). The first case of chronic myelogenous leukaemia (CML) was reported in 1845 in a patient presenting with splenomegaly and hypertrophy of the liver that resulted in death due to suppuration of the blood (Virchow, 1845; Bennett, 1845). This was followed by the discovery of a new clinical entity, primary myelofibrosis (PMF) that included extramedullary haematopoiesis, osteosclerosis and bone marrow fibrosis (Heuek and Assistenzarzt, 1879). The first description of polycythaemia vera (PV) reported evidence of excessive and persistent erythrocytosis (Vaquez, 1895). This was confirmed to be a new clinical entity and distinctions later

observed between relative and secondary polycythaemia (Osler, 1903; Osler, 1908). Essential thrombocythaemia (ET) was among the later diseases classed as a clinical entity and was associated with haemorrhagic thrombocythaemia and elevated platelet along with evidence of sclerotic spleen (Epstein and Goedel, 1934). These diseases presented with highly diverse symptoms and their aetiology remained obscure, however, these were assumed to be potentially related diseases from the same origin due to the similarities in clinical manifestation (Hirsch, 1935; Vaughan and Harrison, 1939).

In 1951, William Dameshek grouped the four clinicopathologic entities, CML, ET, PV and PMF under the rubric 'myeloproliferative disorders' (MPD) (Dameshek, 1951; Tefferi and Pardanani, 2015). Dameshek primarily highlighted that bone marrow cells such as erythroblasts, megakaryocytes and granulocytes proliferate *en masse*, indicating that these cells are mass produced during physiological conditions. Dameshek therefore speculated that the overlapping clinical and morphological features of these disorders were attributed to the myeloproliferation in the bone marrow. Dameshek further suggested that an as-yet undiscovered 'myelostimulatory' factor was responsible for driving the development of these diseases (Tefferi, 2008).

Following the work of Dameshek, work exploiting polymorphisms in the X-linked glucose-6-phosphate dehydrogenase (G-6-PD) locus successfully determined these disorders all have clonal origin (Fialkow et al., 1967; Adamson et al., 1976; Jacobson et al., 1978; Fialkow et al., 1981; Shlush, 2018). The principle uses polymorphic G-6-PD isozymes as a marker system for identifying clonality is

dependent on the randomness of X-chromosome inactivation (Chen and Prchal, 2007), and was adapted for analysis of clonal origins of neoplasms. Using this assay, normal tissues would be expected to exhibit equivalent expression of both G-6-PD isozymes due to random X-inactivation, whereas neoplasms derived from a single 'ancestral' cell would exhibit skewed expression of one G-6-PD isozyme due to domination of an ancestral clone. Neoplasms with a multicellular origin should also express both isozymes equivalently, as seen in unaffected tissues (Fialkow et al., 1967; Shlush, 2018). Using this assay, analysis of erythrocytes, granulocytes and platelets derived from female PV patients showed skewed levels of one G-6-PD isozyme expression indicative of clonal haematopoiesis, whereas skin fibroblasts demonstrated no evidence of skewing (Adamson et al., 1976; Shlush, 2018). Further analysis of CML, ET and PMF patients similarly demonstrated that these disorders are all established from a single stem cell clone. At the same time, the identification of BCR-ABL as the disease-initiating mutation in CML led to the new classification that separated CML from ET, PV and PMF, and the latter three disorders were renamed as chronic myeloproliferative neoplasms (MPN) (Nowell, 2002; Tefferi, 2008).

The current view therefore of the classical myeloproliferative neoplasms (MPN) (also termed as BCR-ABL-negative MPNs) are as a group of clonal, haematopoietic stem cell disorders that are characterised by overproduction of fully functional terminally differentiated blood cells of the myeloid lineage (Nangalia et al., 2016; Levine, 2012). The three classical MPNs are ET, PV and MF, and are defined primarily on the haematopoietic lineage(s) affected. ET is characterised by an elevated platelet count accompanied by megakaryocytic

hyperplasia, PV is characterised by an increase of erythrocytes and predominant erythroid lineage involvement with variable hyperplasia of the granulocytic/megakaryocytic lineages, and PMF presents a heterogeneous disorder defined by megakaryocytic hyperplasia and bone marrow fibrosis. In all cases, the disease arises as a result of the acquisition of MPN-initiating somatic mutations in an HSC that provides the MPN HSCs with a clonal advantage over normal HSCs to drive myeloid differentiation and expansion and leads to increased production of an affected myeloid lineage. In addition, all three disorders collectively have a tendency to transform into secondary acute myeloid leukaemia (AML) through an accumulation of additional lesions at various cooperating loci encoding genes such as epigenetic regulators, splicing factors and TP53. Post-MPN AML presents with poor prognosis and survival (Yogarajah and Tefferi, 2017).

1.4.2 Role of cytokine signalling in the pathophysiology of MPN

All MPN entities are derived from a single somatically mutated HSC that clonally expands within the bone marrow and contributes to over-proliferation of various myeloid lineages. This pathophysiology has been attributed to hypersensitivity of haematopoietic progenitors from MPN patients to various cytokines. It was shown that *in vitro* culture of bone marrow cells from PV patients (but not non-diseased individuals) could give rise to erythroid colonies in the absence of cytokines such as Epo (Prchal and Axelrad, 1974; Dupont et al., 2007). This phenomenon of endogenous erythroid colony (EEC) formation is characteristic of PV, and was subsequently observed in a subset of patients with ET and PMF also (Adamson, 1968; Zanjani et al., 1977; Gewirtz et al., 1983; Juvonen et al.,

1993; Griesshammer et al., 1998; Kawasaki et al., 2001; Hofmann, 2015). These reports were followed by evidence of hypersensitivity of MPN cells to other cytokines such as interleukin-3 (IL-3), granulocyte-macrophage colony-stimulating factor (GM-CSF), insulin-like factor 1 (IGF1) and stem cell factor (SCF) (Dai et al., 1992; Correa et al., 1994; Montagna et al., 1994; de Wolf et al., 1989; Dai et al., 1997; Hammarén et al., 2019). Collectively, these reports suggest a potentially critical role for deregulation of cytokine signalling in mediating the MPN phenotype.

In line with a key role for cytokine signalling in MPNs, it was also shown that aberrant STAT activation was a common feature of primary cells of MPN patients. STAT3/5 hyperactivation (as gauged by DNA binding ability in gel shift assays) was a primary molecular aberration in granulocytes from PV patients (Röder et al., 2001). STAT5 activation was also seen to correlate with the anti-apoptotic protein BCL-xL following Epo stimulation, indicating a potential role of STAT5 signalling in inhibiting apoptosis (Silva et al., 1999; Ishida et al., 2018). Furthermore, constitutive activation of PI3K and AKT was also reported in erythroid progenitors of PV patients following incubation with SCF or EPO (Nishigaki et al., 2000; Dai et al., 2005). Taken together, these reports indicate a significant role of STATs and PI3K/AKT in the pathobiology of MPN cells and are consistent with a role of aberrant cytokine signalling in driving the myeloid expansion observed in MPN.

1.4.3 Mutational Landscape of MPN

Given the prominent role of cytokine receptors in MPN pathobiology, it was initially theorised that gain-of-function mutations in these receptors could be responsible for MPNs. Early studies however revealed no mutations in the coding and non-coding regions of the *EPOR* gene or the *MPL* gene in a limited number of ET, PV and MF patients (Hess et al., 1994; Le Couedic et al., 1996; Mittelman et al., 1996; Wang and Hashmi, 2003; Randi et al., 2005). These findings prompted a search for causative MPN lesions in other parts of the JAK-STAT signalling cascade.

1.4.3.1 JAK2V617F

In 2005, the breakthrough came when four independent groups identified a somatic gain-of-function mutation in the *JAK2* gene that is present in a majority of MPN subtypes (James et al., 2005; Levine et al., 2005; Baxter et al., 2005; Kralovics et al., 2005). The lesion was a G>T transversion in nucleotide 1849 in exon 14 of the *JAK2* gene. This resulted in a substitution from valine to phenylalanine in codon 617 (*JAK2V617F*). Over 95% of PV patients and ~50-60% of ET and MF patients were found to harbour the *JAK2V617F* mutation (James et al., 2005; Levine et al., 2005; Baxter et al., 2005; Kralovics et al., 2005), making it the most common genetic lesion in MPN patients regardless of subtype (**Figure 1.3**).

The effect of the V617F mutation on *JAK2* activity is constitutive hyperactivation of *JAK2* kinase activity. This is achieved by disrupting the normal activity of the valine-617 amino acid residue which is located within the JH2 pseudokinase

domain and is required to inhibit the activity of the adjacent JH1 kinase domain (Saharinen and Silvennoinen, 2002) to ensure that JAK2 is kept at an inactive state in the absence of phosphorylation. The valine-617 substitution to phenylalanine caused by the V617F mutation thus leads to loss of inhibitory activity by the JH2 pseudokinase domain, decreased suppression of JH1 kinase activity, and constitutive increase in JAK2 kinase activity (Bandaranayake et al., 2012).

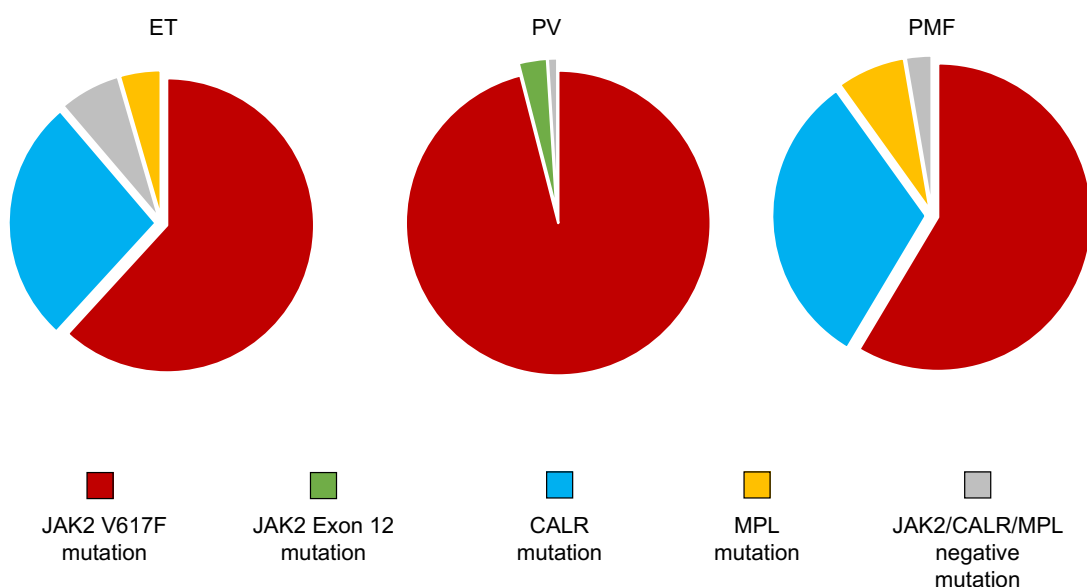


Figure 1.3 Mutational Frequencies of MPN. Distribution of somatic mutations in MPN patients according to phenotype. Colours indicate percentage of somatic mutations within each subtype.

This discovery stimulated follow-up research efforts to elucidate the role of JAK2V617F in disease initiation and myeloproliferation (Silvennoinen and Hubbard, 2015). Bone marrow transplantation studies confirmed that over-expression of JAK2V617F is sufficient to induce a PV-like phenotype in mice (Wernig et al., 2006), but its activity was shown to heavily rely on the presence

of specific cytokine receptors, such as erythropoietin (EpoR), thrombopoietin (MPL) or granulocyte colony-stimulating factor (GCSFR) (Lu et al., 2005). Various knock-in mouse models expressing physiological levels of Jak2V617F exhibited a range of MPN-like phenotypes, including ET (Li et al., 2010), PV (Mullally et al., 2010) and MF (Akada et al., 2010; Marty et al., 2010). The discrepancies in the phenotypes are likely to reflect differences in the species of the JAK2 cDNA employed in the construction of the mice, with murine Jak2 cDNA giving rise to more severe phenotypes. Nevertheless, these studies confirmed that JAK2V617F alone was able to directly engender an MPN phenotype *in vivo*.

Further analysis subsequently revealed the crucial mediators downstream of JAK2V617F that are essential for MPN pathogenesis. A crucial role of STAT5 in the pathogenesis of PV was confirmed in mouse studies whereby Jak2V617F was incapable of giving rise to an MPN phenotype in a Stat5-null context (Yan et al., 2012; Walz et al., 2012). In contrast, although ERK, AKT and STAT3 are often constitutively activated in JAK2V617F cells, these signalling pathways were shown to be dispensable for mediating haematopoietic transformation (Zou et al., 2011; Yan et al., 2012). Follow up studies demonstrate that deletion of STAT3 increases thrombopoiesis and reduced overall survival suggesting that STAT3 could in fact negatively regulate MPN induced by JAK2V617F (Yan et al., 2015; Yan and Mohi, 2013; Grisouard et al., 2015). Finally, STAT1 play differential roles in the pathogenesis of various MPN subtypes, with STAT1 activation associated with enhanced megakaryocytic differentiation in ET (Chen et al., 2010). Collectively, these data suggest that cytokine activation and

downstream activation of STAT1 and 5 are necessary for JAK2V617F-mediated transformation.

1.4.3.2 JAK2 Exon 12 mutations

For the small fraction of PV patients that were JAK2V617F-negative, it was hypothesised that acquired mutations in either another JAK family members or elsewhere in JAK2 could account for these patients. Sequencing of all 25 JAK2 exons in granulocyte DNA obtained from a JAK2V617F-negative PV patient revealed an additional area of sequence change in exon 12: a three-nucleotide substitution from CAA to ATT in positions 1614 through 1616 resulting in a H538QK539L mutation (Scott et al., 2007). This alteration was only present at low levels in granulocytes and was absent in T-cells, implying that this alteration was acquired. Furthermore, this variant was also seen in clonally derived EECs at a similar level as heterozygous mutation. An independent sequencing of JAK2 exons in a second JAK2V617F-negative patient yielded a 6 bp in frame deletion at positions 1611 to 1616 (also in exon 12), resulting in F537-K539delinsL mutation. Despite the heterogeneity with respect to sequence changes in these cases, both variants targeted H538 and K539 residues. Analysis of eight additional JAK2V617F-negative PV patients subsequently revealed four additional exon 12 allele variants that all presented with changes affecting conserved residues between K537 and E543 whilst three of the alleles identified contained a K539L substitution. Sequence analysis of granulocyte DNA from patients with JAK2V617F-positive PV, JAK2V617F-negative ET and JAK2V617F-negative cases of idiopathic myelofibrosis showed no evidence of JAK2 exon 12 mutations (Scott et al., 2007; Pardanani et al., 2007; Colaizzo et

al., 2007; Williams et al., 2007). Following this discovery, further cases have identified JAK2 exon 12 mutations in numerous reports (Martínez-Avilés et al., 2007; Butcher et al., 2008; Ohyashiki et al., 2009). The mechanism of action for these mutations is thought to be similar to that of JAK2V617F, specifically *via* de-repression of the pseudokinase inhibitory activity.

Functional studies confirmed that JAK2 exon 12 variants are MPN driver mutations. Bone marrow transplantation of mouse bone marrow cells transduced with JAK2-K529L resulted in mice which exhibited high levels of haemoglobin, reticulocytosis and leukocytosis (Scott et al., 2007), and transgenic mice with JAK2-N542-E543del (the most frequent exon 12 variant) also presented with elevated haemoglobin and reduced overall survival but normal platelet and neutrophil counts (Grisouard et al., 2016). Molecular characterisation of these mice demonstrated increased signalling of STAT3 and ERK1/2 pathway and deregulation in iron metabolism that favoured increased erythropoiesis. Interestingly, these mice showed no significant up-regulation in STAT5 signalling, unlike JAK2V617F mice. Furthermore, although a modest increase of pSTAT1 was reported, it was shown that STAT1 does not play a crucial role in mediating the signalling consequences of JAK2 exon 12 mutations on erythropoiesis or megakaryopoiesis (Grisouard et al., 2016; Godfrey et al., 2016).

1.4.3.3 Thrombopoietin receptor (MPL) mutations

As described above, thrombopoietin receptor (MPL) and its ligand, thrombopoietin (TPO) play an essential role during megakaryopoiesis. In 2006,

mutations in exon 10 of gene encoding *MPL* was identified in JAK2-unmutated ET and MF cases at a frequency of 3-5% and 8-11%, respectively (Pikman et al., 2006; Pardanani et al., 2006). This mutation is located in the juxtamembrane region of MPL with the most common mutation being a substitution in codon 515 leading to tryptophan-to-leucine (W515L) and tryptophan-to-lysine (W515K) (Beer et al., 2008). Other MPL mutations such as W515S, W515A and S505N have also been discovered in some cases of hereditary thrombocytosis (Chaligné et al., 2008; Teofili et al., 2007). Overall, these mutations lead to inappropriate receptor homodimerisation that results in aberrant activation of JAK-STAT, MAPK, ERK and Akt signalling pathways (Pikman et al., 2006). The molecular mechanism of MPL activation in normal and diseased states is discussed more extensively in Chapter 4.

Functional studies confirmed that *MPL* variants are true MPN driver mutations. MPLW515L-mutant mice exhibit disease phenotype similar to ET and MF (Li et al., 2011; Pecquet et al., 2010), but does not cause PV-like phenotypes seen in JAK2V617F murine models. These differences however accord with the fact that MPL mutations are only present in ET and MF patients and may suggest that the MPLW515L exerts its primary effects on megakaryocytic lineages *in vivo*.

1.4.3.4 Calreticulin (CALR) mutations

In 2013, two groups reported that mutations in the gene encoding ER-resident chaperone calreticulin (CALR) can be detected in ~25-30% of ET and MF patients, and represent the most common genetic lesion in JAK2-unmutated MPN patients (Klampfl et al., 2013; Nangalia et al., 2013). CALR mutations

reside in the exon 9 of *CALR* gene, and are a heterogeneous set of insertion-deletion (indel) mutations that give rise to a +1 bp frameshift that results in the replacement of the C-terminal tail of the wild-type *CALR* protein with a mutant-specific C-terminus encoded in an alternative reading frame. Of the mutations identified, the 52-bp deletion (type I) mutation (L367fs*46) and a 5-bp insertion (type II) mutation (K385fs*47) are the most common (Nangalia et al., 2013). Across all *CALR*-mutated MPN patients, over 65% of patients harbour a type I mutation, 32% of patients exhibited a type II mutation and 3% of patients exhibited other variants. The frequency of type I mutation was also significantly higher in PMF patients (75%) than in ET patients (48%).

The mechanism by which *CALR* mutations confer MPN has not been fully elucidated. In contrast to other MPN driver mutations, the link between *CALR* and aberrant cytokine signalling, the emblematic feature of MPN biology, is not immediately obvious, and the mechanism by which *CALR* mutations activates *MPL* remains a topic of active investigation. In the next section, I will provide a summary of the relevant literature on the normal biology of *CALR*, followed by a summary on the mechanism of action of mutant *CALR* in MPN pathogenesis.

1.5 Calreticulin

1.5.1 Cellular functions of calreticulin

Since its first isolation in 1974, *CALR* has been extensively studied by various groups that were interested in identifying its significance and function (Ostwald

and MacLennan, 1974; Michalak et al., 1996; Van Duyn Graham et al., 2010; Zimmerman et al., 2013). The primary function of CALR is to act as a molecular chaperone in the endoplasmic reticulum (ER) and to interact with various newly synthesised glycoproteins to facilitate proper protein folding and quality control and engage in the “calreticulin-calnexin cycle” (**Figure 1.4**) (Peterson et al., 1995; Parodi, 2000). In this process, nascent polypeptide chains enter the lumen, and glucosidase I exposes the outermost glucoses to show the $\text{Glc}_1\text{Man}_9\text{GlcNAc}_2$ epitope (Helenius and Aebi, 2004). This epitope is subsequently recognised by CALR or its closely related homologue calnexin (CANX), which binds to these monoglucosylated glycans. This binding is then followed by the removal of the innermost glucose by glucosidase II which frees the glycoprotein from the lectin anchor of CALR or CANX. Deglucosylated glycoprotein substrates can then be bound by UDP-Glc:glycoprotein glucosyltransferase (UGGT), an enzyme that functions as a conformational sensor. If UGGT senses that the substrate protein exhibits a non-native three-dimensional structure, it will reglucosylate the protein, thus making it a substrate for CALR or CANX, and susceptible to glucosidase II activity again. Thus, the glycoprotein binding and liberation by CALR or CANX continually occurs in a cycle, catalysed by competing activities of glucosidases II and UGGT until the glycoproteins attain their desired native structures whereupon the glycoprotein exits the cycle and are allowed to continue their transit through the secretory pathway (Ware et al., 1995; David et al., 1993). These reactions are frequently dependent on the recruitment other molecular chaperones and folding enzymes such as ERp57 to promote efficient folding by enhancing the formation of disulphide bonds (Zapun et al., 1998). Known client proteins of CALR include insulin receptor (Bass et al., 1998), and major histocompatibility complex (MHC)

class I and class II molecules (Blees et al., 2017; Raghavan et al., 2013; Wijeyesakere et al., 2015; Degen et al., 1992).

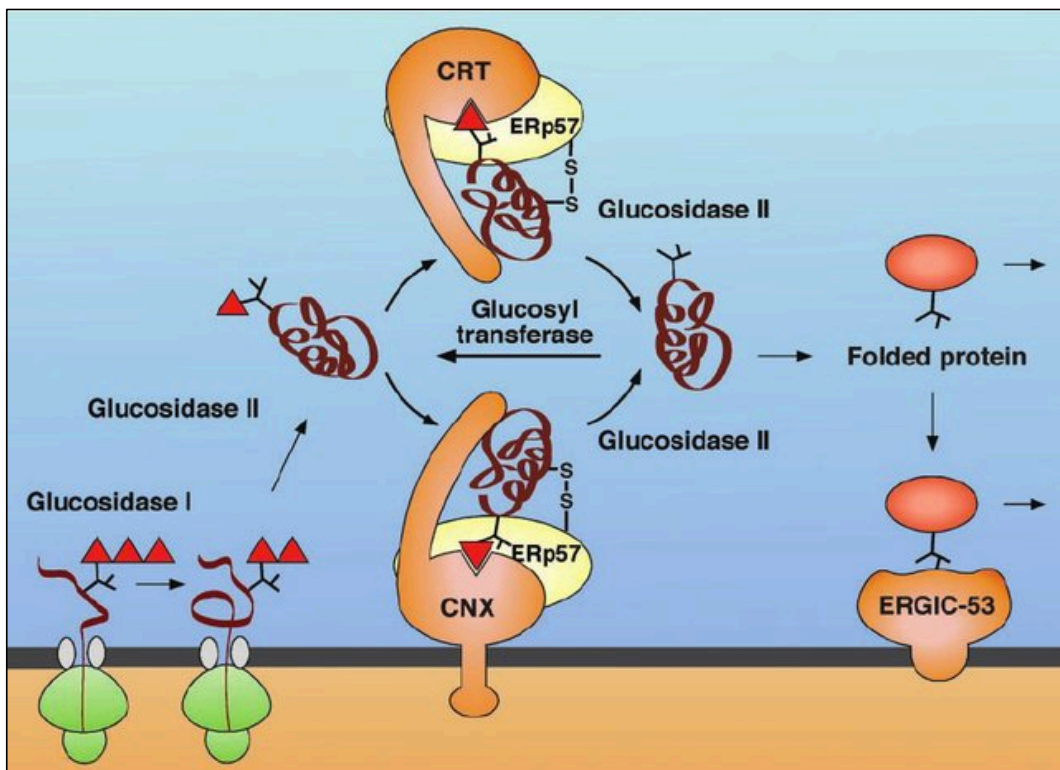


Figure 1.4 Calnexin/calreticulin cycle. When the first two glucose in the N-linked core glycans have been processed by glucosidase I and II, the nascent glycoproteins are recognised by ER lectins, calnexin (CNX) and calreticulin (CRT). These glycoproteins are also recognised by ERp57 that catalyse disulphide formation in glycoproteins. When the third glucose residue is trimmed by glucosidase II, the complex dissociates. If the glycoproteins are not folded correctly, the oligosaccharides are reglycosylated by ER glucosyltransferase and reassociates with CNX or CRT. Once the glycoproteins are correctly folded, it is no longer glucosylated and will be processed for ER removal by ERGIC-53. This figure is adapted from Helenius and Aebi, 2001.

Another major role of CALR in the cell is to regulate calcium (Ca^{2+}) stores within the ER lumen (Pozzan et al., 1994). As Ca^{2+} ions cannot remain free in the ER lumen, various proteins are required for efficient mechanisms of storage. CALR, along with other ER-resident Ca^{2+} binding proteins such as CANX, BiP, GRP94, calumenin, reticulocalbins and calsequestrin, is able to act as a calcium sink by binding free Ca^{2+} (Coe and Michalak, 2009; Pozzan et al., 1994).

Finally, in addition to its chaperone functions and calcium buffering activity within the ER, CALR has also been associated with numerous cellular processes occurring outside the ER (Burns et al., 1994; Dedhar et al., 1994; Coppolino et al., 1997; Bibi et al., 2011). CALR was shown to function as a modulator that bind to the DNA binding domain of glucocorticoid receptor and prevent subsequent binding to its glucocorticoid response element (Burns et al., 1994), as well as able to bind to androgen receptor and retinoic acid receptor to regulate its transcription factor activity (Dedhar et al., 1994; Coppolino et al., 1997; Holaska et al., 2002). CALR has also been demonstrated to play a critical role in facilitating the assembly of major histocompatibility complex (MHC) class I molecules (Gao et al., 2002; Wearsch and Cresswell, 2008), and has also been localised in other parts of the cell such as the outer cell surface, in the cytosol and in the extracellular matrix (ECM) and plays a role in cell adhesion, phagocytosis, migration, proliferation and wound healing (Gold et al., 2010; Johnson et al., 2001). Finally, CALR plays a role as a marker of phagocytosis as a facultative recognition ligand in apoptotic cells (Martins et al., 2010; Kuraishi et al., 2007; Ogden et al., 2001).

1.5.2 Structural Analysis of CALR Protein

1.5.2.1 Overview of CALR and CANX Structure

Biochemically, CALR protein is a 46 kDa protein that contains three highly conserved functional domains: (i) a globular N-domain that encompasses the key CALR enzymatic activities including chaperone activity, lectin binding and polypeptide binding (residues 18-197); (ii) a proline-rich P-domain (residues 198-307) and (iii) a C-domain (residues 308-417) (**Figure 1.5A**). CALR also contains a 17 amino acid signal peptide domain at the N-terminus which is required for translocation into the ER during polypeptide synthesis.

Early efforts to interrogate the structure of CALR heavily relied on the existing knowledge of its membrane-bound homologue CANX. CALR and CANX share similar domain structures, with the exception that CALR lacks a transmembrane domain and thus exists soluble within the ER lumen (**Figure 1.5A**). Pioneering crystallographic analysis of a fragment from CANX representing its luminal domains (lacking the transmembrane domain and C terminus) was able to derive an atomic model for CANX with a 2.9Å resolution (**Figure 1.5B**) (Schrag et al., 2001). It was revealed the luminal portion of CANX was a highly asymmetric molecule with two distinct domains: a compact globular lectin domain that is essential for binding to glycans, and a flexible 145-residue long extended arm that stretched 140Å away from the globular domain which can hook around client proteins. The original crystal structure indicated that the extended P-domain hooked around another CANX protein and inserted into the adjacent protein's lectin domain in an intermolecular interaction, but it is likely that these interactions reflect crystal packing forces and that the P domain is more likely to

interact with protein moieties within substrate proteins rather than with the glycan of an adjacent CANX molecule (Schrag et al., 2001).

Structural data for CALR have been restricted to an NMR structure of the P-domain derived from rat CALR, an X-ray crystallography structure of the CALR N-domain, and a cryo-EM reconstruction of CALR in complex with 6 other proteins as part of the human MHC-I peptide-loading complex (**Figure 1.5C**) (Blees et al., 2017; Ellgaard et al., 2001; Chouquet et al., 2011; Kozlov et al., 2010). Overall, these studies reveal that the shape of CALR adopts a conformation that includes a prominent globular domain with an extended hook, similar to that seen with CANX. In this section, I will discuss the insights gleaned from these studies on the structure of the wild-type CALR protein, with an emphasis on specific motifs within individual domains.

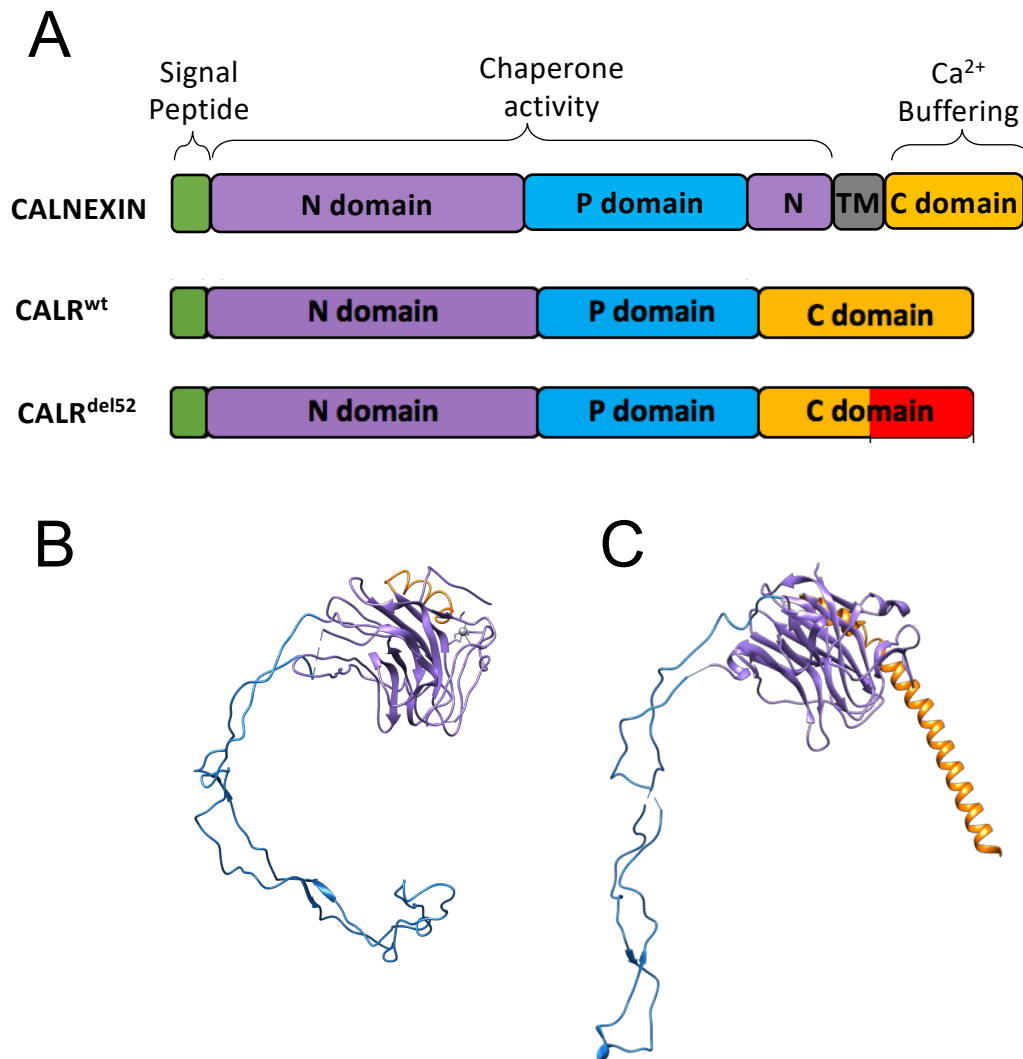


Figure 1.5 Structural model of calnexin and calreticulin. (A) Linear domain structures of calnexin and calreticulin feature similar structures consisting of a signal peptide (green), N-terminal globular lectin domain (purple), flexible P-domain (blue) and C-terminal domain (orange). (B-C) 3D crystal model structure of calnexin (B) and calreticulin (C). The globular domain (purple) consists of a lectin motif that functions as an oligosaccharide binding site, a zinc binding domain and a DNA binding site. The P-domain has a high-affinity calcium binding site. The C-domain is a highly acidic region, has a high capacity calcium binding site and an ER retrieval signal, KDEL. The transmembrane domain of calnexin is shown in this model.

1.5.2.2 CALR N-domain

Of the three CALR functional domains, the most is known about the N-domain. An X-ray structure of the human CALR N-domain has recently been resolved, and reveals that the N-domain adopts a highly structured globular domain characterised by a jelly-roll fold derived from one convex and one concave anti-parallel beta sheets (Chouquet et al., 2011). In addition, the atomic modelling highlighted several critical features that are relevant for CALR activity. These include:

- (i) Binding to monoglucosylated client glycoproteins during the engagement of the calreticulin-calnexin cycle is dependent on a highly conserved lectin motif. The lectin motif was found to reside on the surface of the globular domain (Leach et al., 2002). Based on the structure, essential residues in the lectin motif were C105 and C137 that were involved in the formation of a disulphide bridge; G107, Y109, Y128, M131, P134, D135 which were localised in the middle of this cluster; and K111, H145 and I147 on the edge (Chouquet et al., 2011). Follow-up mutational analysis of the carbohydrate-binding region of CALR confirmed several specific residues such as Y109, K111, Y128 and D135 as being essential for lectin activity as their loss led to complete abrogation of oligosaccharide binding when mutated (Kapoor et al., 2004; Thomson and Williams, 2005) whereas other residues such as M131, D317 and D160, were also involved in the lectin site of CALR but demonstrated weaker affinity towards trisaccharide and their loss had a partial effect on CALR oligosaccharide binding ability (Thomson and Williams, 2005). Further studies demonstrated that the lectin site was

essential in mediating interactions between CALR and many of its substrates, including MHC class I and glucocorticoid receptor (Del Cid et al., 2010; Wearsch et al., 2011).

- (ii) A high affinity zinc (Zn^{2+}) binding site in its N-domain defined by four histidine residues (H42, H99, H145 and H170) (Baksh et al., 1995; Chouquet et al., 2011). Independent studies also revealed that the capacity to coordinate Zn^{2+} regulates the ability of CALR to suppress aggregation of non-glycoproteins and protection against thermal inactivation (Saito et al., 1999; Guo et al., 2003).
- (iii) A patch of conserved residues comprised of D166, H170, D187 and W347 with strong sequence conservation which suggests there is a possible association with important function. The activity of these residues in CALR activity remains unclear.

1.5.2.3 CALR P-domain

The P-domain consists of a proline-rich sequence that forms a flexible arm and contains a high-affinity binding site for Ca^{2+} and this arm is also known to associate to co-chaperones such as ERp57 (Michalak et al., 2009). Pioneering structural data of CALR have been provided through NMR structural analysis of its P-domain (Ellgaard et al., 2001). This central proline-core of the P-domain is characterised by a series of triplicate copies of repeated amino acid sequences that are arranged in a characteristic “111222” pattern (Ellgaard et al., 2001), suggesting that the structure exists as a hairpin fold involving the entire polypeptide chain stabilised by three anti-parallel beta sheets similarly seen in that of CANX. These repeats are thought to have weak lectin-like function, but

are likely to be more heavily involved in mediating protein-protein interaction to co-chaperones such as ERp57. The P-domain also share sequence similarities to other known Ca^{2+} binding chaperones such a CALNUC and CANX (Bergeron et al., 1994; Lin et al., 1999) and has been previously demonstrated to be structurally similar to that of CANX, but is shorter since it consists of 3 proline-containing modules (Pocanschi et al., 2011).

1.5.2.4 CALR C-domain

Finally, the C-domain contains a series of acidic amino acids (predominantly glutamic acid and aspartic acid) that enable low affinity, high capacity binding to Ca^{2+} . The C-terminal tail also possesses the Lys-Asp-Glu-Leu (KDEL) sequence motif that allows targeting and retention of CALR in the lumen of ER. An *in silico* analysis of the wild-type C-domain reported that it possesses an isoelectric point (pI) of 3.98 and has a high probability of being structurally disordered (Shivarov et al., 2014). Given this intrinsic disorder, very little is known about the structure of the C-domain at atomic resolution.

1.5.3 Pathophysiology of calreticulin mutations in MPN

As described above, CALR mutations in MPN are indel mutations that introduce a +1 frameshift in the CALR reading frame that leads to the creation of a mutant-specific C-terminal tail (**Figure 1.5A**). In total, a minimal common mutant-specific tail of 36 amino acid is created in which the acidic amino acids in the wild-type C-terminus are replaced with basic amino acids in the mutant-specific C-terminus.

The first understanding of how mutant CALR (CALR^{del52}) engenders MPN was demonstrated using cytokine-dependent cell lines such as the Ba/F3 lymphoblastoid cell line. Ba/F3 cells are normally dependent on exogenous cytokines (such as IL-3) for survival in culture, but can be prompted to survive and proliferate in cytokine-depleted conditions when over-expressing various MPN driver mutations. Using this system, it was shown by multiple groups that CALR^{del52} alone was insufficient to confer cytokine-independent growth of Ba/F3 cells, but rather, CALR^{del52} required the co-expression of the cytokine receptor MPL, suggesting synergy between these two genes in mediating cytokine-independent growth (Chachoua et al., 2016; Araki et al., 2016; Elf et al., 2016). Moreover, MPL activation was associated with induction of constitutive STAT5 activation (Chachoua et al., 2016). In contrast, other type I haematopoietic cytokine receptors such as EpoR and G-CSFR failed to support CALR^{del52}-mediated oncogenic activity (Araki et al., 2016; Elf et al., 2016). These findings therefore demonstrated that CALR^{del52} drives transformation *via* MPL and by activating the MPL-JAK2-STAT5 signalling axis (**Figure 1.6**) (Marty et al., 2016).

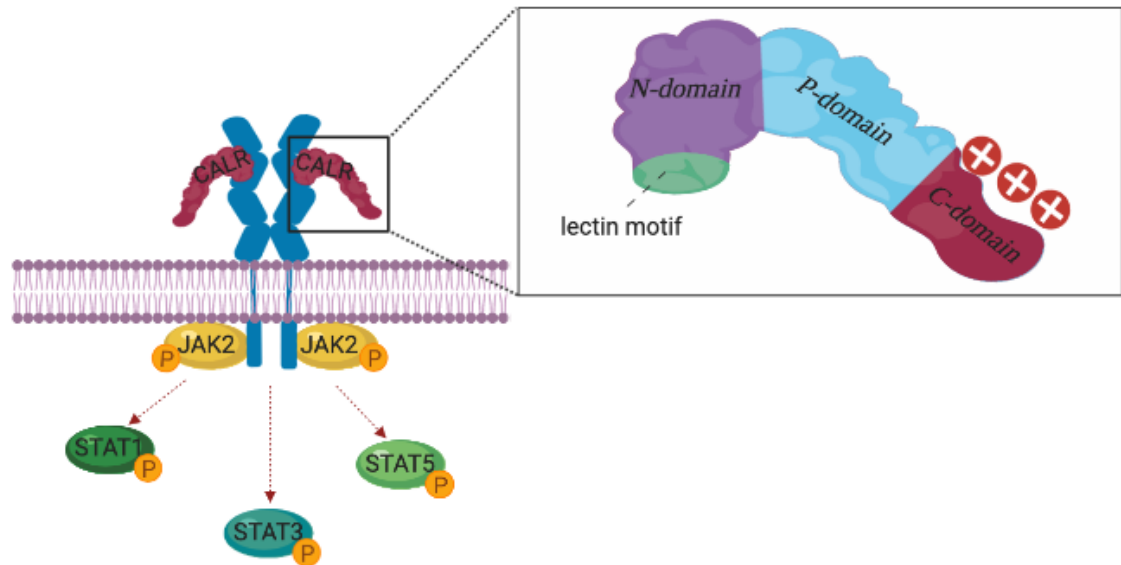


Figure 1.6 Possible mechanism of mutant CALR-mediated MPL activation and JAK-STAT signalling. Mutant CALR (red) requires the presence of both MPL and JAK2 to activate JAK-STAT signalling and oncogenic transformation. Multiple groups have also demonstrated that mutant CALR physically associates with the extracellular domain of MPL, an event that correlates with its transforming activity. Mutagenesis of C-terminus indicate that it is essential but is not sufficient by itself for oncogenic activity. Studies have showed that the lectin motif within the globular domain of CALR (inset) is critical for MPL binding and subsequent oncogenic transformation.

Next, attempts were made to understand the role of the novel mutant-specific C-terminus of CALR^{del52} in its transforming capacity (Elf et al., 2016; Araki et al., 2016). Mutagenesis assays were performed that generated a panel of mutagenised versions of CALR^{del52} where individual domains were deleted (**Table 1.1**) (Elf et al., 2016). This assay revealed four key findings. Firstly, complete truncation of the mutant-specific C-terminus resulted in an inability to confer cytokine-independence, suggesting that the mutant C-terminus was in fact essential for CALR^{del52} transforming activity. Secondly, expression of the mutant-specific C-terminus alone was incapable of driving cytokine independence indicating that the C-terminus was necessary but not sufficient for transformation and that the N and/or P-domains of CALR were still necessary. Thirdly, removing successive 8-10 amino acid blocks of the mutant C-terminus failed to abrogate cytokine independent growth in any mutant analysed, which suggested that the transforming ability of CALR^{del52} is not sequence specific. And fourthly, mutagenising all 18 basic K/R residues within the C-terminal tail to glycine abrogated CALR^{del52} oncogenic activity, whereas mutagenising all non-basic K/R residues did not affect oncogenic activity, suggesting that the oncogenic activity of CALR^{del52} was due to the C-terminus's positive electrostatic charge (**Table 1.1**). These data allow the conclusion that the dependence of CALR^{del52} on the C-terminus for oncogenic activity is not sequence-specific, but rather based on a threshold of positively-charged residues. Moreover, this threshold of positively-charged residues likely cooperates with the N-domain in an unknown manner to engender cytokine-independence (Elf et al., 2016).

	CALR variant	C-terminus sequence	Activity
	CALR ^{WT}	...QDEEQRLKEEEEDKKRKEEEEAEDKEDDEDKDEDEEDEDKEEEDVPGQAKDEL	-
	CALR ^{MUT}	...QDEEQRTRRMMRTKMRMRMRRTRRKMRRKMSPARPRTSCEACLQGWTEA	+
charge	CALR ^{MUT} -positive	...QDEEQRGRGGGRGKGRGRRGRRGRRKGGGGRGGGGEACLQGWTEA	+
	CALR ^{MUT} -neutral	...QDEEQGTGGMMGTGMGMGGGGTGGGGMSPAGPGTSCGEACLQGWTEA	-
truncation	CALR ^{MUT} Δ10	...QDEEQRTRRMMRTKMRMRMRRTRRKMRRKMSPARPRTSR	+
	CALR ^{MUT} Δ18	...QDEEQRTRRMMRTKMRMRMRRTRRKMRRKMSP	+
	CALR ^{MUT} Δ28	...QDEEQRTRRMMRTKMRMRMRRT	+
	CALR ^{MUT} Δ36	...QDEEQRTRRMMRTKM	-
	CALR ^{MUT} Δ47	...QDEE	-
blocks	CALR ^{MUT} 37_47del	...QDEE RMRMRRTRRKMRRKMSPARPRTSCEACLQGWTEA	+
	CALR ^{MUT} 29_36del	...QDEEQRTRRMMRTKM RRKMRRKMSPARPRTSCEACLQGWTEA	+
	CALR ^{MUT} 19_28del	...QDEEQRTRRMMRTKMRMRMRRT SPARPRTSCEACLQGWTEA	+
	CALR ^{MUT} 10_18del	...QDEEQRTRRMMRTKMRMRMRRTRRKMRRKM EACLQGWTEA	+

Table 1.1 Variations of mutant specific C-terminal domain of CALR^{del52} performed in study. Amino acid sequence highlighted in red are sequences specific to CALR^{del52}. + refers to ability to confer cytokine-independent growth; – refers to inability to confer cytokine-independent growth.

Finally, attempts were made to understand the dependency of CALR^{del52} on MPL for oncogenic activity. Pulldown experiments demonstrated that CALR^{del52} and MPL directly interact in co-immunoprecipitation assays (Elf et al., 2016; Araki et al., 2016; Chachoua et al., 2016) and that this interaction required an intact lectin motif within the N-domain in addition to the positively-charged amino acids within the C-domain (Elf et al., 2018). Moreover, there was significant correlation between oncogenic transformation and MPL binding across the large panel of engineered versions of CALR^{del52} encompassing alterations introduced in the N- and C-domains, which suggests that CALR^{del52} binding to MPL is a necessary prerequisite event in order to activate it (**Figure 1.6**).

1.6 Overview of Thesis

As mentioned, various studies have reported the significance of the mutant C-terminal tail in the oncogenic activity of CALR^{del52} to bind and induce activation of MPL. However, there are still numerous gaps in our understanding of the molecular pathology of CALR^{del52}, in particular, if other regions of CALR contribute to its oncogenic activity and if specific regions of MPL are essential in supporting its oncogenic activity.

On the basis of these gaps in our understanding, the following thesis seeks to address three main hypotheses:

- (i) Specific regions of CALR^{del52} (other than the mutant-specific C-terminus) contribute to its oncogenic activity;
- (ii) Specific regions of MPL are essential for transducing CALR^{del52} oncogenic signalling;
- (iii) Structural and functional analysis of CALR^{WT} and CALR^{del52} proteins can provide important insights in the molecular pathology of CALR^{del52}

Chapter 3 will discuss the results from an alanine mutagenesis screen where I identified two functional motifs essential for CALR^{del52} activity: the lectin and zinc-binding motifs. This chapter describes in detail the downstream functional assays that confirmed the initial findings from the alanine screen and identify the specific role of these residues in the oncogenic activity of CALR^{del52}, and

describe evidence that zinc homeostasis plays a role in CALR^{del52} oncogenic activity.

Chapter 4 investigates the role of canonical signalling of MPL in its ability to support CALR^{del52}-mediated cellular transformation. Moreover, important residues on MPL primarily involved in TPO and eltrombopag binding were also examined and their significance in CALR^{del52} oncogenic activity was assessed.

Chapter 5 describes in detail efforts to express and purify CALR^{WT} and CALR^{del52} in *E. coli*. Furthermore, this chapter will also discuss preliminary structural studies of CALR^{del52} following successful purification.

Finally, Chapter 6 will summarise the work done for this thesis and discuss future work that should be undertaken to better understand the molecular pathology of CALR^{del52} in MPN.

Chapter 2

Materials and Methods

Chapter 2

Materials and Methods

2.1 Cell Lines and Tissue Culture

HEK293T human embryonic kidney tissue epithelial cells were obtained from the American Type Culture Collection (ATCC) (DuBridge et al., 1987; Pear et al., 1993). HEK293T cells were maintained in Dulbecco's Modified Eagle's Medium (DMEM) (Lonza) supplemented with 10% Foetal Bovine Serum (FBS) (heat inactivated), 1% L-glutamine and 1% penicillin/streptomycin. 293T cells were subcultured every 2-3 days. Briefly, cells were rinsed in 1x PBS, 1 mL of trypsin-EDTA solution (Sigma Aldrich) was added and incubated for approximately 5 minutes to allow cell detachment and seeded in fresh complete growth medium at a sub cultivation ratio of 1:10. Cells were grown at 37°C in 5% CO₂.

Ba/F3 cells are IL-3 dependent murine pro B cells and were a generous gift from Professor Tony Green (University of Cambridge). Ba/F3 cells were maintained in Roswell Park Memorial Institute (RPMI) 1640 medium (Sigma Aldrich) supplemented with 10% FBS, 1% L-glutamine, 1% penicillin/streptomycin and 10ng/mL recombinant murine IL3 (Peprotech). Ba/F3 cells were subcultured at a ratio of 1:7 every 2-3 days. Ba/F3 cells were grown in T-25 vented flask at 37°C with 5% CO₂.

Ba/F3-MPL cells are a derivative of Ba/F3 cells and were generated in-house by transduction of Ba/F3 cells with retroviruses expressing human MPL (hMPL) cDNA (described in Section 2.4). Following transduction, cells were cultured in the presence of 50 ng/mL recombinant human thrombopoietin (Peprotech) to select the hMPL-expressing cells.

2.2 Drug Treatments

N, N, N' N'- tetrakis(2-pyridylmethyl)ethylenediamine (TPEN) stock solutions were prepared by dissolving TPEN powder (Sigma Aldrich) in 99% ethanol. For TPEN treatment, Ba/F3-MPL cells were seeded into 6 well plates at a density of 1×10^5 cells per well, and various doses of TPEN from 0-10 μ M were added directly to RPMI culture medium. The samples are collected at various time points for further analysis.

2.3 Freezing and Thawing Cells

Cells were stored for long-term storage at -80°C . Confluent cells were centrifuged at $450 \times g$ for 5 minutes and the cell pellet was resuspended in 1mL of freezing media. Freezing media for 293T cells are composed of 70% DMEM medium, 20% FBS and 10% DMSO. The freezing media for Ba/F3 cells consists of 70% RPMI media, 20% FBS and 10% DMSO. The cells are then transferred into cryovials and placed into Mr. Frosty freezing container (Thermo Fisher Scientific) to allow a rate of cooling of $-1^{\circ}\text{C}/\text{minute}$, the optimal rate for cell preservation. For cell thawing, the cryovials were thawed in gel bead bath at 37°C and were resuspended in pre-warmed media. Cells

were centrifuged at 450 x g for 5 minutes, and cell pellet was resuspended with fresh culture media and transferred into a cell culture flask, cultured in optimal conditions and allowed to recover.

2.4 Lentiviral infection of Ba/F3 and Ba/F3-MPL cells

Lentivirus generation was performed using HEK293T cells. HEK293T cells were seeded in 6 well dishes at a density of 1.5×10^5 cells/mL. After 24 hours, each well was transfected with a total of 2.5 μ g plasmid DNA, which includes 1.2 μ g CALR cDNA in pLeGO-iv2 lentiviral vector backbone (Riecken, 2015) 0.65 μ g pVSV-G and 0.65 μ g pPAX2, and mixed with 7.5 μ L TransIT-LT1 transfection agent (Mirus). DNA:cationic lipid mixture was incubated for 15 minutes at room temperature and then added to HEK293T cells in a dropwise manner. Cells were incubated at 37°C for 5 hours and then subjected to a media change. Twenty-four hours post-transfection, conditioned media (containing viral supernatants) was collected, passed through a 0.22 μ m filter and used to transduce Ba/F3 or Ba/F3-MPL cells. For each transduction, 3×10^5 cells Ba/F3 or Ba/F3-MPL cells were added into a well of a 6-well dish, combined with 1 mL of the viral supernatant, supplemented with 8 ng/mL polybrene and subjected to spin-infection at 1100 x g with slow acceleration and deceleration for 2 hours. After spin-infection, viral supernatant was removed and cells were grown in fresh media supplemented with appropriate cytokines for 24-48 hours prior to downstream applications.

2.5 Cytokine Withdrawal Assays

To quantify cell proliferation following cytokine withdrawal, transduced Ba/F3 or Ba/F3-MPL cells were washed three times with PBS to completely remove traces of cytokines and seeded in triplicate at a density of 2×10^5 cells/mL in complete RPMI media in the absence of cytokines.

2.6 Cell Counting

Cell viability of transduced Ba/F3-MPL cells following cytokine withdrawal were performed in one of 3 ways: (i) Trypan blue dye exclusion - cells were mixed with trypan blue solution (Sigma Aldrich) at a 1:1 ratio and cell numbers were counted under an inverted phase contrast microscope by a haemocytometer; (ii) MTT assay – cells were aliquoted into 96-well microtitre plates to achieve a density of 1×10^5 cells/well. After 24 hours, culture medium was replaced with 100 μ L (3-(4,5-Dimethylthiazol-2-yl)-2,5-Diphenyltetrazolium Bromide (MTT) solution (5 mg/mL MTT diluted with phenol red-free IMDM media to achieve a final concentration of 1 mg/mL). After 3 hours incubation in 5% CO₂ at 37°C, the remaining MTT media was aspirated, 100 μ L isopropanol was added to initiate the formazan colorimetric reaction, and colour change was measured using BioRad plate reader at an absorbance of 570nm; (iii) flow cytometry – cell numbers were quantified using a CytoFLEX flow cytometer (Beckman Coulter) by measuring the number of events in a fixed volume analysed at day 3 versus day 0 counts (Figure 2.1).

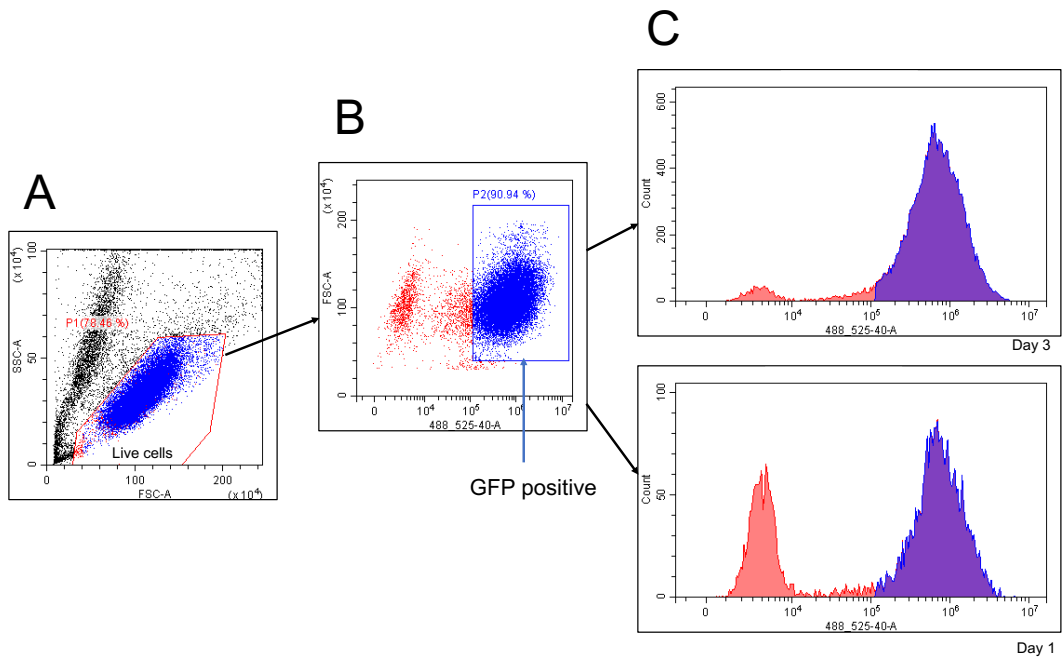


Figure 2.1 Gating strategy for FACS acquisition and downstream analysis of cell counts. (A) Initial acquisition gate used to identify live cell population following collection of a fixed volume of 50 μ L. (B) Second acquisition gate was used to identify and distinguish GFP⁺ cells within the live cell population. (C) Histograms depicting cell count in day 3 (top panel) versus day 1 (bottom panel).

2.7 Coimmunoprecipitation assays

For CALR-MPL coimmunoprecipitation assays, 293T cells were first seeded at a density of 2×10^5 cells/mL in a 6 well plate overnight, followed by transfection with 1.25 μ g of FLAG-tagged CALR variants in a pSPORT6 backbone and 1.25 μ g of pLeGO-iT2-hMPL using 7.5 μ L of TransIT-LT1 (Mirus). Mixtures were added to cells dropwise and were incubated for 24 hours in 5% CO₂ at 37°C. The next day, transfected 293T cells were harvested and washed with 1X PBS, pelleted and resuspended in 450 μ L NP40 lysis buffer (20 mM Tris HCl pH 8, 137 mM NaCl, 2 mM EDTA 1% NP-40 supplemented with protease inhibitors) and incubated on ice for 30 minutes. The samples were centrifuged at 17000 g for 10 minutes at 4°C, and supernatant were retained for immunoprecipitation. For each sample, 50 μ L of Protein G magnetic beads (BioRad) was washed with IP Wash Buffer (PBS with 0.1% Tween-20) three times and combined with 1 μ L FLAG M2 antibody (Sigma Aldrich) and incubated for 15 minutes by gentle rotation at room temperature. Bead-antibody mixtures were then washed with IP Wash Buffer and applied to 400 μ L lysate supernatants for 1 hour at room temperature with gentle rotation. Beads were washed on the Surebead magnetic bead system (BioRad), and washed beads were resuspended in 100 μ L of 1x SDS Laemmli buffer and eluted by incubating the beads for 10 minutes at 70°C.

2.8 Western Immunoblotting

Cells were harvested and washed with 1x PBS and lysed with 100 μ L of RIPA+ buffer. Samples were incubated on ice for 30 minutes and centrifuged at 17000 g for 10 minutes and supernatants were then collected and transferred into a new microcentrifuge tube. The protein concentration was determined using a Bradford assay with BSA standards at known protein concentration ranging from 0.5-4 mg/mL. The samples are measured in triplicates and absorbance is measured using the spectrophotometer plate reader at 595 nm. Proteins were readied for loading by addition of sufficient quantities of 2X SDS Laemmli buffer (Biorad). The samples were boiled at 95°C for 10 minutes and stored in -20°C until required.

Protein samples were subjected to SDS-PAGE on a 10% polyacrylamide gel for 90 minutes at 100V or until the proteins reach the end of the tank. Proteins were then transferred to nitrocellulose membrane (Amersham) using the Trans-blot Turbo transfer system (Biorad) for 30 minutes. The membranes were stained with Ponceau S to ensure efficient protein transfer. Membranes were blocked using 5% skimmed milk in 1x PBST (PBS supplemented with 0.05% Tween-20) at room temperature for 1 hour. The membranes were incubated with appropriate antibodies overnight at 4°C (See **Table 2.1** for all antibodies used). The membranes were washed three times with PBST, then incubated with the appropriate secondary antibodies for 1 hour at room temperature, washed three times PBST, and blots were visualised using SuperSignal West Pico ECL Plus Chemiluminescent substrate kit (Thermo Fisher Scientific) according to the manufacturer's instructions. The blots were

exposed using Image Lab. Analysis of the blots were performed using Image Lab software.

Antibody	Catalogue Number	Dilution	Species	Company
Calreticulin (D3E6) XP	12238	1:1000	Rabbit	CST
Calreticulin	PA3-900	1:1000	Rabbit	Invitrogen,
Mutated Calreticulin (CAL2)	DIA-CAL-250	1:1000	Mouse	Dianova
FLAG	F1804	1:1000	Mouse	Sigma
FLAG	SAB4301135	1:1000	Rabbit	Sigma
β -actin	A1978	1:10000	Mouse	Sigma
MPL (CD110)	562137	1:1000	Mouse	BD Biosciences
V5	13202	1:500	Rabbit	CST
6-His	906110	1:1000	Mouse	BioLegend
Phospho-Stat5 (Tyr694) (D47E7)	4322	1:1000	Rabbit	CST
Phospho-Stat5 (Tyr694) (C11C5)	9359	1:1000	Rabbit	CST
Stat5	9363	1:1000	Rabbit	CST
Phospho-Stat3 (Tyr705) (D3A7)	9145	1:1000	Rabbit	CST
Stat3 (124H6)	9139	1:1000	Mouse	CST
Anti-rabbit IgG, HRP-linked	7074S	1:5000	Goat	CST
Anti-mouse IgG, HRP-linked	7076S	1:5000	Horse	CST

Table 2.1 Antibody Table. Details of sources and concentrations of antibodies used for immunoblotting in this study. Abbreviations: CST, Cell Signalling Technology; HRP, horse radish peroxidase

2.9 Intracellular Phosphoprotein Flow Cytometry Analysis

Ba/F3-MPL cells expressing CALR variants were starved of cytokines for 4 hours. Harvested cells were transferred into flow tubes and washed with FACS Buffer (1X PBS + 2% FCS) twice to remove residual RPMI media and centrifuged at 750 x g for 5 minutes. Fixation and permeabilisation of cells were performed using Fix&Perm Kit (Nordic MUBio, GAS-002-1). These cells were fixed with 100 μ L of reagent A (fixation medium) and incubated for 15 minutes at room temperature and washed with 5 mL of FACS Buffer by centrifuging for 5 minutes at 750 x g and discarding supernatant. The fixed cell pellet was resuspended with reagent B (permeabilisation medium) and 5 μ L each of PE Mouse anti-Stat3 (pY705) and Alexa Fluor 647 anti-Stat5 (pY694) (BD Biosciences Phosphoflow). Staining was carried out for 1 hour at room temperature in the dark. Cells were washed after staining using the FACS Buffer, resuspended in 500 μ L of FACS Buffer and analysed using a CytoFLEX flow cytometer (Beckman Coulter). Data analysis was performed with CytExpert V2.2 (**Figure 2.2**).

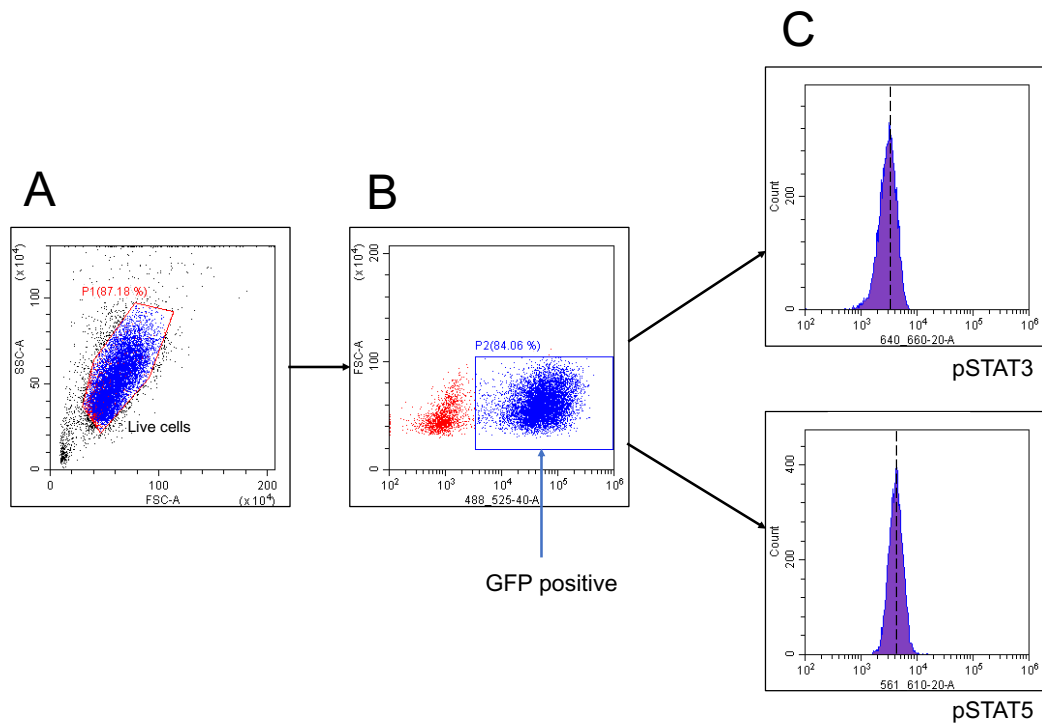


Figure 2.2 Gating strategy for FACS acquisition and downstream analysis of intracellular phosphoflow STAT3 and STAT5 signalling. (A) Initial acquisition gate used to identify live cell population following collection of a fixed volume of 50 μ L. (B) Second acquisition gate was used to identify and distinguish GFP⁺ cells within the live cell population. (C) Histograms showing cell count in day 3 (top panel) versus day 0 (bottom panel).

2.10 Annexin and Propidium iodide Staining

Ba/F3-MPL expressing CALR variants cells were collected into flow tubes and centrifuged for 5 minutes at 750 x g. Cells were washed with FACS Buffer and centrifuged for 5 minutes. The pellet was resuspended in 500 μ L Annexin V binding buffer and centrifuged for 5 minutes. Annexin V-specific antibody (Biolegend), RNase A and propidium iodide (PI) were added to the cell suspension and incubated on ice for 15 minutes in the dark, followed by analysis on the CytoFLEX flow cytometer (**Figure 2.3**)

2.11 Site Directed Mutagenesis

Site-directed mutagenesis was performed using the Q5 Site-Directed Mutagenesis Kit (New England Biolabs) according to manufacturer's protocols. Briefly, the following reagents were assembled in a thin-walled PCR tube for exponential amplification of the template DNA: 1X Q5 Hot Start High-Fidelity 2X Master Mix, 0.5 μ M forward primer, 0.5 μ M reverse primer, 10 ng template DNA and nuclease-free water. The reagents were then transferred into a thermocycler. The following thermocycling setup was used: initial denaturation 98°C for 30 seconds, 25 cycles at 98°C for 10 seconds 50-72°C for 10-30 seconds, 72°C 30 seconds, final extension at 72°C and hold at 4°C. Next, the following reagents were assembled for Kinase, Ligase and DpnI (KLD) treatment: 1 μ L PCR product, 1X KLD reaction buffer, 1X KLD enzyme mix and nuclease free water. The mixture was incubated at room temperature for 1 hour. The KLD mixture was added to competent *E. coli* cells and incubated on ice for 30 minutes. The sample was heat shocked at 42°C

for 30 seconds and was placed on ice for 5 minutes. Super optimal broth (SOC) media was added into the mixture and incubated at 37°C for 1 hour with shaking. The mixture was spread onto a selection plate (LB agar with Ampicillin (Sigma Aldrich) and placed in a plate incubator overnight at 37°C. At least 3 colonies were picked per sample the following day and transferred into 2 mL of LB with Ampicillin and incubated with shaking overnight. The plasmid DNA was purified using QIAprep Spin Miniprep Kit (Qiagen). DNA was quantified using Nanodrop 8000 spectrophotometer (Thermo Fisher Scientific) and sent for sequencing to confirm if mutagenesis was successful.

2.12 Confocal Microscopy

293T cells were seeded into 35 mm, high, μ -Dish with an ibidi polymer coverslip bottom and were incubated overnight at 37°C. Transient co-transfection of pSPORT6 mCherry-CALR variant-FLAG with psMSCV-GFP-MPL was performed. Following 24 hours post-transfection, the cells were gently washed with 1X PBS and resuspended with phenol free DMEM culture medium. The cells were imaged using Zeiss LSM 880 inverted confocal microscopy. A pinhole of 0.8 airy unit (AU) was used to enhance the resolution. The objective used are Plan-Apochromat 20x/0.8 and Plan-Apochromat 40x/1.4 Oil DIC. FRET was measured by exciting sample at donor excitation of 488 nm and measuring the acceptor excitation absorbance at 610 nm. FRET intensity was calculated by using sensitised emission.

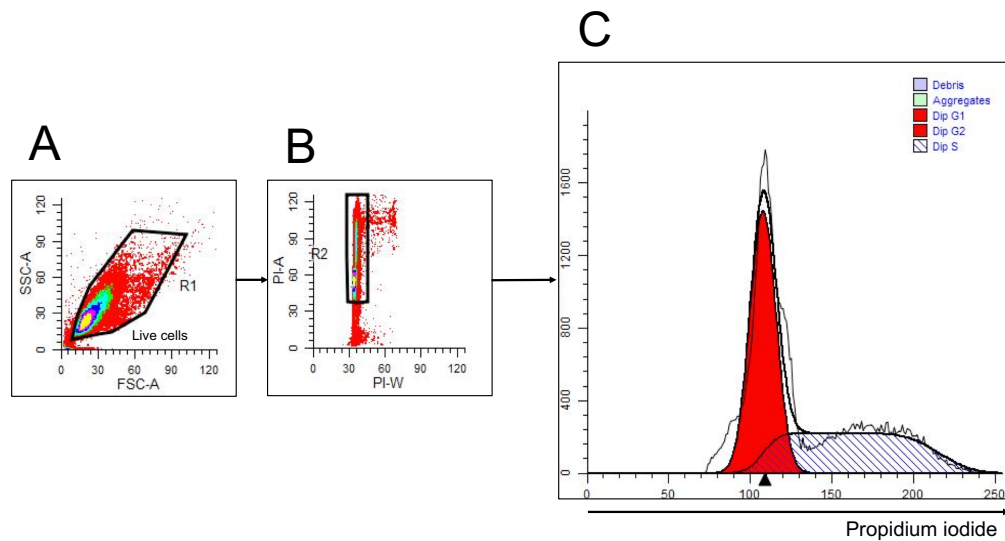


Figure 2.3 Gating strategy for FACS acquisition and downstream analysis of cell cycle. (A) Initial acquisition gate used to identify live cell population by 10000 events. (B) Second acquisition gate was used to exclude clumps and doublets by using propidium iodide (PI) fluorescence. (C) Identification of debris (purple), aggregates (green), G₁ (red), S (stripe) and G₂/M phase (red).

2.13 Zinc binding assay

Cell lysates were prepared in NP40 lysis buffer (as described in Section 2.7) and applied to zinc chelating resin (G Biosciences) and incubated with rotation for 20 minutes at room temperature. The resin was centrifuged for 5 minutes, and resuspended with elution buffer with mechanical rotation for 5 minutes. The resin was pelleted by centrifugation for 5 minutes and supernatant (which contains the zinc-bound fraction) was collected and retained for SDS-PAGE. 2x SDS-loading buffer was added to supernatant at a 1:1 ratio, and the mixture was boiled in 70°C for 10 min. Samples were then analysed using SDS-PAGE and western blotting.

2.14 Cloning of CALR cDNA into pOPIN vectors

For cloning of CALR cDNA into the pOPIN vector, NEBuilder HiFi DNA assembly (New England BioLabs) was used. The cloning reaction was set up in a 5:1 ratio of insert vector and pOPIN vector. 10 µL HiFi DNA assembly master mix was added to DNA mixtures and incubated at 50°C for 1 hour. The cloning reaction was used to transform competent DH5α cells and colonies were picked following overnight incubation into LB agar supplemented with kanamycin and chloramphenicol (Sigma Aldrich). Plasmid DNA was purified using QIAprep Spin miniprep kit (Qiagen) and quantified using Qubit 4 Fluorometer (Thermo Fisher Scientific) for fluorometric quantification. The plasmid DNA were submitted for DNA sequencing to check if cloning was successful.

Confirmation of successful cloning was performed using two methods: (i) Diagnostic restriction digest was performed to analyse the plasmid DNA. The reagents were assembled into an Eppendorf tube: NEB Cutsmart buffer (2 μL), NEB NcoI (0.5 μL), NEB HindIII (0.5 μL), 10 μL of plasmid DNA and nuclease free water. The samples were incubated at 37°C in a water bath for 1 hour. Following the restriction digest, the samples were analysed on 1% agarose gel using gel electrophoresis. (ii) Diagnostic PCR was performed using 10 μM CALR forward primer (0.5 μL , 10 μM CALR reverse primer (0.5 μL), 1X OneTaq Quick-Load Master Mix with standard buffer (12.5 μL), 2 μL plasmid DNA and nuclease free water for a total reaction volume of 20 μL . Veriti PCR machine was used using pre-programmed Q5 settings with the following parameters: 1 cycle of initial denaturation (98°C), 30 cycles of denaturation (98°C), annealing (60°C), elongation (72°C), final extension (72°C) and 1 cycle on hold (4°C).

2.15 Small scale protein purification

Small scale expression screening was performed using Promega MagneHis purification system (Promega) to screen clones for recombinant CALR protein expression. The plasmid DNA were introduced into various *E. coli* bacterial expressing cells, namely, BL21 (DE3) (New England Biolabs), BL21 (DE3) pLysE (Sigma-Aldrich), BL21 (pLysS) (Promega), NiCo21(DE3) (New England Biolabs), Lemo21 (DE3) (New England Biolabs), BL21 Rosetta (DE3) (Merck), Rosetta-Gami2 (DE3) pLysS (Merck), ArcticExpress (DE3) (Agilent) and BL21 Rosetta2 (DE3) (Merck) and cultured on LB-agar plates

supplemented with ampicilli and chloramphenicol. Individual colonies were plucked and expanded in LB media in 24-well plates with ampicillin and chloramphenicol. Once the OD₆₀₀ reached 0.6, 0.1M IPTG was added and incubated at 18°C and 25°C with shaking at 220 RPM (MaxQ8000 incubators) overnight.

Following the overnight growth, the 24-well plates were centrifuged at 4000 g for 10 minutes and culture media was discarded. An automated MagneHis protocol program to run a standard protein purification protocol based on the manufacturer's protocols was performed using the Hamilton robot, which involved five steps: MagneHis Particle Dispense, Cell Pellet Resuspension/Lysis, Protein binding to MagneHis Ni-Particles, Washes and Elution (Promega Corporation, 2019). At the conclusion of the purification, 2x protein loading dye was added to the various eluted proteins and ran using Biorad 10% SDS-Page gels for 200V for 45 minutes. The gels were then stained in InstantBlue Coomassie protein stain (Expedeon) for 1 hour. Gels were imaged using Syngene G:Box Chemi XRQ (Syngene). If necessary, western immunoblotting was also performed using CALR-specific or His tag-specific antibodies to identify bands.

2.16 Large scale protein purification

pOPIN-CALR^{WT} plasmids were propagated in Rosetta cells, while pOPIN-CALR^{del52} plasmids were propagated in Rosetta 2 cells. A single colony was expanded into a 3 mL starter culture of LB with ampicillin (100µg/mL) (Sigma

Aldrich) and chloramphenicol (34 μ g/mL) overnight at 37°C with shaking at 220 RPM. The culture was then transferred into 100 mL culture and grown overnight, followed by inoculating 1L cultures. These cultures were grown at 37°C with shaking at 180 RPM until the OD₆₀₀ reaches ~0.6. The cultures were then induced with 0.1M IPTG per mL (Sigma Aldrich) of culture (4 mL of IPTG per 1L of culture) and then grown at 18°C for 12 hours. The cells were centrifuged at 4000 g for 30 minutes at 4°C, the media was discarded and the pellet was resuspended in 20 mL Low Salt Buffer (50 mM Tris pH 7.6, 300 mM NaCl, 20 mM imidazole, 5% v/v glycerol, 0.075% β -mercapethanol, supplemented with protease inhibitor EDTA free (1 mg) and 30 mg of lysozyme) per litre of the original culture. The bacterial lysate was incubated on ice for 20 minutes with an end-to-end mixing. The samples were then sonicated for 30 seconds on and 60 seconds off at 30%, and then subjected to a cell disrupter until samples were at a good consistency. The samples were then centrifuged at 35000 g for 45 minutes at 4°C. The supernatant was pooled together and stored in 4°C.

2.17 Affinity Chromatography

Large scale purification was performed using AKTA pure purification system (GE Healthcare Life Sciences). The standard methodology for large scale purification was performed following CIP process: capture, intermediate purification and polishing. The capture step was performed by affinity chromatography using a Nickel column to capture His-tagged proteins. The column used was a nickel-charged IMAC column for high resolution his-

tagged protein purification with high binding capacity for maximised recovery. AKTA setup involved following pre-programmed standardised method. Sample application was performed using sample pump at a rate of 1 mL/minute. The column was washed with 5 column volumes of Low Salt buffer, 5 column volumes of High Salt Buffer (50 mM Tris pH 7.6, 500 mM NaCl, 20 mM imidazole, 5% v/v glycerol, 0.075% β -mercapethanol), and 5 column volumes of Low Salt Buffer. The samples were eluted using His Elution Buffer (50 mM Tris pH 7.6, 300 mM NaCl, 400 mM imidazole, 5% v/v glycerol, 0.075% β -mercapethanol) at a gradient elution. The column is then washed and stored in 70% ethanol at 4°C.

2.18 Ion Exchange Chromatography

Ion exchange chromatography was carried out using a HiTrap Q HP anion exchange chromatography column (GE Life Sciences). The following pre-programmed method was used on the AKTA pure purification system: sample prime and pump washes, equilibration to prepare the column to the desired start conditions, sample application and wash using a sample pump, elution in HEPES elution buffer (50mM HEPES, 150 nM NaCl, 1 μ M TCEP) whereby the proteins will be released from the ionic exchanger by a change of buffer pH from 7.5 to 4, and a final regeneration step to remove all proteins still bound to the column.

2.19 Size Exclusion Chromatography

Size exclusion chromatography was performed using the HiLoad 26/600 Superdex 200 prep grade column (GE Healthcare Life Sciences). The column was primed and equilibrated prior to use to ensure that the desired buffer fills the entire column. The sample is injected manually and the pre-programmed method for gel filtration.

2.20 GST Cleavage

GST cleavage was performed both manually and by AKTApure. For the cleavage using AKTA pure, the following method was used: sample application using a sample pump, unbound samples were washed off and the 3C-His protease was injected into the column and incubated for 12 hours at 4°C. Following incubation, 5 column volumes of PBS was used to wash the column, and His elution buffer was applied to elute the protease and any uncleaved samples. A final elution using elution buffer containing glutathione was applied into the column to elute the GST tag and any uncleaved samples still present within the column. Manual cleavage followed a similar principle using GST Pierce Glutathione Agarose (Thermo Fisher Scientific). The GST agarose beads were washed and equilibrated with the PBS for 5 minutes and incubated at 4°C with end-to-end mixing. The beads were then centrifuged at 500 g for 5 minutes at 4°C. This was repeated twice. Purified GST fusion protein samples were applied and incubated for 4 hours with an end-to-end mixing to allow binding to GST beads. The 3C-His protease was then added and incubated for 12 hours. Samples were washed with PBS and centrifuged

for 5 minutes at 500 g and at 4°C to elute the cleaved proteins. His Elution Buffer was then added into the sample and incubated for 1 hour to allow the remaining protease to elute. The samples were then centrifuged for 5 minutes at 500 g, the supernatant was collected, GST elution buffer added into the solution and incubated for 1 hour to elute the GST tag and residual uncleaved proteins still bound to the bead. This is then centrifuged for 5 minutes at 500 g to pellet the bead.

2.21 Negative EM staining

Grids for electron microscopy were kindly provided by the staff of the FBS Electron Microscopy unit. A Cressington glow discharge unit was used to perform the glow discharge to transfer negative charge onto the carbon of the grid that renders the surface hydrophilic. A 1% solution of uranyl acetate was used to negatively stain the protein samples. Staining was performed using a single droplet method. In brief, 5 µL of the protein of interest was dropped onto the grid and incubated for 5 minutes to allow the proteins to stick to the grid. All samples examined were quantitated prior to application onto grids, and had a concentration of >0.2µg/mL. The grid was carefully washed with 10 µL of distilled water to remove unbound samples 5 times. Next, 5 µL of uranyl acetate stain was carefully applied onto the grid and incubated for 1 minute, and any excess stain was removed using a wedge of a filter paper. The stained grid was then left to air dry prior to imaging. Negative stain imaging was performed using a FEI Tecnai G2-spirit with an electron source of Lab6. The camera used is Gatan Ultra Scan 4000 CCD, voltage of 120

KeV and the software was Digital Micrograph (DM) with a Cs of 6.3 mm. The screen down nominal mag used during imaging is 26.5 with a screen up nominal mag of 30 (kx) and a pixel size of 0.37 nm (EM Facility). Each micrograph has an image size of 3.74 Å.

2.22 Negative EM staining image analysis

Electron micrographs were saved as a .dm3 file and were converted into .mrc file prior to processing into RELION 3.0 software. The fbsdpcu058 and abs-lwkstn04 was used a local GPU machine to access the RELION software. Sample analysis was performed using the work flow described in Table 2.2.

2.23 Biological replicates and statistical analysis

All experiments were performed throughout this thesis have at least one replicate. All figures in Chapter 3 were representative of three independent experiments. Statistical analysis used throughout this thesis is a student's t-test.

Data Conversion	<ul style="list-style-type: none"> • Convert .dm3 to .mrc <code>module load imod</code> <code>2proc2d.py *.dm3 @.mrc</code>
Launch RELION and import micrographs	<ul style="list-style-type: none"> • Launch relion and import micrographs <code>module load relion</code> <i>Import tab, on I/O tab:</i> <i>Input files: micrographs/*.mrc</i> <i>Node type: 2D micrographs/tomograms (.mrc)</i>
CTF estimation	<ul style="list-style-type: none"> • CTF estimation <i>On I/O tab:</i> <i>Input micrographs STAR file: job01/micrographs.star</i> <i>Use micrograph dose-weighting: No</i> <i>Spherical aberration (mm): 2.7 Voltage (kV): 120, amplitude contrast: 0.1, magnified pixel size (Angstrom): 3.74, amount of astigmatism (A): 100</i> <i>On Searches tab:</i> <i>FFT box size (pix): 512, min. resolution (A): 30, max. resolution (A): 7.1, min. defocus value: 5000, max. defocus value: 50000, defocus step size: 500</i> <i>On Gctf tab:</i> <i>Use Gctf instead: Yes, Gctf executable: wherever_it_is, ignore 'searches' parameters: Yes, perform equi-phase averaging: Yes</i>
Manual picking	<ul style="list-style-type: none"> • Manual pick <i>On I/O tab:</i> <i>Input micrographs: job02/micrographs_ctf.star</i> <i>On Display tab:</i> <i>Particle diameter (A): 100, scale for micrographs: 0.2, sigma contrast, 3, white value: 0, black value: 0, low pass filter (A): 20, highpass filter (A): -1, pixel size (A): -1, Pick-start-end coordinate helices: No, Scale for CTF images: 1</i>
Particle extraction	<ul style="list-style-type: none"> • Particle Extraction <i>On I/O tab:</i> <i>Micrograph STAR file: job03/micrographs_ctf.star, input coordinates: job03/cords_suffix_manual_pick.star, OR re-extract refined particles?: No</i> <i>On extract tab:</i> <i>Particle box size (pix): 80, invert contrast? No, Normalise particles? Yes, diameter background circle: -1, stdev for white dust removal: -1, stdev for black dust removal: -1, rescale particles? No</i>
2D Classification	<ul style="list-style-type: none"> • 2D Classification <i>On I/O tab:</i> <i>Input images STAR file: extract/particles.star</i> <i>On CTF tab:</i> <i>Do CTF-correction? Yes, have data been phase-flipped? No, ignore CTFs until first peak? No</i> <i>On optimization tab:</i> <i>Number of classes: 50, regularization parameter T: 2, number of iterations: 25, use fast subsets? Yes, mask diameter (A): 250, mask individual particles with zeros? Yes, Limit resolution E-step to (A): -1</i> <i>On Sampling tab:</i> <i>Perform image alignment? Yes, in-plane angular sampling: 6, offset search range (pix): 5, offset search step (pix): 1,</i> <i>On compute tab:</i> <i>Use parallel disc I/O: Yes, number of pooled particles: 5000, pre-read all particles into RAM? Yes, combine iterations through disc? No, use GPU acceleration? Yes</i>
3D Initial Model	<ul style="list-style-type: none"> • 3D Initial Model <i>On I/O tab:</i> <i>Input images STAR file: 2D_class/particles.star</i> <i>On CTF tab:</i> <i>Do CTF-correction? Yes, have data been phase-flipped? No, ignore CTFs until first peak? No</i> <i>On optimization tab:</i> <i>Number of classes: 4, Mask diameter (A): 250, flatten and enforce non-negative solvent? Yes, symmetry: C1, initial angular sampling: 15 degrees, offset search range (pix): 6, offset search step (pix): 2</i> <i>On SGD tab:</i> <i>Number of initial iterations: 50, number in between iterations: 200, number of final iterations: 50, write-out frequency: 10, initial resolution (A): 35, final resolution (A): 15, initial mini-batch size: 100, final mini-batch: 500,</i> <i>On computer tab:</i> <i>Use parallel disc I/O? Yes, number of pooled particles: 5000, skip padding: No, pre-read all particles RAM? Yes</i>

Table 2.2 Summary of the negative stain EM analysis work flow.

Chapter 3

Zinc dependent homomultimerisation of mutant calreticulin is required for MPN pathogenesis

Chapter 3

Zinc dependent homomultimerisation of mutant calreticulin is required for MPN pathogenesis

3.1 Introduction

Recurrent somatic mutations in the CALR gene have been found in 25-30% of ET and MF patients, and represent the most commonly affected gene in JAK2/MPL-unmutated MPN patients (Klampfl et al., 2013; Nangalia et al., 2013). CALR encodes calreticulin, an ER-resident calcium-binding chaperone that transiently associates with nascent unfolded proteins to assist with protein folding and regulate cellular proteostasis (Peterson et al., 1995). Wild-type CALR is comprised of three conserved functional domains: (i) the N globular domain that consists of lectin-, polypeptide- and zinc-binding motifs and is essential for CALR chaperone activity; (ii) a proline-rich P-domain that forms as an arm-like hairpin that binds to co-chaperones such as ERp57; and (iii) a highly acidic C-terminal tail that consists of negatively charged amino acid residues responsible for calcium buffering activity and contains an ER-retention signal sequence (KDEL) (**Figure 3.1**) (Michalak et al., 1999). MPN-associated CALR mutations are a heterogeneous set of indel mutations that result in a +1 bp frameshift that generates a novel C-terminal tail of 36 amino acids encoded in an alternative reading frame, with the most common mutations being a 52-bp deletion (type I; L367fs*46) and a 5-bp insertion (type II; K385fs*47) (Klampfl et al., 2013; Nangalia et al., 2013). The mutant-specific C-terminus replaces most of the negative-charged amino

acids of the wild-type protein with a preponderance of positively-charged arginine (R) and lysine (K) residues.

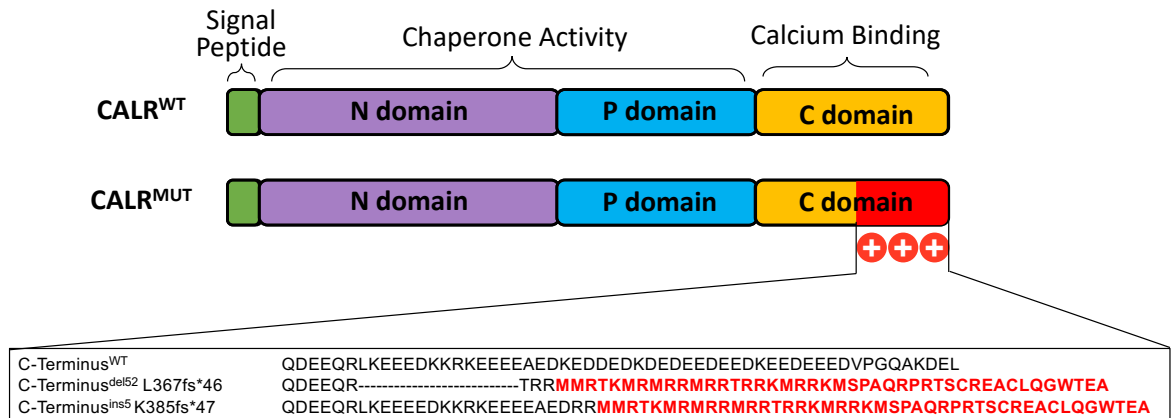


Figure 3.1 Domain structure of calreticulin. CALR comprise of three domains: signal sequence peptide (green), globular N-domain (purple), flexible P-domain (blue), terminal C-domain (yellow). CALR 52bp deletion or 5bp insertion mutations introduce a positively charged novel C-domain.

Multiple studies have now provided direct links between mutant CALR (CALR^{del52}) and the MPL-JAK2 signalling axis. An important pathognomonic feature of all MPN driver mutations is the ability to confer cytokine-independent growth. Multiple studies have reported that expression of CALR^{del52} confers cytokine-independent growth in conjunction with increased JAK-STAT signalling in Ba/F3 and UT7 cell lines co-expressing the thrombopoietin receptor MPL, but not EPO receptor or GM-CSF receptor (Chachoua et al., 2016; Elf et al., 2016; Araki et al., 2016). In addition, consistent with an essentiality of MPL in mediating CALR^{del52}-associated disease, CALR^{del52} was unable to induce MPN-like disease in mice lacking *Mpl* or *Tpo* (the ligand for Mpl) (Marty et al., 2016). Finally, multiple groups

have reported that CALR^{del52} physically associates with the extracellular domain of MPL, an interaction that correlates to its transforming activity (Chachoua et al., 2016; Elf et al., 2016; Araki et al., 2016). Cumulatively, these data lead to the hypothesis that CALR^{del52} physically interacts with MPL to promote its inappropriate activation.

Domain swapping studies have elucidated crucial features of CALR^{del52} essential for its oncogenic activity. Firstly, it was demonstrated that the capacity of CALR^{del52} to confer cytokine-independent growth and to bind MPL was critically dependent on the mutant-specific C-terminus's positively-charged nature, as mutagenising all 18 K/R residues within the C-terminal tail to glycine residue abrogated CALR^{del52} oncogenic activity (including conferring cytokine-independence, activating JAK-STAT signalling, and binding to MPL), whereas mutagenising all non-K/R residues did not affect oncogenic activity (Elf et al., 2016). Secondly, neither the N-domain nor the mutant-specific C-domain in isolation had the ability to confer cytokine-independent growth (Araki et al., 2016; Elf et al., 2018). And thirdly, a (Araki et al., 2016; Elf et al., 2018)(Araki et al., 2016; Elf et al., 2018)(Araki et al., 2016; Elf et al., 2018)(Araki et al., 2016; Elf et al., 2018)specific region within the N-domain of CALR^{del52} – namely, its lectin motif - were identified as being required for CALR^{del52} oncogenic activity (Araki et al., 2016; Elf et al., 2018). Cumulatively, these data suggest that the mutant C-terminus is necessary but not sufficient for transformation, and that the N-domain of CALR^{del52} could play a significant contributory role in its oncogenic activity. However, the

manner(s) by which the N-domain contribute to CALR^{del52} oncogenic activity, have not been clarified fully.

3.2 Aims and Hypothesis

There is significant evidence that the N-domain of CALR^{del52} contributes to its transforming ability. I therefore hypothesise that key residues within the N-domain (that are associated with specific CALR functionalities) are essential for CALR^{del52} oncogenic activity and can be uncovered using a mutagenesis-based strategy. In this chapter, I will describe results associated with these aims:

- I. Perform alanine screening of the CALR^{del52} N- domain to identify candidate residues that are critical for CALR^{del52} functionality;

- II. Functional validation of identified N-domain residues, including testing whether candidate residues are essential for abrogation of known CALR^{del52} oncogenic functionalities such as ability to confer cytokine-independent growth of Ba/F3-MPL cells, activation of JAK-STAT signalling and binding to MPL.

3.3 Results

3.3.1 Alanine mutagenesis screen identified residues in the CALR^{del52} N-domain essential for oncogenic activity

In collaboration with A. Baral and R. Smyth in the lab, a comprehensive alanine mutagenesis screen was performed for the entire N-domain of CALR^{del52} encompassing residues 18-197 (excluding residues 1-17 which comprise the signal peptide and 3 alanine residues). Each individual alanine-mutant was confirmed by Sanger sequencing (data not shown), and subsequently assessed for the ability to confer cytokine independent growth in Ba/F3-MPL cells. Ba/F3-MPL cells were lentivirally transduced with CALR^{del52} alanine-variants and the number of cell divisions was assessed 3 days post-hTPO withdrawal. Analysis of all 177 alanine-mutants revealed that the majority of the single-residue alanine mutants were unaffected in their ability to confer cytokine-independent growth (**Figure 3.2**). In total, only 9 residues out of 177 were identified which, when mutated, affected the capacity for cytokine-independent growth by a factor greater than one standard deviation away from the mean. These residues were put forward for further analysis.

Four residues (Cys105, Lys111, Gly133 and Asp135) were identified which, upon mutation, resulted in the complete impairment of the ability of CALR^{del52} to confer cytokine independence. These residues have previously been implicated in the lectin motif of wildtype CALR (Chouquet et al., 2011), and Asp135 has previously been shown to be required for CALR^{del52} oncogenic

activity (Elf et al., 2018; Chachoua et al., 2016). Quantitation of cell growth using a time-course confirmed that loss of Cys105, Lys111, Gly133 and Asp135 resulted in total impairment in the ability of CALR^{del52} to confer cytokine independence (**Figure 3.3, left panel**), which was associated with decreased levels of phosphorylated STAT3 and STAT5 as assessed by intracellular flow cytometry (**Figure 3.4A**) and western immunoblotting (**Figure 3.4B**). Moreover, FLAG pulldown assays showed that these CALR^{del52} alanine mutants lost the ability to bind directly to MPL in 293T cells (**Figure 3.5**), consistent with previous theories that MPL binding correlated with cytokine-independence.

In addition to these four residues, two additional residues (Tyr109 and Tyr128) that have also been implicated in lectin activity exhibited only a partial effect on conferring cytokine independence when mutated (**Figure 3.3, right panel**), with no significant difference on STAT3 and STAT5 phosphorylation (**Figure 3.4A-B**) and MPL binding (**Figure 3.5**) when compared with CALR^{del52}. Furthermore, other residues also implicated in the wildtype calreticulin lectin activity (Met131, Cys137 and Ile147) had no significant effect on cytokine independent growth (**Figure 3.3**). These data agree with previous findings that the lectin motif of CALR^{del52} is essential in facilitating MPL binding, but suggests that different residues within the lectin motif could have differential effects in facilitating CALR^{del52} binding to MPL.

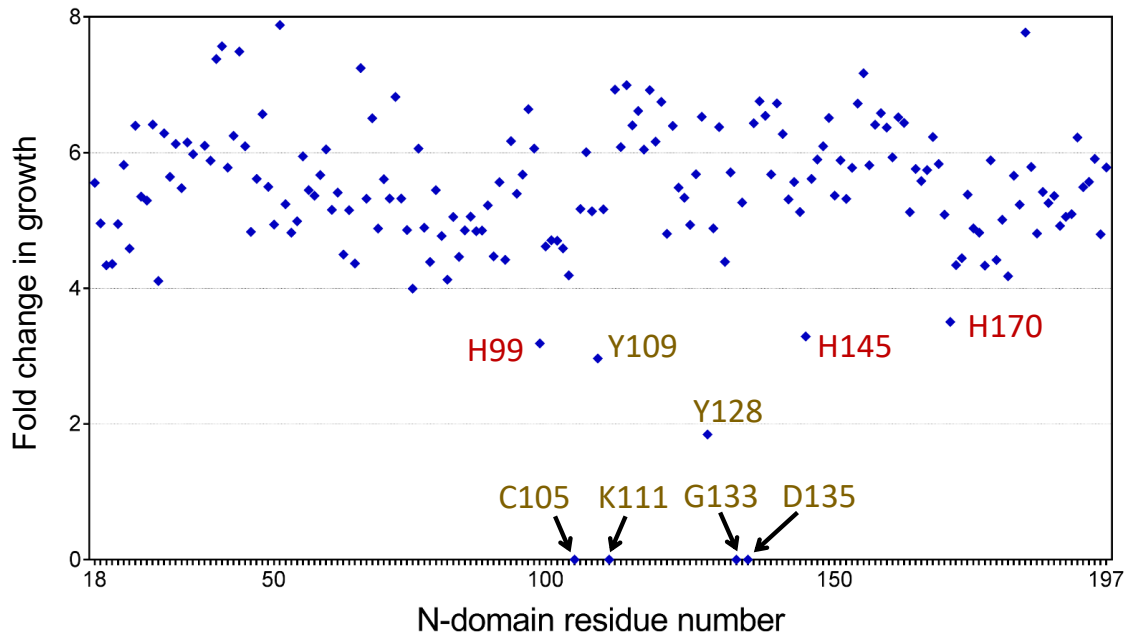


Figure 3.2 Alanine screening mutagenesis identified essential CALR^{del52} residues involved in the ability to confer cytokine independent growth.

Three histidine residues (H99, H145 and H170) (shown in red) associated with zinc binding motif when mutated was partially impaired their ability to grow following cytokine withdrawal. Residues associated with lectin motif demonstrated either complete abrogation (C105, K111, G133, D135) or partial abrogation (Y109, Y128) (shown in gold) to confer cytokine independent growth. Named residues were repeated three independent times for validation. The data in this figure were generated in collaboration with A. Baral and R. Smyth.

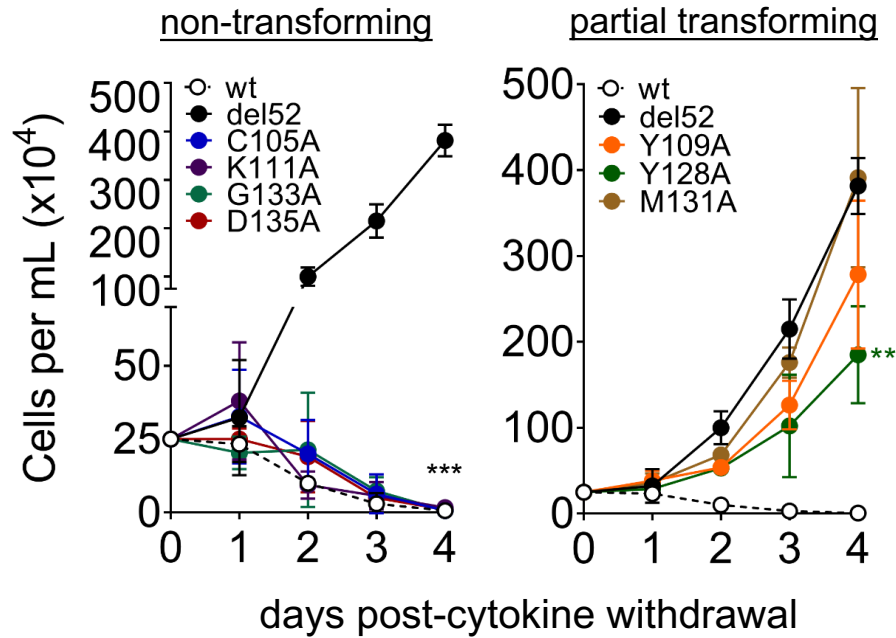
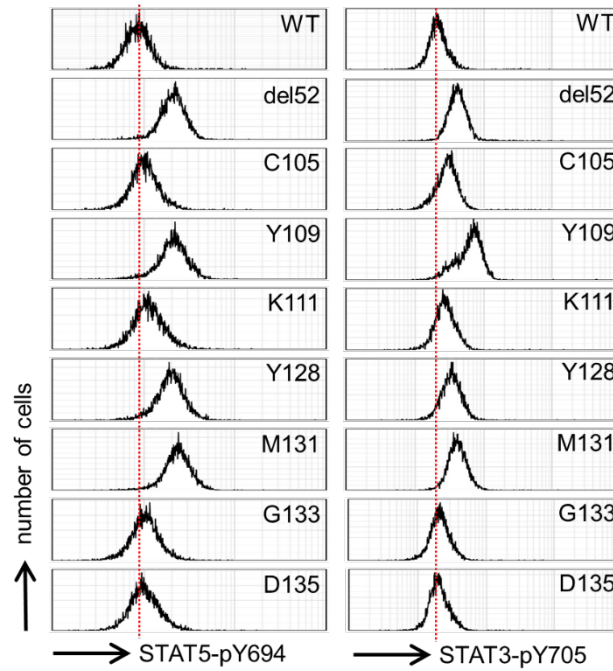


Figure 3.3 Growth curves of cells expressing CALR^{del52} lectin variants. Left panel shows CALR^{del52} lectin motif variants that were unable to confer cytokine independent growth. Right panel shows CALR^{del52} lectin motif variants which confer partial cytokine-independence. Error bars denote standard error. Testing for statistical significance was performed using a student's t-test (**: p<0.01; ***: p<0.001). Results are representative of 3 independent experiments.

A



B

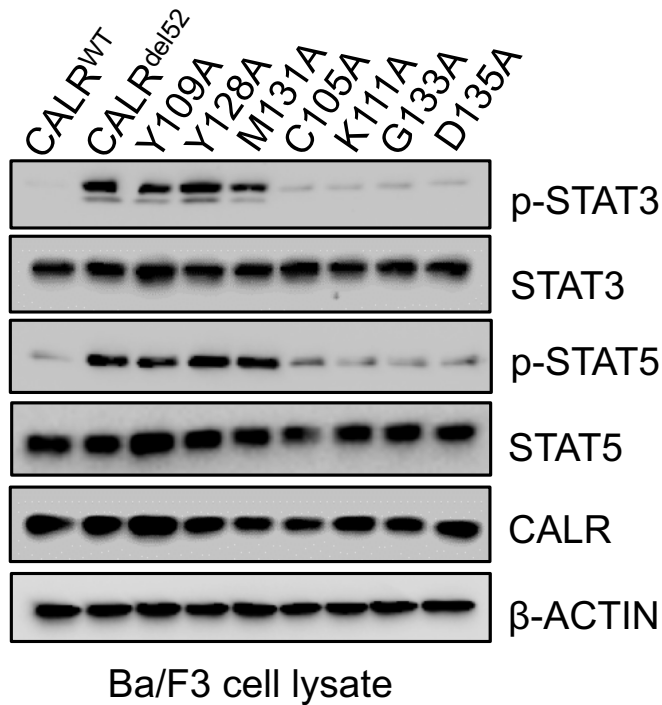


Figure 3.4 Non-transforming CALR^{del52} lectin variants lead to impaired STAT3 and STAT5 phosphorylation. (A-B) Intracellular phosphorylation flow cytometry (Panel A) and western immunoblotting (Panel B) demonstrate diminished STAT3 and STAT5 phosphorylation in Ba/F3-MPL cells expressing non-transforming CALR^{del52} lectin variants. Results are representative of 3 independent experiments.

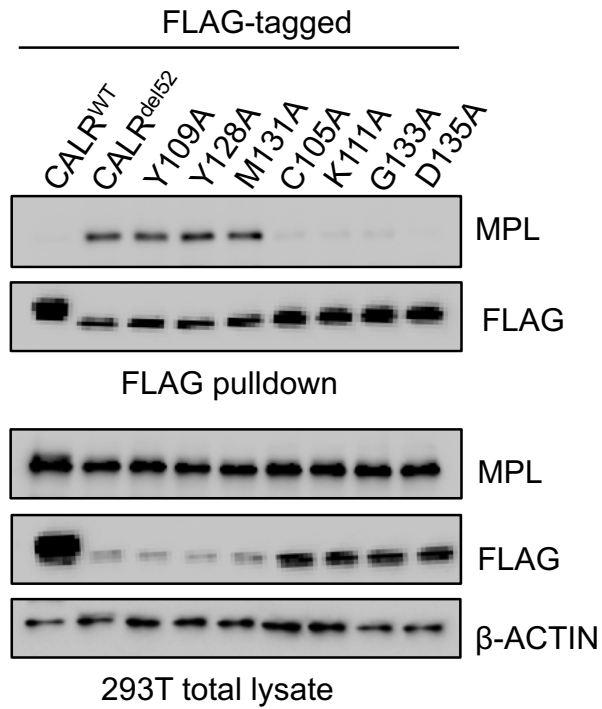


Figure 3.5 Non-transforming CALR^{del52} lectin variants do not bind to MPL. Non-transforming lectin residue variants demonstrate abolished MPL binding, whilst partially transforming lectin residues variants show binding capacity relative to CALR^{del52}. Results are representative of 2 independent experiments.

3.3.2. A triad of histidine residues in the N-domain regulates CALR^{del52} oncogenic activity

The remaining 3 residues identified in the initial alanine screen were histidine residues (His99, His145, His170) that have previously been implicated in the ability of wild-type CALR to bind zinc (Baksh et al., 1995). In the initial alanine screen, each single His (1His) mutant led to partial abrogation of cytokine-independent growth (**Figure 3.2**).

I subsequently undertook more detailed follow-up studies to functionally characterise these residues by generating CALR^{del52} cDNAs harbouring two histidine mutations in combination (2His) or harbouring all three histidine mutated (3His). This was based on the rationale that these histidine residues were involved in zinc coordination, which frequently requires multiple histidine residues simultaneously (Guo et al., 2001), and therefore, combined loss of multiple histidine residues could have a more significant impact on CALR^{del52} functionality. Firstly, these CALR^{del52} variants were lentivirally transfected into Ba/F3-MPL cells and assessed for cytokine-independent growth. I confirmed that loss of any single histidine residue (1His) led to the consistent partial abrogation of cytokine independent growth in a time-course assay (**Figure 3.6**), whereas loss of two or three histidine residues led to a significant impairment in the capacity to confer cytokine independent growth (**Figure 3.6**). This finding was further supported by cell cycling analysis (**Figure 3.7**). In particular, His99 was observed to play a key role in this process, since its loss in combination with either His145 or His170 led to complete abrogation of cytokine independence, whereas combined loss of

His145 and His170 retained some capacity for cytokine-independent growth, albeit somewhat attenuated. As expected, 1His variants were associated with sustained levels of phosphorylated STAT3 and STAT5 comparable with CALR^{del52}, whereas 2His and 3His variants exhibited attenuation of STAT3 and STAT5 phosphorylation by intracellular flow cytometry (**Figure 3.8A**) and western immunoblotting (**Figure 3.8B**).

To ensure that the effects of these histidine residues are specific to these specific putative zinc-binding residues and not due to a general effect on CALR^{del52} stability following mutagenesis of excessive number of residues, 1His CALR^{del52} variants were combined with loss of His42, which is predicted to lie on the opposite face of the globular domain and is not thought to coordinate with His99, His145 and His170 to bind to zinc (Chouquet et al., 2011; Guo et al., 2003). As previously, these variants were transfected into Ba/F3-MPL cells and assessed for their ability to confer cytokine-independent growth and constitutively activate STAT3 and STAT5 phosphorylation. Loss of His42 individually or in combination with His99, His145 and His170 did not significantly impair the ability of CALR^{del52} to confer cytokine-independent growth (**Figure 3.9A**) and elicited comparable levels of STAT3 and STAT5 phosphorylation as CALR^{del52} (**Figure 3.9B-C**).

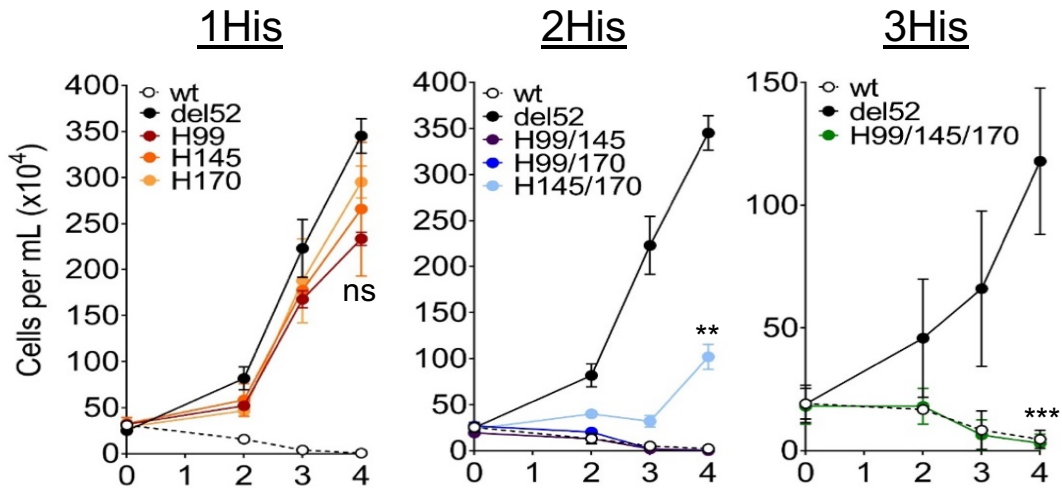


Figure 3.6 Loss of two or more histidine residues within the zinc binding domain of CALR^{del52} leads to impaired ability to confer cytokine independent growth. Growth curves of Ba/F3-MPL cells stably expressing CALR^{del52} single (1His), double (2His) and triple (3His) histidine variants were measured over a period of 4 days following cytokine withdrawal. Error bars denote standard error. Testing for statistical significance was performed using a student's t-test (ns: no significance; **: $p < 0.01$; ***: $p < 0.001$). Results are representative of 3 independent experiments.

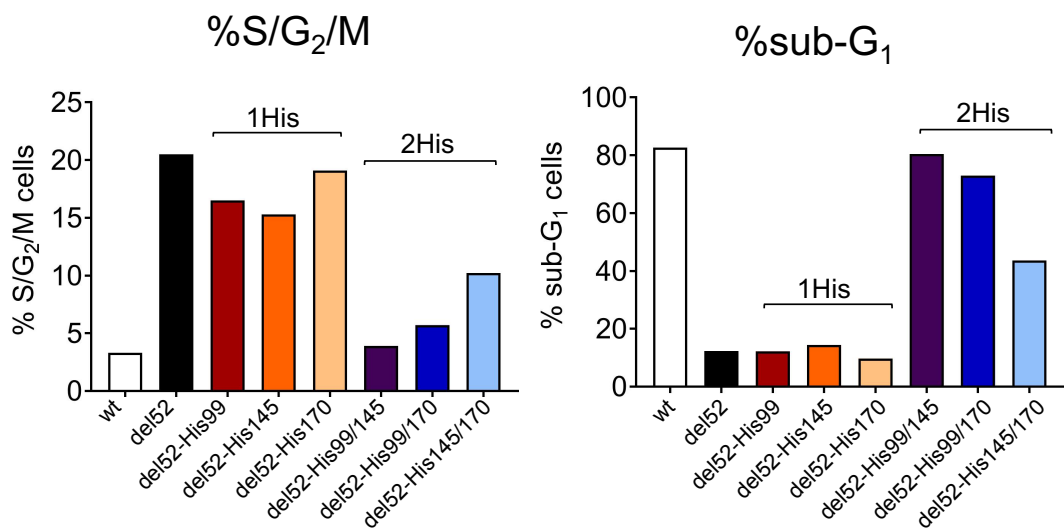


Figure 3.7 Loss of two or more histidine residues within the zinc binding domain of CALR^{del52} leads to impaired ability to confer cytokine independent growth. Loss of two or more histidine residues is associated with increased sub-G₁ cells and decreased S/G₂/M cells compared to Ba/F3-MPL cells expressing CALR^{del52}. Results are representative of one independent experiment.

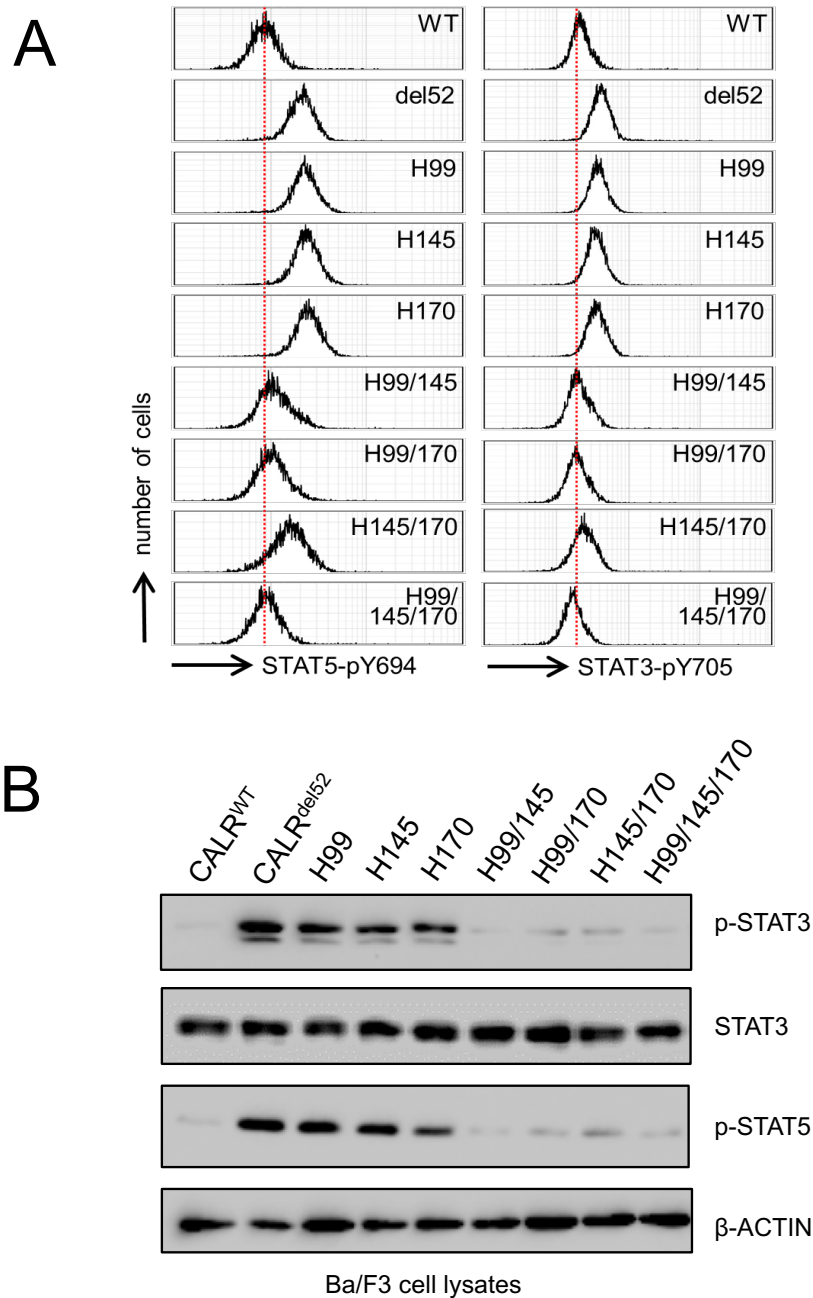


Figure 3.8 Loss of two or more histidine residues in CALR^{del52} lead to diminished STAT3 and STAT5 phosphorylation. (A-B) Intracellular phosphorylation flow cytometry (Panel A) and immunoblotting (Panel B) demonstrate diminished STAT3 and STAT5 phosphorylation in Ba/F3-MPL cells expressing 2His- and 3His-CALR^{del52} variants. Results are representative of 3 independent experiments.

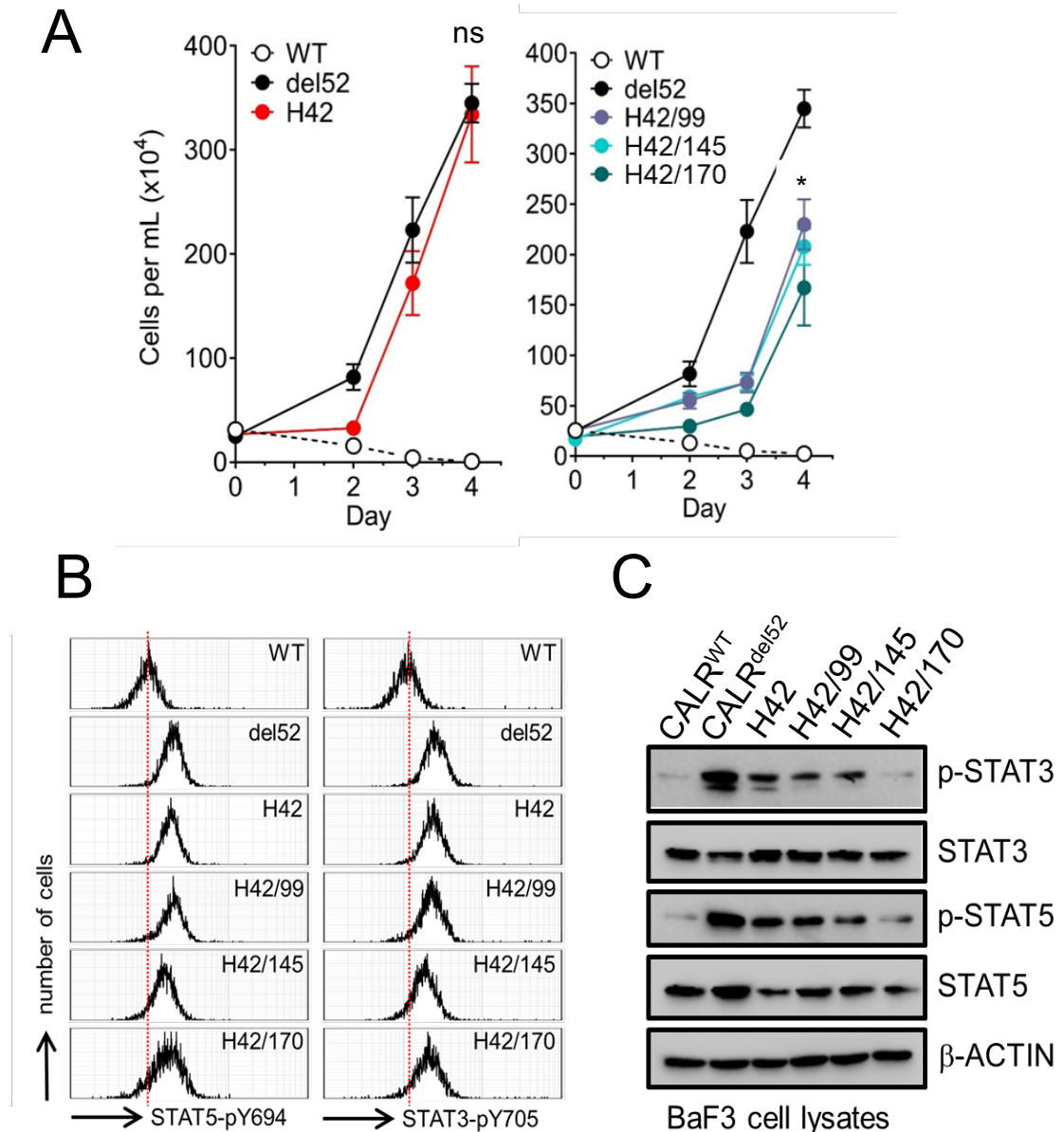


Figure 3.9 Loss of His42 does not affect CALR^{del52} activity. (A) Growth curves in Ba/F3-MPL cells expressing CALR^{del52} variants harbouring loss of His-42 alone or in combination with His-99, His-145 or His-170. (B-C) Intracellular phosphorylation flow cytometry (Panel B) and immunoblotting (Panel C) demonstrate robust STAT3 and STAT5 phosphorylation in Ba/F3-MPL cells expressing CALR^{del52} variants harbouring loss of His-42 alone or in combination with His-99, His-145 or His-170. Error bars denote standard error. Results are representative of 3 independent experiments. Testing for statistical significance was performed using a student's t-test (ns: no significance; *: p<0.01).

Next, I tested whether histidine-deficient CALR^{del52} can bind to MPL. This was achieved using two different assays. Firstly, FLAG-pulldown assays demonstrated that 1His variants retained the ability to bind to MPL, but not 2His or 3His variants (**Figure 3.10**). Secondly, I used fluorescence resonance energy transfer (FRET)-based immunocytochemistry to test the ability of histidine-deficient CALR^{del52} variants to colocalise intracellularly with MPL. To achieve this, 1His-, 2His- and 3His-CALR^{del52} variants were generated fused to an mCherry fluorescent marker and transfected into 293T cells in conjunction with a MPL-GFP fusion protein, and colocalisation was measured by quantification of energy transfer of the mCherry donor to the GFP acceptor. Significant FRET was observed for mCherry-tagged CALR^{del52} and MPL-GFP indicative of intracellular colocalisation, whereas minimal FRET was observed for mCherry-tagged wild-type CALR and MPL-GFP (**Figure 3.11A-C**). Similar analysis applied to histidine-deficient CALR^{del52} variants indicated that MPL colocalised strongly with 1His-CALR^{del52} variants, but not with 2His and 3His variants (**Figure 3.11A-C**).

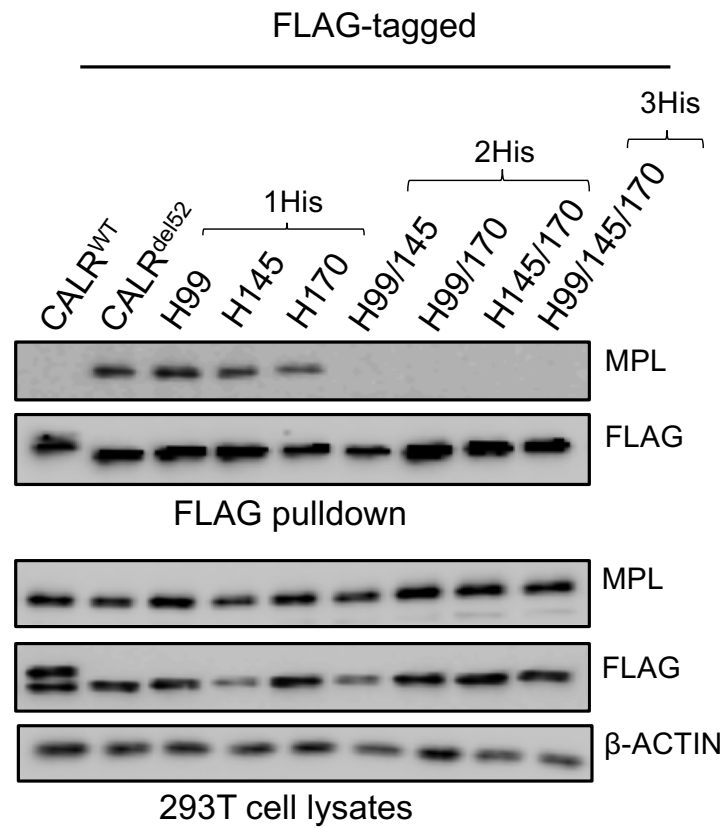


Figure 3.10 Loss of two or more histidine residues in CALR^{del52} lead to impaired capacity to bind to MPL. Co-immunoprecipitation demonstrate 1His variants retained MPL binding capacity, whilst 2His and 3His exhibit loss of MPL binding capacity. Results are representative of 3 independent experiments.

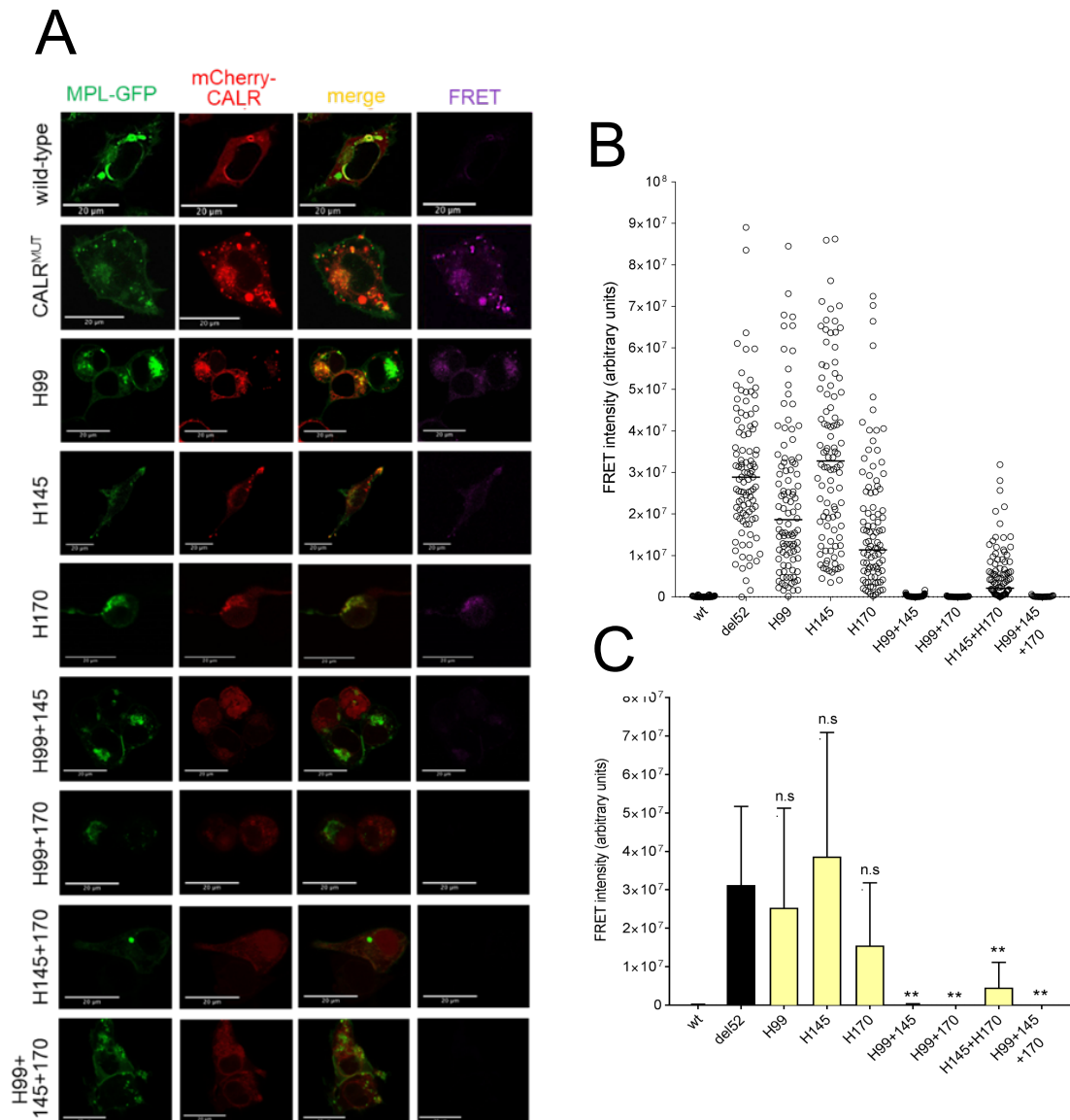


Figure 3.11 Assessment of colocalisation of histidine-deficient CALR^{del52} variants and MPL by FRET. (A) Representative confocal images of 293T cells expressing MPL-GFP fusion protein (green), mCherry-fused histidine-deficient CALR^{del52} variants fused to mCherry fluorophore (red) and areas of signal overlap (yellow). Quantitation of energy transfer by FRET are denoted in pseudocolour (magenta). (B) FRET energy transfer between mCherry-tagged histidine-deficient CALR^{del52} protein and MPL-GFP in arbitrary fluorescence units for 103 single cells. (C) Average FRET intensity depicting energy transfer in arbitrary fluorescence units. The data represent mean \pm S.D. of all cells. Testing for statistical significance was performed using a student's t-test in comparison with the CALR^{del52} sample (*: $p < 0.05$; **: $p < 0.01$; ***: $p < 0.001$). Results are representative of 5 independent experiments.

3.3.3. Histidine-mutated CALR^{del52} variants lose the capacity to homomultimerise, an essential property for MPL binding activation

A recent study reported that CALR^{del52} but not its wildtype counterpart is capable of forming homomultimers (Araki et al., 2019). I was able to confirm similar conclusions by assessing the ability of FLAG-tagged CALR^{del52} (bait) to complex and co-immunoprecipitate with a V5-tagged CALR^{del52} species (prey) in 293T cells (**Figure 3.12A**), and demonstrated that CALR^{del52} is capable of interacting with CALR^{del52} but exhibited impaired ability to bind to wildtype CALR (**Figure 3.12B**). In line with previous reports, the capacity for homomultimerisation was dependent in part on the mutant C-terminus, as CALR^{del52} was less efficient at pulling down two CALR^{del52} truncation variants lacking significant portions of the mutant-specific C-terminal tail ($\Delta 36$ and $\Delta 47$) (**Figure 3.12B**) (Araki et al., 2019).

I next tested if the same phenomenon was observed with lectin-deficient and histidine-mutated CALR^{del52} variants using the same co-immunoprecipitation approach. I observed that the lectin-deficient CALR^{del52} were able to retain its capacity to homomultimerise (**Figure 3.13**). Moreover, 1His-CALR^{del52} was also shown to be able to form homomultimers (**Figure 3.14**). In contrast, the 2His and 3His-CALR^{del52} showed an impaired capacity to homomultimerise (**Figure 3.14**). Taken together, these data suggest that the lectin activity and the capacity to homomultimerise are co-requisites to facilitate MPL binding.

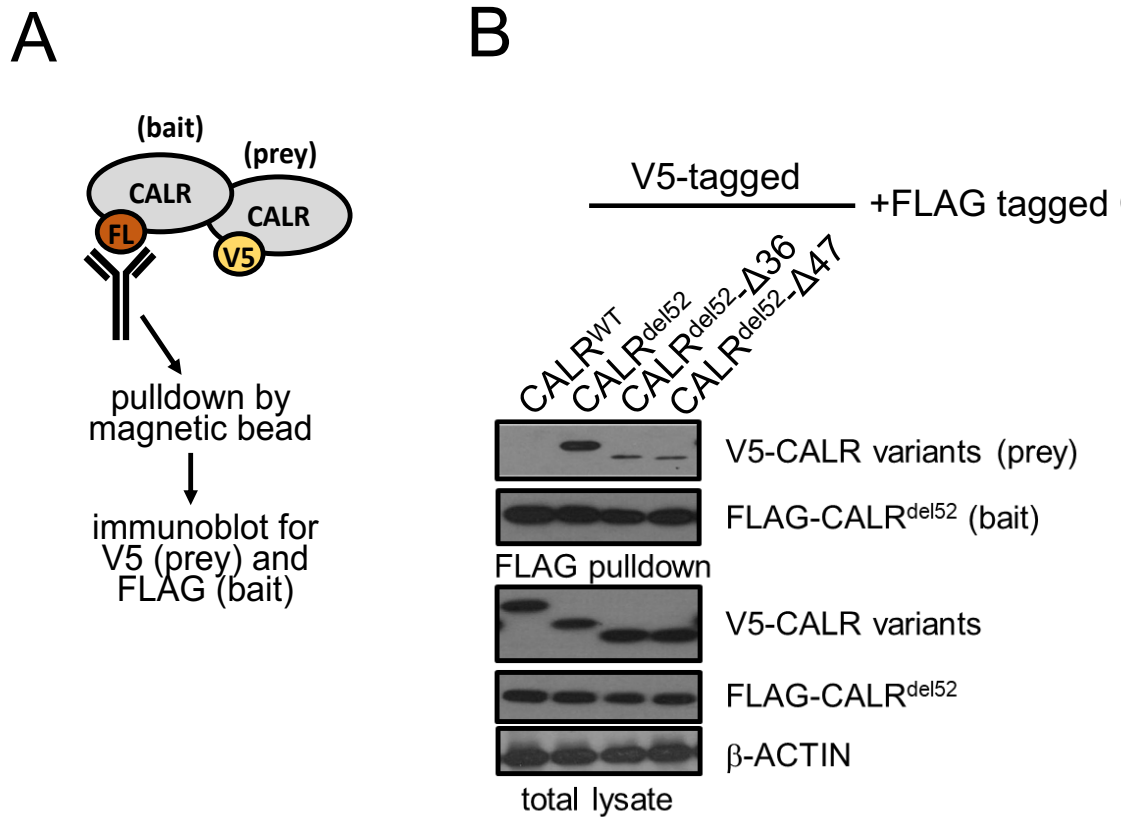


Figure 3.12 CALR^{del52} is capable of homomultimerisation. (A) Schematic depicting co-IP assay for detecting homomultimerisation of FLAG-tagged CALR variant and V5-tagged CALR^{del52}. **(B)** FLAG-pulldown assays demonstrating CALR^{del52} is capable of binding to a V5-tagged CALR^{del52} truncation mutants lacking the terminal 36 amino acids (CALR^{del52}-Δ36) or the terminal 47 amino acids (CALR^{del52}-Δ47). Results are representative of 2 independent experiments.

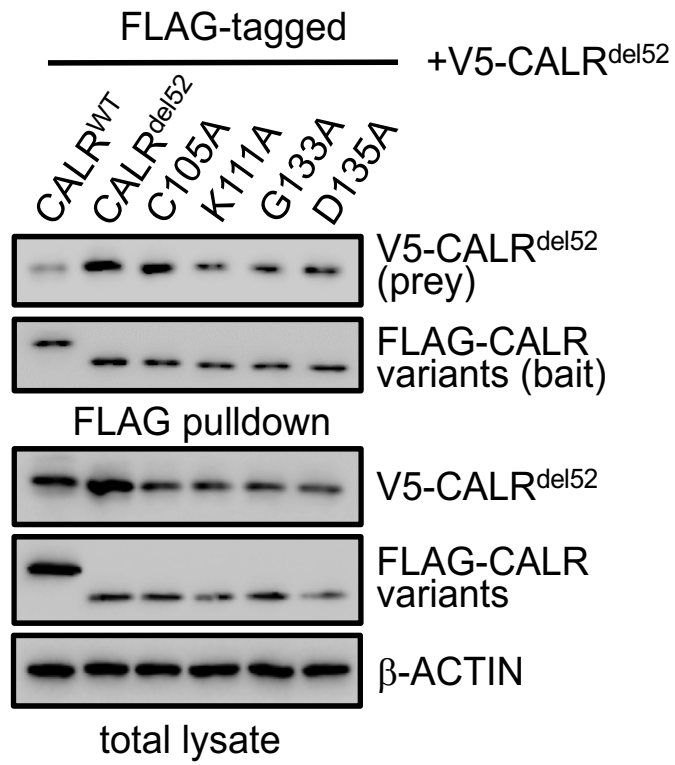


Figure 3.13 Lectin-deficient CALR^{del52} retained their ability to homomultimerise. FLAG-pulldown assays demonstrating CALR^{del52} lectin variants retain the ability to bind to V5-CALR^{del52}. Results are representative of 3 independent experiments.

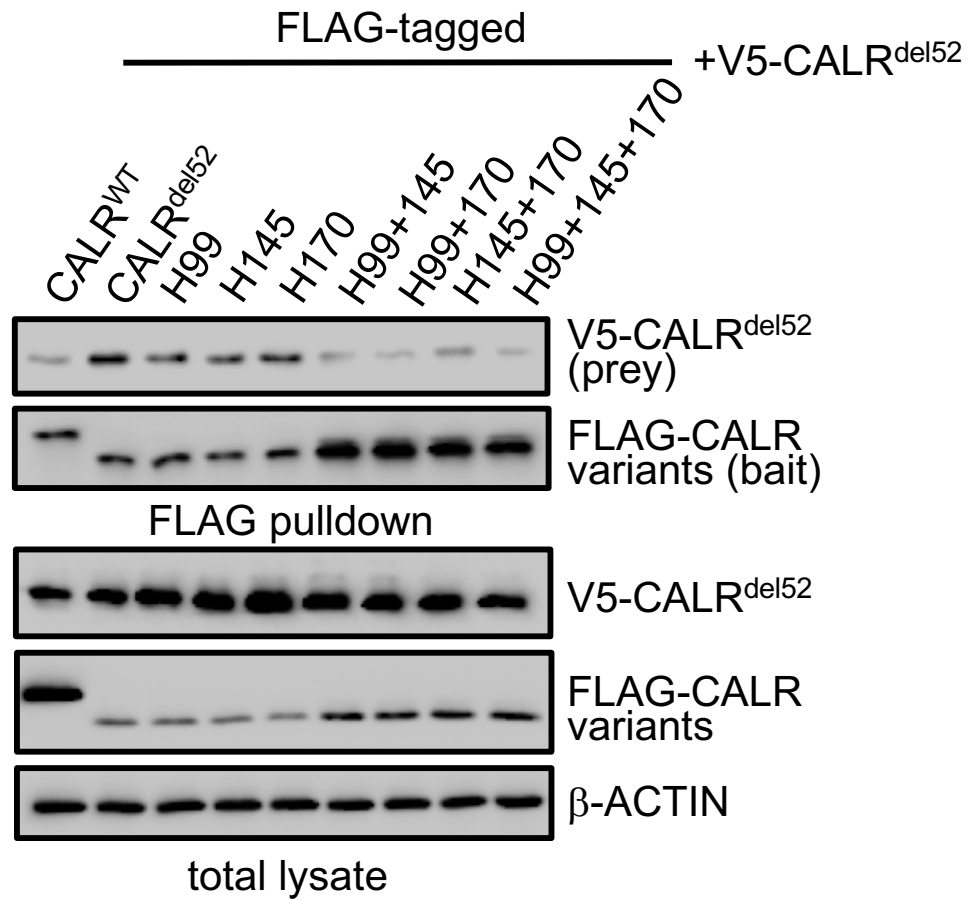


Figure 3.14 Loss of two or more histidine residues in CALR^{del52} lead to impaired homomultimerisation. FLAG-pulldown assays demonstrating 2His- and 3His-CALR^{del52} are compromised in their ability to bind V5-CALR^{del52} compared to 1His-CALR^{del52}. Results are representative of 3 independent experiments.

3.3.4. Zinc chelation impairs CALR^{del52} homomultimers and CALR^{del52}-MPL complexes

As previously stated, His99, His145 and His170 have previously been implicated in the zinc binding capacity of wildtype calreticulin. To identify if these histidine-deficient CALR^{del52} variants exhibit impaired zinc binding by affinity chromatography, cell lysates of 293T cells expressing FLAG-tagged 1His-, 2His- or 3His-CALR^{del52} variants were applied onto a zinc resin to test for the ability of histidine-deficient CALR^{del52} variants to be retained on the column. CALR^{del52} and 1His-CALR^{del52} were both able to be isolated in the zinc-resin, whereas 2His- and 3His-CALR^{del52} were not retained on the zinc column suggestive of impaired zinc binding capacity (**Figure 3.15**).

These findings led to the hypothesis that perturbation of intracellular zinc levels could affect CALR^{del52} activity. To test this, FLAG- and V5-tagged CALR^{del52} and MPL were heterologously expressed in 293T cells and were treated with agents that modulate zinc levels followed by pulldown assays to assess CALR^{del52}-MPL co-immunoprecipitation. Treatment of cells with ZnCl₂ (which increases free intracellular Zn²⁺) resulted in a modest increase in CALR^{del52} homomultimerisation in a dose-dependent manner, as well as increased MPL binding within heteromeric complexes (**Figure 3.16**). On the other hand, treatment with varying concentrations of the zinc chelator TPEN (which decreases free intracellular Zn²⁺) for 6 hours resulted in decreased CALR^{del52} homomultimer formation and decreased CALR^{del52}-MPL heteromeric complexes (**Figure 3.17**). These data suggest that modulation

of zinc levels can regulate the formation of CALR^{del52}-MPL signalling complexes

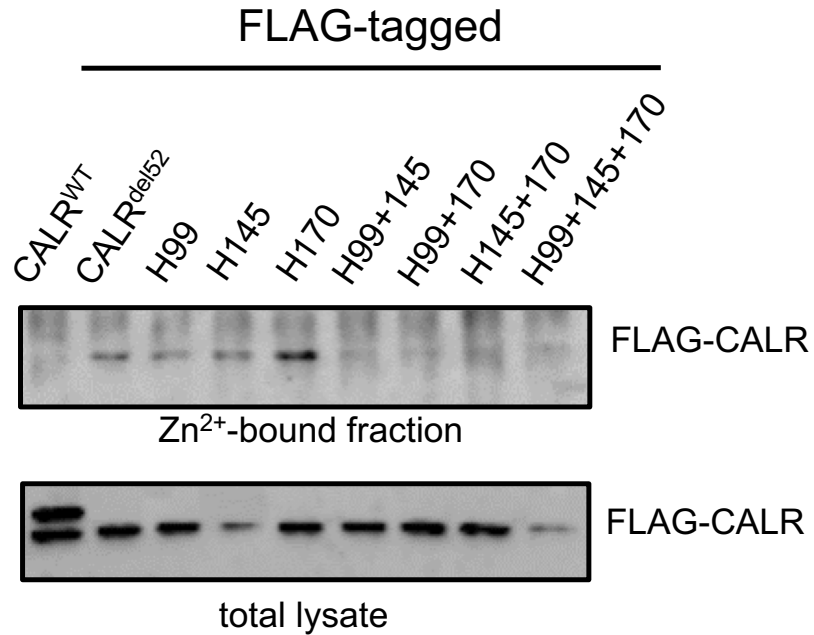


Figure 3.15 Loss of two histidine residues lead to an impairment of zinc binding. Zinc affinity pull down of 293T cells co-expressing CALR^{del52} variants demonstrates 2His- and 3His-CALR^{del52} variants are unable to bind zinc. Results are representative of 2 independent experiments.

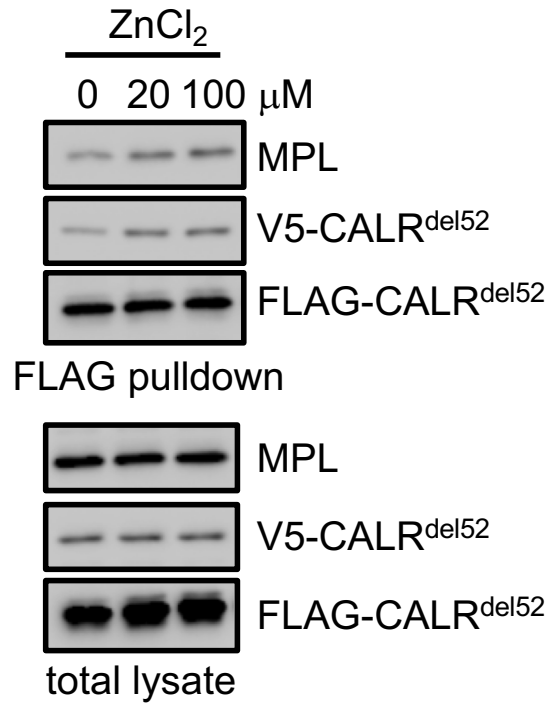


Figure 3.16 Zinc chloride enhances CALR^{del52} homomultimerisation and MPL binding. FLAG-pulldown assays demonstrating ZnCl₂ treatment enhances CALR^{del52} homomultimerisation and MPL binding in 293T cells. Results are representative of 2 independent experiments.

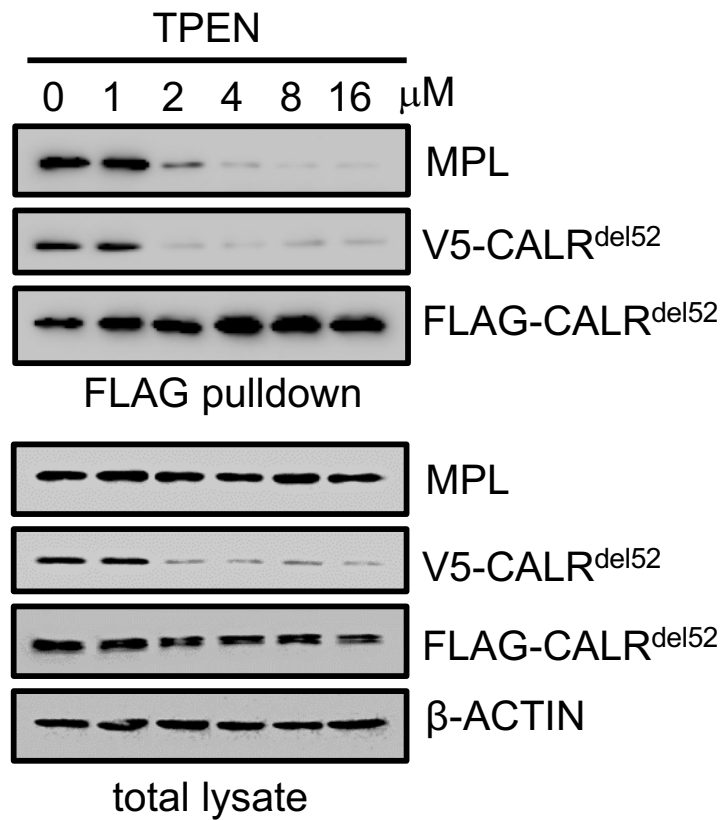


Figure 3.17 TPEN chelation diminishes CALR^{del52} homomultimerisation and MPL binding. FLAG-pulldown assays demonstrating zinc chelator TPEN treatment disrupts CALR^{del52} homomultimerisation and MPL binding in 293T cells. The data are representative of 2 independent experiments. Results are representative of 3 independent experiments.

Given these findings in 293T cells, I next tested whether zinc chelation affected formation and function of the CALR^{del52}-MPL signalling complex in hematopoietic cells. Cytokine-independent FLAG-tagged CALR^{del52}-expressing Ba/F3-MPL cells (Ba/F3-MPL-CALR^{del52}) were treated with TPEN for 4 hours and analysed for CALR^{del52}-MPL binding by co-immunoprecipitation. In line with data in transiently transfected 293T cells, zinc chelation led to decreased association between CALR^{del52} and MPL in Ba/F3-MPL-CALR^{del52} cells in a dose-dependent manner (**Figure 3.18**), in conjunction with decreased STAT3/5 phosphorylation as assessed by intracellular flow cytometry (**Figure 3.19A**) and immunoblotting (**Figure 3.19B**). Diminution of free intracellular zinc was confirmed by staining with an intracellular Zn²⁺ selective fluorescent probe zinquin (**Figure 3.20A-B**). Quantitation of pSTAT3/5 and zinc mean fluorescence intensities suggest that the extent of the pSTAT3/5 reduction was directly correlated with the levels of intracellular zinc following TPEN treatment (**Figure 3.20C**). To assess the specificity of TPEN on CALR^{del52}-associated oncogenic processes, the effect of TPEN was also tested on Ba/F3 cells transformed with an alternate MPN oncogene MPL^{W515L} (Ba/F3-MPL^{W515L}), which would be not be predicted to be dependent on zinc to facilitate complex formation for oncogenic activity. TPEN was equally effective at reducing intracellular zinc levels in Ba/F3-MPL^{W515L} cells (**Figure 3.20C top panel**). In contrast, TPEN treatment was less effective on reducing STAT3/5 phosphorylation in Ba/F3-MPL^{W515L} cells compared to Ba/F3-MPL-CALR^{del52} cells (**Figure 3.20**) and there was weaker correlation between zinc levels and pSTAT3/5 reduction (**Figure 3.20C bottom panel**). These data suggest that sensitivity

to zinc homeostasis is not a common feature of all MPN diseases but rather, is a potentially unique feature of CALR^{del52}-associated disease.

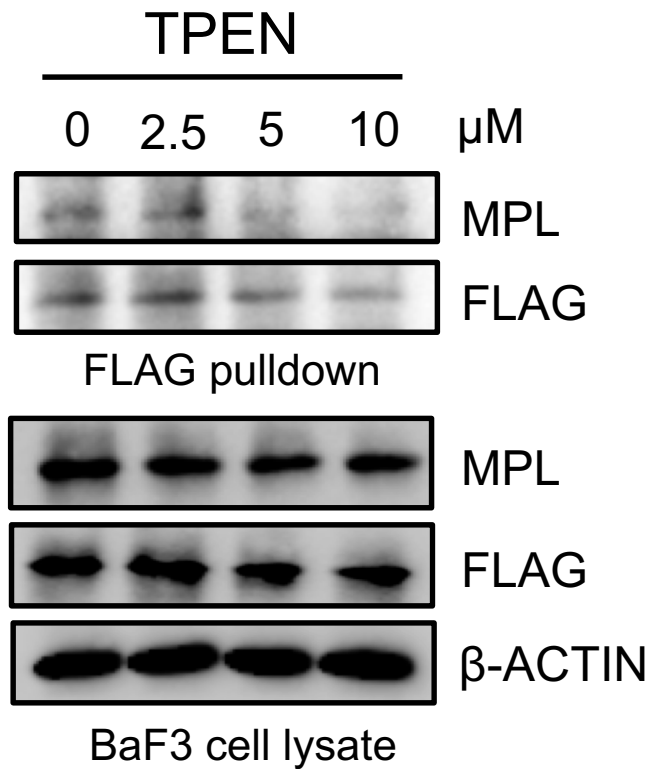
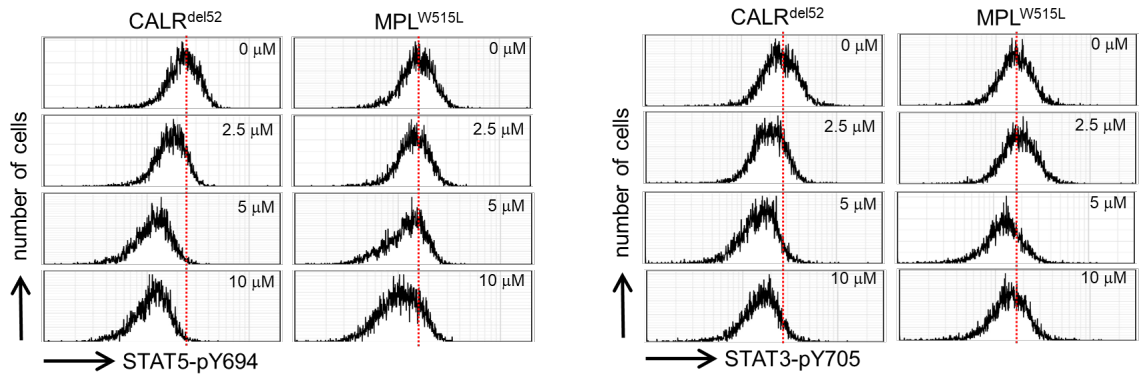


Figure 3.18 TPEN chelation in Ba/F3-MPL cells stably expressing CALR^{del52} decreases MPL binding in a dose dependent manner. Immunoblotting of FLAG-immunoprecipitated proteins and whole cell lysates from Ba/F3-MPL cells expressing CALR^{del52} demonstrates TPEN chelation disrupts CALR^{del52} homomultimerisation and MPL binding. Results are representative of 3 independent experiments.

A



B

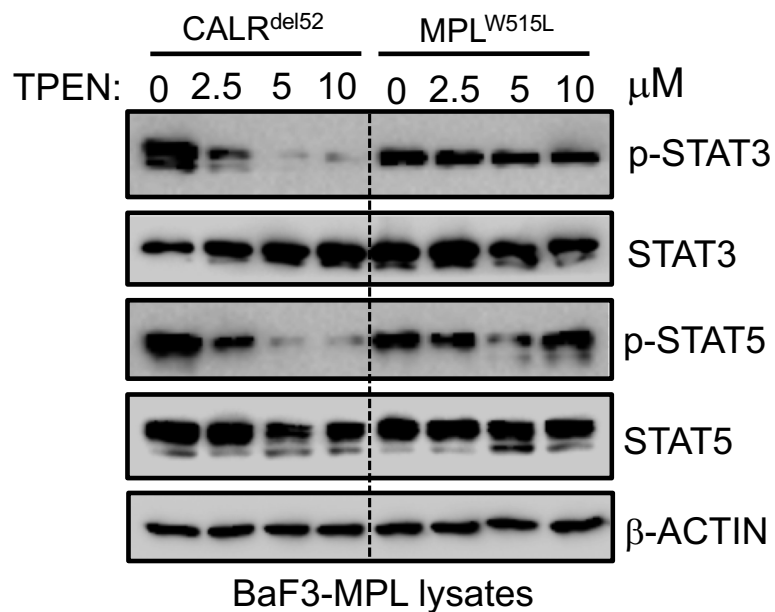


Figure 3.19 Effect of TPEN chelation on JAK-STAT signalling is specific to CALR^{del52}. (A) Intracellular phosphorylation flow cytometry analysis of pSTAT5 (left) and pSTAT3 (right) following TPEN chelation demonstrate no effect in MPL^{W515L} cells. (B) Immunoblotting of Ba/F3-MPL cells expressing CALR^{del52} or MPL^{W515L} demonstrate diminished STAT5 and STAT3 phosphorylation in response to TPEN is specific to CALR^{del52}-expressing cells. Results are representative of 3 independent experiments.

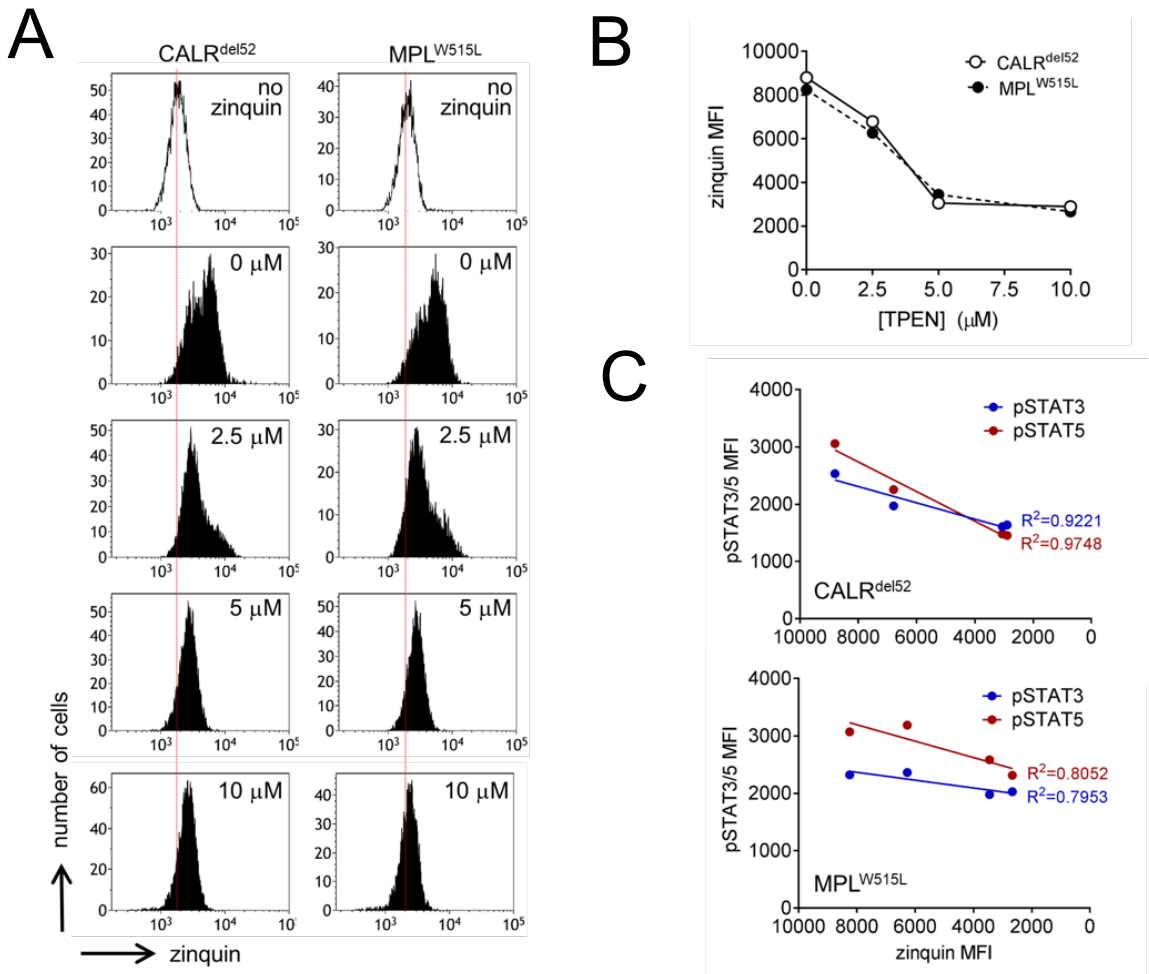


Figure 3.20 Zinc chelation abrogates CALR^{del52}-induced JAK-STAT signalling. (A) Zinquin staining quantitation of free intracellular zinc levels in TPEN-treated CALR^{del52} and MPL^{W515L} Ba/F3 cells by flow cytometry. **(B)** Correlation between zinquin mean fluorescence intensity (MFI) and TPEN dosage reveals similar extent of zinc chelation in both CALR^{del52} and MPL^{W515L} Ba/F3 cells. **(C)** Correlation between zinquin MFI and pSTAT3/5 MFI reveals strong correlation between zinc chelation and STAT3/5 signalling in CALR^{del52}-expressing Ba/F3-MPL cells and weaker correlation in Ba/F3-MPL^{W515L} cells. Results are representative of 3 independent experiments.

3.4 Discussion

Multiple studies have now provided evidence that CALR mutations leverage the MPL-JAK2 signalling axis to engender an MPN phenotype and that this is achieved by direct interaction between CALR^{del52} and the MPL extracellular domain (Chachoua et al., 2016; Elf et al., 2016; Araki et al., 2016). In this chapter, I have attempted to provide further molecular insights into how the CALR^{del52}-MPL binding event is governed.

These data confirm the essentiality of the lectin motif in CALR^{del52} oncogene function. It was somewhat surprising that residues thought to be essential for wild-type CALR lectin activity (such as Tyr109, Tyr128 and Met131) only had a partial effect on CALR^{del52} activity when mutated. A recent X-ray crystallography structural comparison suggested two surface patches in common within the lectin domain between calreticulin and calnexin, could provide a possible explanation (Chouquet et al., 2011). Specifically, although Tyr109, Tyr128 and Met131 are localised in the middle of the lectin patch, they were found to be 40-80% buried with the exception of its hydroxyl group and is positioned adjacent to Met131 and Tyr128 (**Figure 3.21A**). This may suggest that these residues contribute to the lectin motif but are less essential in certain contexts. In addition, structural analysis indicated that Cys105, Lys111 (neighbouring edge) and Gly133 and Asp135 (middle of the patch) are essential for formation of disulphide bridges and for mediating key hydrophobic contacts (Chouquet et al., 2011), which may suggest that these types of protein-protein interactions are especially important for mediating

physical interaction with MPL. Further structural analyses of this interaction is required to clarify this question.

These data also successfully reveal the novel finding that a triad of zinc-binding histidine residues within the CALR^{del52} N-domain is required for MPL binding. Consistent with this, loss of any 2 of the 3 histidine residues led to significant abrogation of the ability of CALR^{del52} to bind MPL, activate JAK-STAT signalling and ultimately confer cytokine-independent growth of Ba/F3 cells. The mechanism by which zinc acts is an essential cofactor to enable CALR^{del52} binding to MPL remains unclear. It was surprising that 2His- and 3His-CALR^{del52} molecules that lack a zinc-binding domain but still retain an intact lectin motif was nevertheless unable to bind MPL. Two potential explanations can be envisioned for this finding. One possibility is that zinc binding is required to ensure proper 3-D conformation of the lectin motif, and that the absence of zinc renders the CALR lectin motif non-functional. This explanation is unlikely to be the sole explanation however for our observations, as structural studies of wild-type CALR have shown that although zinc binding does cause significant intramolecular conformational changes that includes increased exposure of hydrophobic surfaces, *in vitro* functional assays have shown that zinc binding did not impair either its lectin activity or polypeptide-binding capacity but rather led to increased ability to suppress glycoprotein aggregation suggesting that the glycan-binding capacity is intact (Saito et al., 1999). Whether this is the case for CALR^{del52} remains to be tested. Alternatively, a second possibility is derived from our findings that zinc binding-deficient CALR^{del52} variants lose

homomultimerisation capacity. It is therefore possible that CALR^{del52} cannot bind to MPL as a monomer but rather needs to engage MPL as a multimer. Under this scenario, binding by CALR^{del52} to MPL would require both an intact lectin motif and the capacity for zinc-dependent homomultimerisation (**Figure 3.21B**). Of note, ligand multimerisation as a prerequisite for receptor activation is a common phenomenon (Marianayagam et al., 2004). For example, erythropoietin (Epo), the ligand of erythropoietin receptor, has been found to form high molecular weight species when purified (DePaolis et al., 1995; Sytkowski et al., 1998) and Epo dimers have been shown to be biologically active *in vivo* and exhibited more than 26-fold higher activity than its monomeric form.

In addition, there were several residues from the alanine mutagenesis screening that appeared to lead to over proliferation following cytokine withdrawal (**Figure 3.2**), suggesting that these residues might have a negative regulatory role in conferring MPL activation. Due to time constraints, these residues were not followed up, but may warrant further investigation.

Finally, these findings have also potential therapeutic implications. These data suggest that drugs which can modulate intracellular zinc levels could be a potentially novel avenue for MPN therapy. Additionally, these data also suggest that inhibition of MPL binding by CALR^{del52} can also be mediated by inhibition of impairing the capacity of CALR^{del52} to homomultimerise, and proteins which can affect the rate of multimerisation could also be an effective therapeutic strategy.

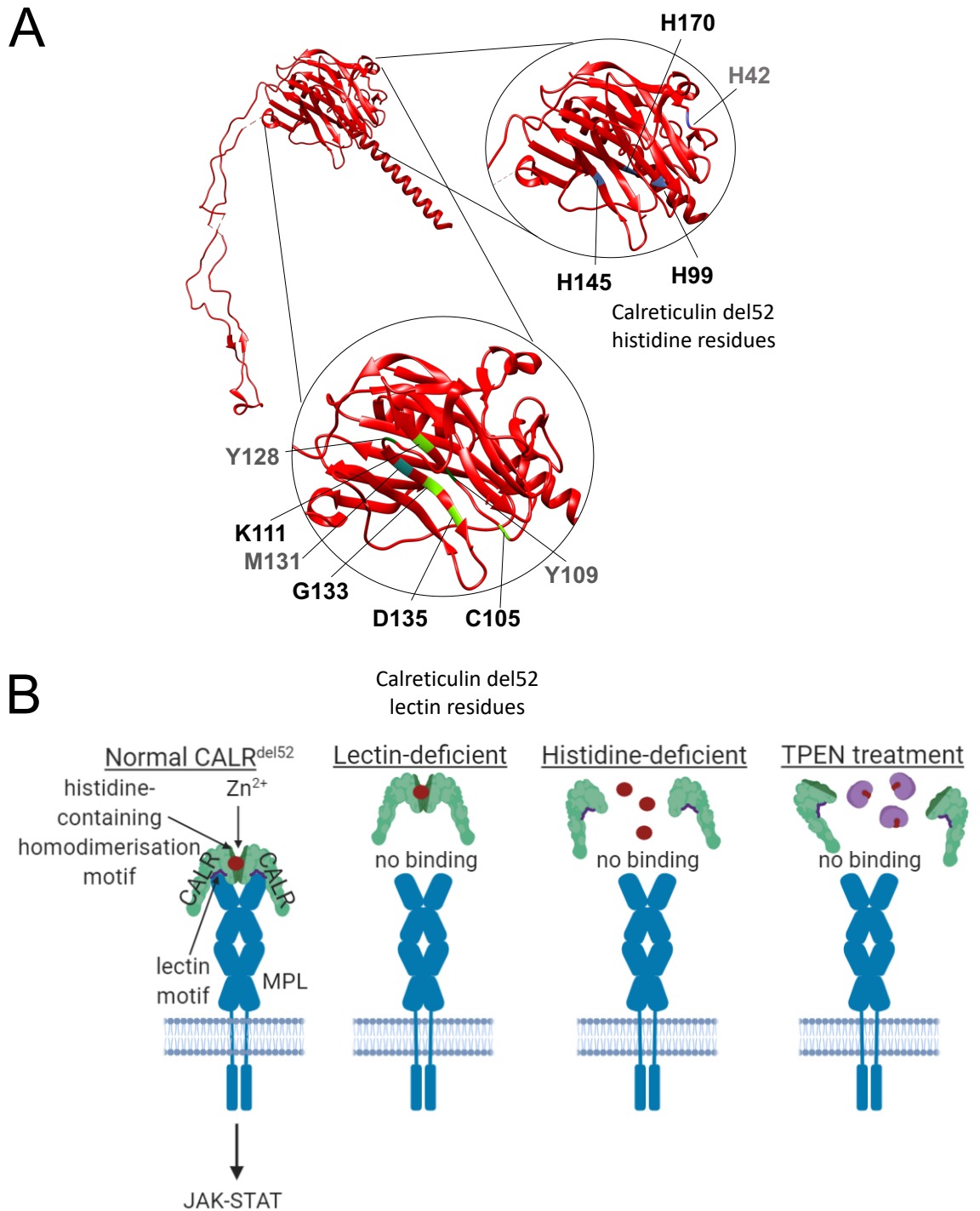


Figure 3.21 Schematic representation of the predicted mechanisms of CALR^{del52} and variants in MPL binding. (A) 3D structure of wildtype calreticulin (from (Blees et al., 2017)) showing positions of histidine and lectin residues within the globular domain. (B) Schematic depiction of role of zinc in mediating interplay between CALR^{del52} multimerization and MPL binding.

Chapter 4

Mutant calreticulin requires Tyr-626 of the thrombopoietin receptor, MPL for oncogenic transformation

Chapter 4

Mutant calreticulin requires Tyr-626 of the thrombopoietin receptor, MPL for oncogenic transformation

4.1 Introduction

The thrombopoietin receptor MPL plays an essential role in megakaryopoiesis and regulating HSC self-renewal, and aberrant activation of MPL signalling results in MPN. Specifically, activating mutations in MPL have been observed in ~5% of ET and PMF patients (Pikman 2006), and co-expression of MPL can support JAK2V617F- and CALR^{del52}-associated oncogenic activity.

Wild-type MPL is activated through binding to its cognate ligand thrombopoietin (TPO) on its extracellular domain, which causes a reorientation of the receptor's transmembrane (TM) and intracellular domains that results in conformational changes leading to receptor activation (**Figure 4.1**) (Varghese et al., 2017). MPL shares homology to other members of the type I cytokine receptor family such as Epo receptor (EpoR) and GCSF receptors (GCSFR) (Geddis et al., 2002; Vigon et al., 1992). The MPL receptor consists of three functional domains: (i) a large extracellular domain that allows binding of ligand at a receptor subunit: ligand stoichiometric ratio of 2:1; (ii) a single-pass membrane spanning transmembrane domain; and (iii) a cytoplasmic/intracellular domain that act as docking sites for JAK binding and various other signalling molecules like STATs.

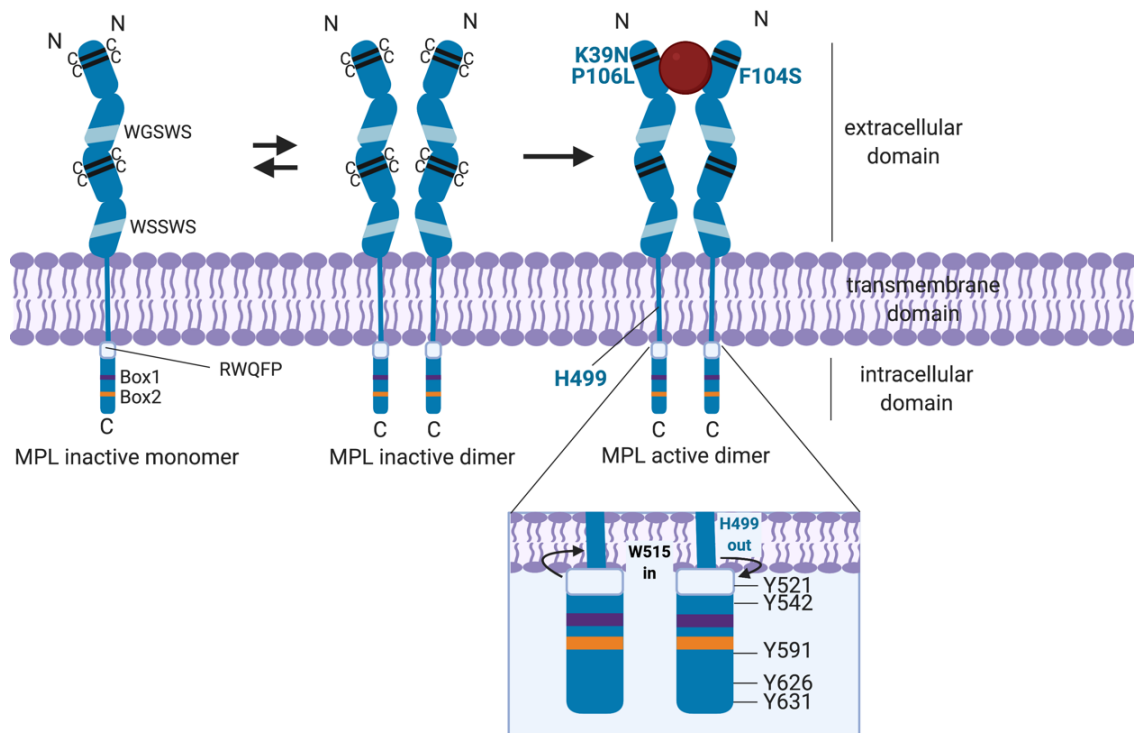


Figure 4.1 Mechanisms of MPL activation. Membrane distal extracellular domain, H499 and the RWQFP motif play vital roles in preventing self-activation in the absence of ligand. H499 creates a break in the helical extracellular juxtamembrane and the TM domain to prevent oncogenic activation and regulate homodimerisation. W515 anchors in the TM domain and is oriented outside of the dimer interface in the opposite direction of H499. In active dimeric state of MPL or upon activating mutations such as W515L or S505N (not shown), W515 is rotated “in” and H499 is rotated “out” leading to JAK2 recruitment and subsequent phosphorylation of tyrosine residues within the intracellular domain of MPL. F104S mutation leads to a defect in TPO binding. K39N or P106L leads to low level MPL cell surface localisation and inability to efficiently clear TPO from circulation. Conserved Box1, Box2 and tyrosine residues are shown above.

4.1.1 Extracellular domain

The extracellular domain (ECD) of the MPL receptor is composed of two copies of cytokine receptor modules (CRM), each of which is composed of a fibronectin-III-like (FNIII) domains characterised by four conserved cysteine residues, a hinge region and a WSXWS motif. The membrane distal CRM (CRM-1) is thought to be primarily responsible for interaction with TPO ligand, as its deletion or replacement with the membrane-proximal CRM (CRM-2) creates a mutant MPL that is incapable of cytokine binding and interaction with TPO (Deane et al., 1997; Sabath et al., 1999). What the role of CRM-2 is in modulating CRM-1 activity and MPL signalling overall remains unclear.

Mutations in the MPL ECD are associated with multiple platelet disorders. Congenital amegakaryocytic thrombocytopaenia (CAMT) is a rare blood disorder characterised by platelet and MK deficiency that have been shown to be caused by inherited mutations in the MPL ECD (Muraoka et al., 1997; Ballmaier et al., 2001; Ihara et al., 1999). The F104S mutation disrupts the membrane distal FNIII-like domain of CRM-1 and has been shown to disrupt the ligand binding site and Ba/F3 cells expressing MPL^{F104S} are unresponsive to TPO stimulation (Fox et al., 2010). Other cases of MPL ECD mutations in CAMT patients also include mutations that affect F45, R102, L103 and P257. Paradoxically, mutations of the MPL ECD have also been identified that lead to reduced global and cell surface expression of MPL, but are associated with thrombocytosis and elevated platelet counts. Specifically, mutation of residue K39N identified in ~7% of African-American populations and of residue P106L seen in a low frequency in Arab populations, causes reduced protein expression in patient-derived

platelets and in Ba/F3 cells but leads to a hereditary thrombocytosis (Molitero et al., 2004; El-Harith et al., 2009; Varghese et al., 2017). The mechanism of how these MPL ECD mutations drive thrombocytosis are not fully understood.

4.1.2 Transmembrane domain

The transmembrane (TM) domain of MPL is responsible for anchoring the receptor to the cell surface. In addition, this domain also plays critical roles in mediating various aspects of receptor activation, including regulating receptor dimerisation and undergoing conformational changes that are necessary for receptor activation (Leroy et al., 2016). The ability of the MPL TM domain to regulate MPL activation principally lies in two sequences which keep MPL inactive in the absence of ligand stimulation. Firstly, a 5-residue amphipathic helical motif RWQFP that is adjacent to the C-terminal tail of the TM domain is critical for keeping the receptor inactive by acting as an anchor in the TM domain to maintain a tilt relative to the lipid bilayer structure that keeps the receptor in an inactive orientation in the absence of ligand (Varghese et al., 2017). Deletion of the motif results in constitutive receptor activation (Staerk et al., 2006). In addition, the MPN-associated W515 mutations that are associated with aberrantly active MPL (described in Section 1.4.3.3) directly disrupts this motif and has been shown by NMR to decrease the tilt angle relative to the lipid bilayer, resulting in an active conformation of the MPL dimer (Defour et al., 2013). Secondly, the H499 residue which lies near the N-terminus of the TM domain is inhibitory to receptor dimerisation. Deuterium-NMR analysis showed that in the absence of ligand stimulation, H499 introduces a kink in the TM helix which negatively influenced the potential for TM domains to dimerise, compared to

murine MPL TM domains (which do not have a H499 paralogue) or a mutated hMPL-TM-H499L variant (Leroy et al., 2016). Furthermore, treatment with eltrombopag (which binds directly to H499) induced a modest increase in hMPL TM domain dimerisation.

4.1.3 Cytoplasmic domain

The intracellular/cytoplasmic domain of MPL that extends into the cytoplasm is the region where signalling intermediates such as JAK2 tyrosine kinases are constitutively bound to act as signal transducers, or where other intracellular proteins such as STATs can be recruited to be phosphorylated.

The intracellular domain of MPL share two conserved elements: Box1 and Box2. Box1 contains a PxxP motif and is required for JAK2 binding, while the function of Box2 remains unclear. In addition, there are three key cytoplasmic tyrosine residues (Tyr591, Tyr626 and Tyr631) located in the intracellular domain that when phosphorylated, can act as docking sites for the SH2-domain-containing proteins, primarily STATs, MAPK, PI3K, protein kinase C (PKC) and LNK to promote cell proliferation and cell survival (Drachman et al., 1995; Rojnuckarin et al., 1999) (**Figure 4.2**). Upon receptor activation, MPL conformational change leads to juxtaposition of Box1-bound JAK2 molecules and trans-autophosphorylation of JAK2 followed by phosphorylation of one or more tyrosine residues within the MPL cytoplasmic domain.

Previous studies have shown that Tyr626 and Tyr631 are essential tyrosine residues that functions as positive regulatory sites for transmitting MPL signals. Mutagenesis studies confirmed that these residues are essential for MPL-mediated STAT3 phosphorylation (and to a lesser extent STAT5) in response to TPO, and acted as critical docking sites for SH2-containing signalling proteins (Drachman et al., 1995). The murine homologue of Tyr626 (Y599) has also been shown to be required for cellular differentiation since abolishment of this residue leads to impaired TPO-dependent Shc phosphorylation and Grb2-Ras signalling (Alexander et al., 1995; Bouscary et al., 2001). Furthermore, Tyr626 is also necessary as a mediator in driving the MPN phenotype. MPL hyperactivation induced by JAK2V617F and MPLW515A was dependent on signalling by Tyr626 (Pecquet et al., 2010), and Tyr626 was found to be required for TPO-independent colony-forming unit megakaryocytes (CFU-Mk) following MPLW515L expression (Yu et al., 2016).

Tyr591 is also phosphorylated in response to TPO (Sangkhae et al., 2014) but has been implicated in the negative regulation of TPO signalling (Hitchcock et al., 2008). MPL variants in which Tyr591 was substituted with phenylalanine conferred a proliferative advantage to Ba/F3 cells in response to TPO. A protein microarray screen of SH2 domain-containing proteins identified spleen tyrosine kinase (SYK) as a Tyr591 binding partner (Sangkhae et al., 2014)(Sangkhae et al., 2014), where it functions as a negative regulator to dampen ERK1/2 signalling (Sangkhae et al., 2014).

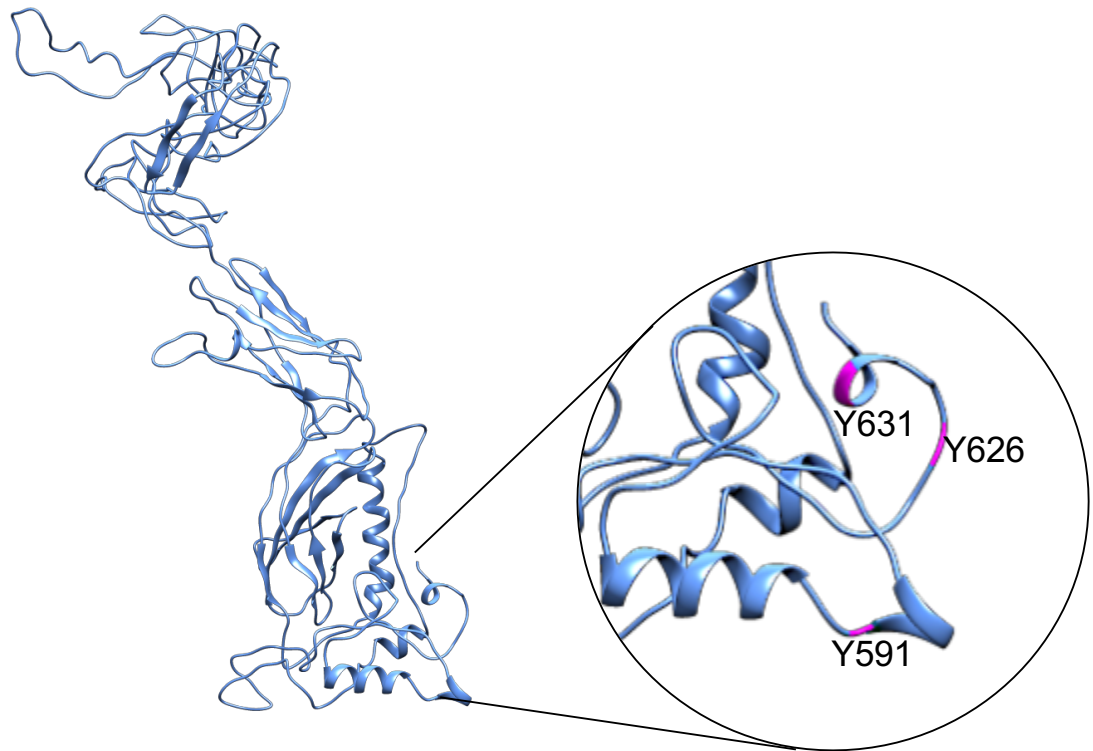


Figure 4.2 Predicted MPL structure using Phyre2 analysis. Residues in pink indicate localisation of tyrosine residues Tyr591, Tyr626 and Tyr631.

4.2 Aims and Hypothesis

Co-expression of wild-type MPL is required in order for CALR^{del52} to transform cells, but it remains unclear which regions of MPL are necessary and sufficient to support this activity. I hypothesise that key regions of MPL exist which are crucial to support cell transformation by CALR^{del52}, which can be uncovered by mutagenesis of potentially critical MPL regions or residues. In this chapter, I will discuss results associated with these aims:

- I. Test the role of MPL intracellular domain tyrosine (Y) residues (Tyr591, Tyr626 and Tyr631) in supporting CALR^{del52} oncogenic activity, using Ba/F3 cytokine-independence assays, activation of JAK-STAT signalling and ability to interact in co-immunoprecipitation assays.
- II. Test the role of CAMT- and hereditary thrombocytosis-associated lesions in MPL extracellular domain (F104S, K39N, P106L) in supporting CALR^{del52} oncogenic activity, using similar assays described in Aim 1.
- III. Test the role of MPL transmembrane domain residue (H499) in supporting CALR^{del52} oncogenic activity, using similar assays described in Aim 1.

4.3 Results

4.3.1 Tyrosine 626 (Tyr626) of the intracellular domain of MPL is critical for CALR^{del52}-mediated transformation

To test the role of MPL intracellular tyrosine residues Tyr591, Tyr626 and Tyr631 in supporting CALR^{del52} oncogenic activity, MPL variants were generated by site-directed mutagenesis where all 3 candidate tyrosine (Y) residues were mutated to phenylalanine (F). Presence of all 3 mutations on the MPL cDNA (Tyr591F/Tyr626F/Tyr631F) (referred hereafter as FFF) was confirmed by Sanger sequencing. Murine IL3 (mIL3)-dependent Ba/F3 cells were co-infected with lentiviruses expressing CALR^{del52} in conjunction with empty lentiviruses (EV), lentiviruses expressing wild-type MPL (YYY) or lentiviruses expressing the triple-mutated MPL (FFF), and the cell growth was monitored for 4 days following mIL3 withdrawal. As expected, absence of MPL co-expression failed to support cytokine independence in the presence of CALR^{del52}, whereas wildtype MPL could support cytokine independence. Strikingly, the MPL-FFF variant demonstrated complete inability to support cytokine-independent growth (**Figure 4.3**). These results indicate that at least one of these 3 tyrosine residues is required for oncogenic transformation of Ba/F3 cells driven by CALR^{del52}. This initial finding prompted further investigations on the specific contribution of individual tyrosine residues.

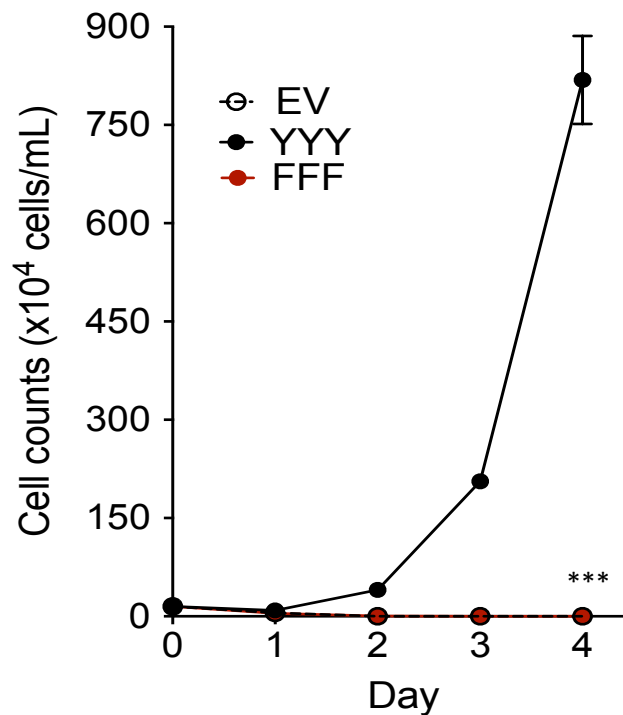


Figure 4.3 Tyr591/626/631 of MPL are required to support CALR^{del52}-induced cytokine independence. Growth curves in Ba/F3 cells stably expressing wild-type MPL (YYY) and MPL variant mutated for Tyr591/626/631 (FFF) four days post-cytokine withdrawal. Error bars denote standard error. Testing for statistical significance was performed using a student's t-test (***: p<0.001). Results are representative of 3 independent experiments.

Therefore, I next generated MPL variants where these three tyrosine (Y) residues were systematically mutated to phenylalanine (F) individually to create single-tyrosine mutants or in tandem to create double-tyrosine mutants. Introduction of correct mutations was confirmed by Sanger sequencing. All MPL variants were expressed in 293T cells and found to physically interact with CALR^{del52} in FLAG-pulldown assays (**Figure 4.4**), consistent with the fact that MPL binding to CALR^{del52} is independent of the intracellular domain. Despite their capacity to bind CALR^{del52}, I tested if these MPL variants were still able to be fully activated by CALR^{del52} by assessing transformation of Ba/F3 cells as above. Analysis of single-tyrosine variants showed that loss of Tyr591 or Tyr631 had no effect on MPL ability to support CALR^{del52} activity, whereas loss of Tyr626 resulted in significant impairment in the ability of MPL to support cellular transformation (**Figure 4.5A**). These findings were corroborated by analysis of the double-tyrosine variants. Double variants in which Tyr626 was disrupted (Tyr591/626 and Tyr626/631) demonstrated an inability to confer cytokine-independence (**Figure 4.5B**). In contrast, a double mutant in which Tyr626 is intact (Tyr591/Tyr631) showed only a partial impairment. Finally, in accord with previous data, triple variants in which all three residues are disrupted (Tyr591/626/631) exhibited no cytokine-independent growth (**Figure 4.5C**). Finally, I next tested whether the capacity for cytokine-independent growth correlated with aberrant JAK-STAT signalling by analysis of levels of phosphorylated STAT5 (pSTAT5) by immunoblotting. Robust STAT5 phosphorylation was a feature of cells expressing intact Tyr626 but was attenuated in variants lacking intact Tyr626 (**Figure 4.6**). Cumulatively, these data suggest that Tyr626 is the key tyrosine residue required to support CALR^{del52}-mediated growth.

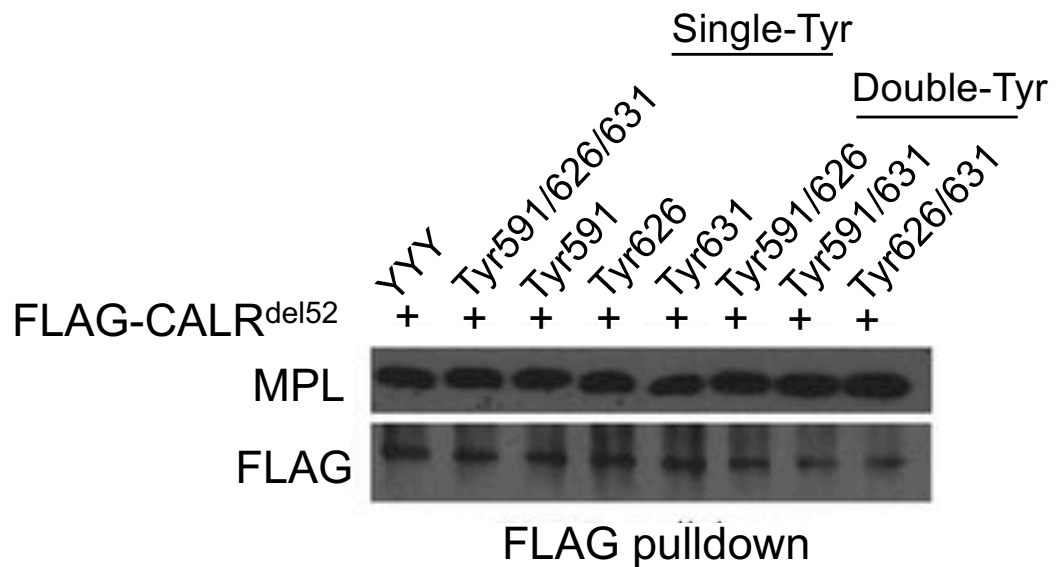


Figure 4.4 MPL tyrosine variants can bind to CALR^{del52}. Immunoblotting of FLAG immunoprecipitated proteins from 293T cells co-expressing FLAG-tagged CALR^{del52} and MPL tyrosine variants demonstrates that mutations of intracellular tyrosine residues on MPL does not affect the ability of CALR^{del52} to bind to MPL. Results are representative of 3 independent experiments.

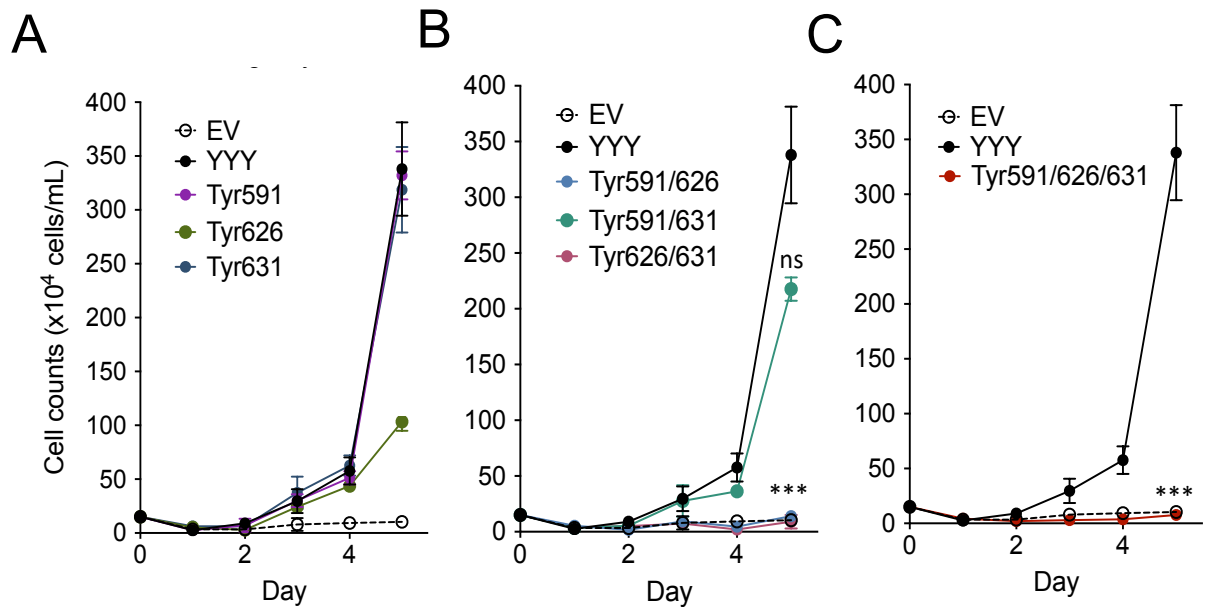


Figure 4.5 Loss of Tyr626 abolishes the ability of MPL to support cytokine independent growth by CALR^{del52}. Growth curves of Ba/F3 cells stably expressing single (A), double (B) and triple (C) MPL tyrosine variants for a period of five days following cytokine (IL-3) withdrawal. Error bars denote standard error. Testing for statistical significance was performed using a student's t-test (ns: no significance, ***: p<0.001). Results are representative of 3 independent experiments.

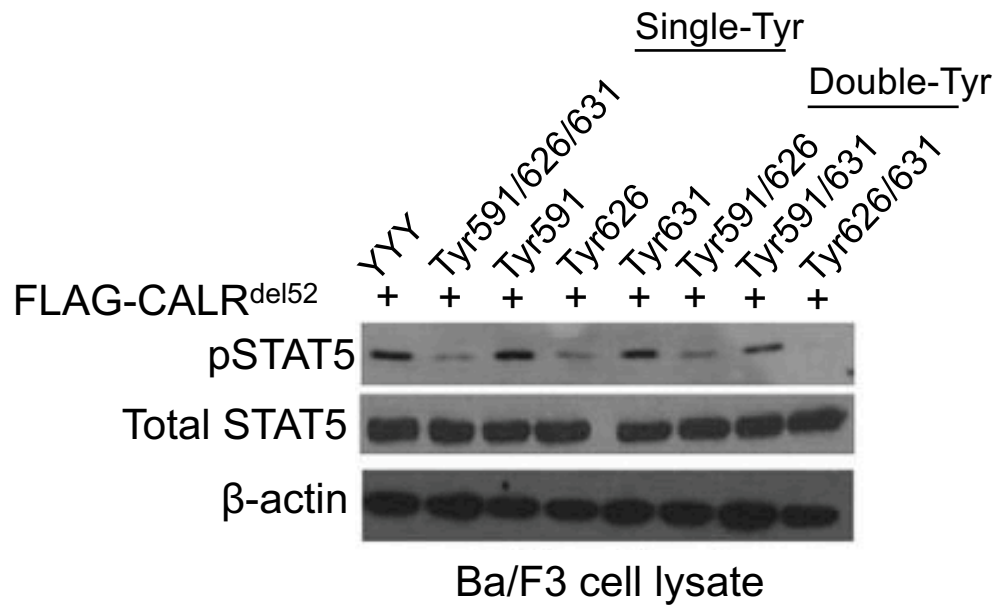


Figure 4.6 Loss of Tyr626 leads to attenuation of pSTAT5 levels. Ba/F3 cells stably co-expressed with MPL tyrosine variants and FLAG-tagged CALR^{del52} demonstrate phosphorylated STAT5 levels were abrogated in cells expressing MPL harbouring loss of Tyr626. Results are representative of 3 independent experiments.

4.3.2 Loss of TPO- and eltrombopag-binding sites does not affect the ability of MPL to support CALR^{del52}-mediated transformation

The previous analysis examined the role of intracellular tyrosines within MPL in transmitting CALR^{del52}-associated oncogenic signals. I next tested whether other residues within MPL, especially within the extracellular domain and in the transmembrane motif, also played a significant role in the ability of MPL to support cytokine independent growth and cellular transformation.

MPL variants were generated harbouring CAMT-associated mutation (F104S), thrombocytosis-associated mutations that decrease the cell surface expression of MPL (K39N, P106L) and the essential transmembrane residue H499 (H499A). Co-immunoprecipitation experiments in 293T cells revealed MPL harbouring K39N, F104S, P106L mutations were able to physically interact with CALR^{del52} in FLAG-pulldown assays, while H499A exhibited weaker binding with CALR^{del52} (**Figure 4.7**). I next proceeded to assess the ability of these variants to support cytokine-independence in Ba/F3 cells in conjunction with CALR^{del52}. Loss of any of these residues did not perturb MPL's ability to support cytokine-independent growth following IL-3 withdrawal (**Figure 4.8**), nor did it have any effect on the ability to induce STAT3/5 phosphorylation (**Figure 4.9**).

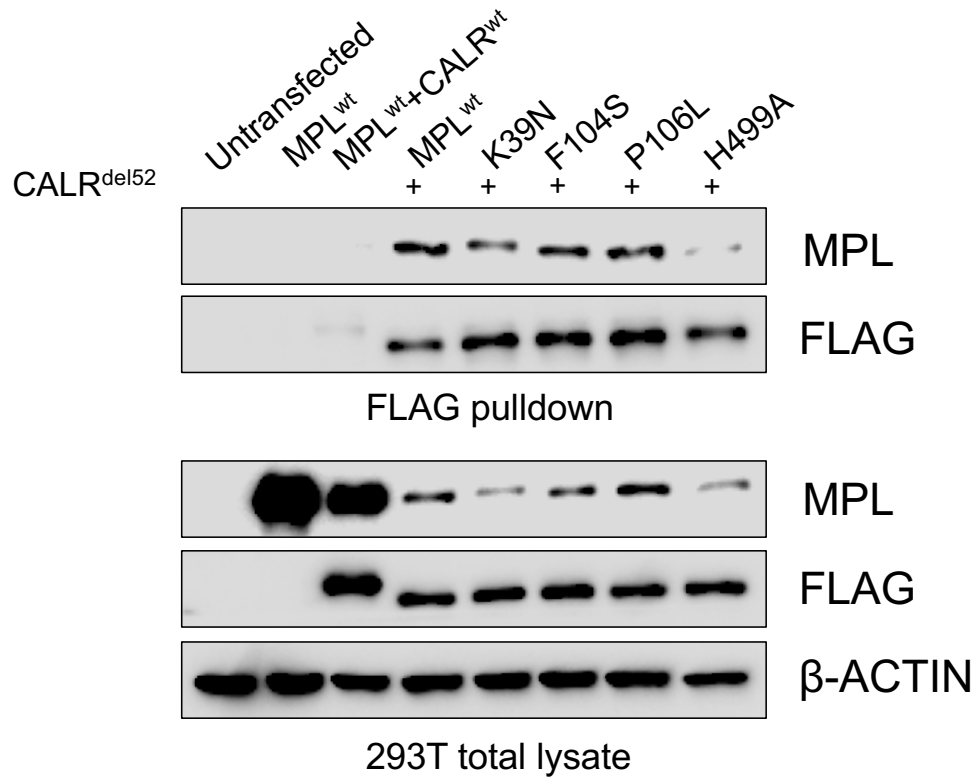


Figure 4.7 MPL variants associated with loss of TPO- and eltrombopag-binding sites does not affect MPL binding capacity to CALR^{del52}. FLAG immunoprecipitated proteins from 293T cells co-expressing FLAG-tagged CALR^{del52} and MPL K39N, F104S and P106L mutants demonstrate no affect in the ability of CALR^{del52} to bind to MPL. Decreased binding between CALR^{del52} and MPL H499A mutants was observed. Results are representative of 2 independent experiments.

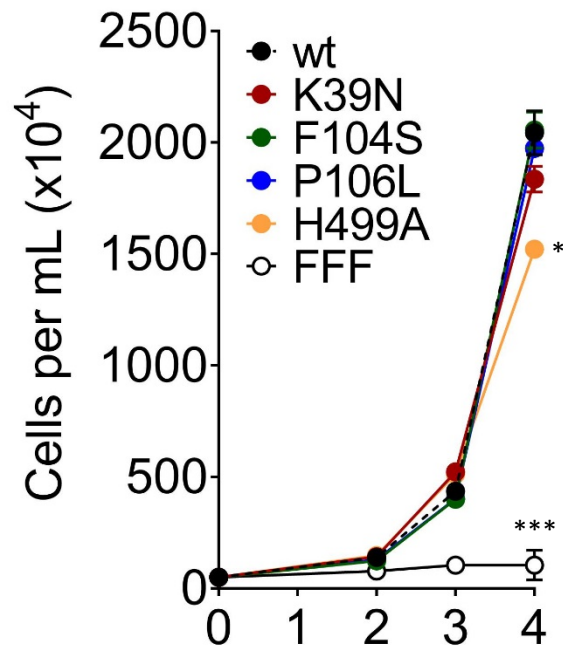


Figure 4.8 MPL variants associated with loss of TPO- and eltrombopag-binding sites does not affect capacity to support CALR^{del52} cellular transformation. Growth curves of Ba/F3 cells stably expressing wild-type MPL and MPL K39N, F104S, P106L and H499A mutants and CALR^{del52} for a period of four days following cytokine (IL-3) withdrawal. Error bars denote standard error. Testing for statistical significance was performed using a student's t-test (*: $p < 0.05$, ***: $p < 0.001$). Results are representative of 2 independent experiments.

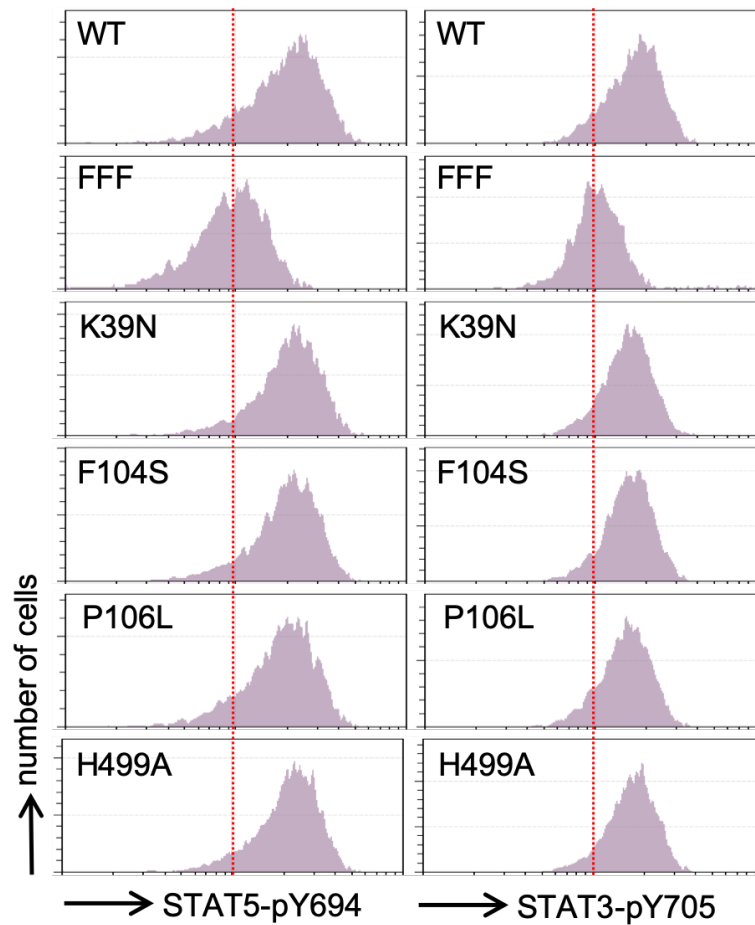


Figure 4.9. MPL variants associated with loss of TPO- and eltrombopag-binding sites does not affect capacity to activate JAK-STAT signalling. Intracellular phospho-flow analysis of pSTAT3/5 demonstrate no significant differences between MPL K39N, F104S, P106L and H499A variants compared to wildtype MPL. Results are representative of one experiment.

4.4 Discussion

Upon ligand binding, the thrombopoietin receptor MPL activates one or more intracellular tyrosine kinases and results in rapid tyrosine phosphorylation of tyrosine residues within its intracellular domain to recruit various STAT proteins such as STAT1, STAT3 and STAT5 (Sattler et al., 1995; Drachman et al., 1995). Following the discovery of MPL mutations as a driver mutation of MPNs as well as its necessity in supporting CALR^{del52}-mediated transformation, there has been significant effort in identifying the precise mechanisms of MPL activation leading to an MPN phenotype. Analysis of functional domains of MPL identified various residues associated with normal TPO signalling (Pecquet et al., 2010; Sangkhae et al., 2014), but it remained unclear which of these (if any) were essential in mediating CALR^{del52}-associated oncogenic signalling.

These data demonstrate a significant contributory role for three tyrosine residues (Tyr591, Tyr626 and Tyr631) localised within the intracellular domain of MPL in supporting CALR^{del52} cellular transformation. By systematically mutating each individual tyrosine residue into phenylalanine in combination, it was deduced that Tyr626 was the essential residue responsible for transmitting CALR^{del52} signals *via* MPL, while Tyr591 and Tyr631 had minor roles in mediating CALR^{del52} signalling. Of note, none of the MPL tyrosine variants analysed resulted in any difference in the ability to physically interact with CALR^{del52}, which is consistent with previous findings that CALR^{del52} binds to MPL on the extracellular domain (Elf et al., 2018). Previous findings investigating the role of Tyr626 also found a central role for it in mediating TPO-dependent signal transduction (Drachman et al., 1995; Staerk et al., 2012) and is absolutely required for STAT3/5 activation.

These data are therefore consistent with a model where CALR^{del52} co-opts canonical MPL activation pathways, by using the same intracellular tyrosine residues as in normal TPO-MPL signalling.

Evidence in literature suggest that Tyr591 is a potential negative regulator of JAK-STAT signalling downstream of MPL, and therefore its minimal contributory role in mediating CALR^{del52} activity is perhaps not surprising. It has been proposed that Tyr591 binds to negative regulatory molecules or trigger receptor internalisation (Hitchcock et al., 2008; Hitchcock et al., 2014), but this negative regulatory activity is insufficient to inhibit the oncogenic consequences and receptor conformational changes induced by MPL^{W515L} mutations. A similar process may be in play in the context of CALR^{del52} where Tyr591 negative regulatory effects may have been overcome by other signalling pathways activated by CALR^{del52} upon binding to MPL (**Figure 4.10**). The exact nature of the crosstalk between Tyr591 and Tyr626 in supporting CALR^{del52} oncogenic activity will likely require further investigation.

Finally, in addition to the tyrosine residues within the intracellular domain, this study also tested numerous residues that exert their functionality in other domains of MPL, including the ligand binding site in the extracellular domain (F104S), in mediating receptor turnover (K39N and P106L) and the binding site for eltrombopag in the transmembrane domain (H499). These data show that loss of any of these residues did not impair the ability of the MPL variant to bind MPL or support CALR^{del52} mediated cellular transformation. These findings have multiple implications. Firstly, this data suggests that the CALR^{del52} binding site

does not overlap with the TPO binding site. This is consistent with previous data where ablation of a putative TPO binding site on MPL (D235/L239) also failed to disrupt its ability to support CALR^{del52} activity (Elf et al., 2018). Secondly, this data also suggests that CALR^{del52} does not act like an eltrombopag mimetic. Eltrombopag is a potent stimulator of megakaryopoiesis that works by binding to H499 within the MPL transmembrane motif to stimulate receptor dimerisation and activation. It is a first-in-class treatment for various bone marrow failure disorders, such as aplastic anaemia. These data shows that loss of H499 (the binding site for eltrombopag) does not curtail the ability of MPL to support CALR^{del52} activity. This also provides evidence of an important distinction between the mechanisms of action between CALR^{del52} and MPL^{W515L}, where loss of H499 is capable of abrogating oncogenic activation of MPL^{W515L}. That the activated MPL receptor is potentially qualitatively different in CALR^{del52}-mutated vs MPL^{W515L}-mutated MPN could have important clinical implications in the design of therapeutic strategies to disrupt MPL signalling.

Cumulatively, the findings presented in Chapters 3 and 4 could be potentially important in the development of therapeutic strategies for mutant CALR-positive MPN. For example, the data in Chapter 3 suggest that zinc chelation could be a novel treatment modality for CALR-mutated MPNs, and the data in Chapter 4 highlight the significance of Tyr626 in CALR^{del52} pathogenesis and suggest that antibodies that detect Tyr626 in MPN cells and could activate T cells and induce a cytotoxic response could be an exploitable strategy. However, in order to rationally design therapies that target the precise nature of the CALR^{del52} and MPL interaction, further structural studies that can reveal the precise nature of

the CALR^{del52}-MPL interaction at the atomic level are crucial. These insights could facilitate therapies involving the design of antibodies, affimers or nanobodies that are able to specifically target CALR-mutant cells.

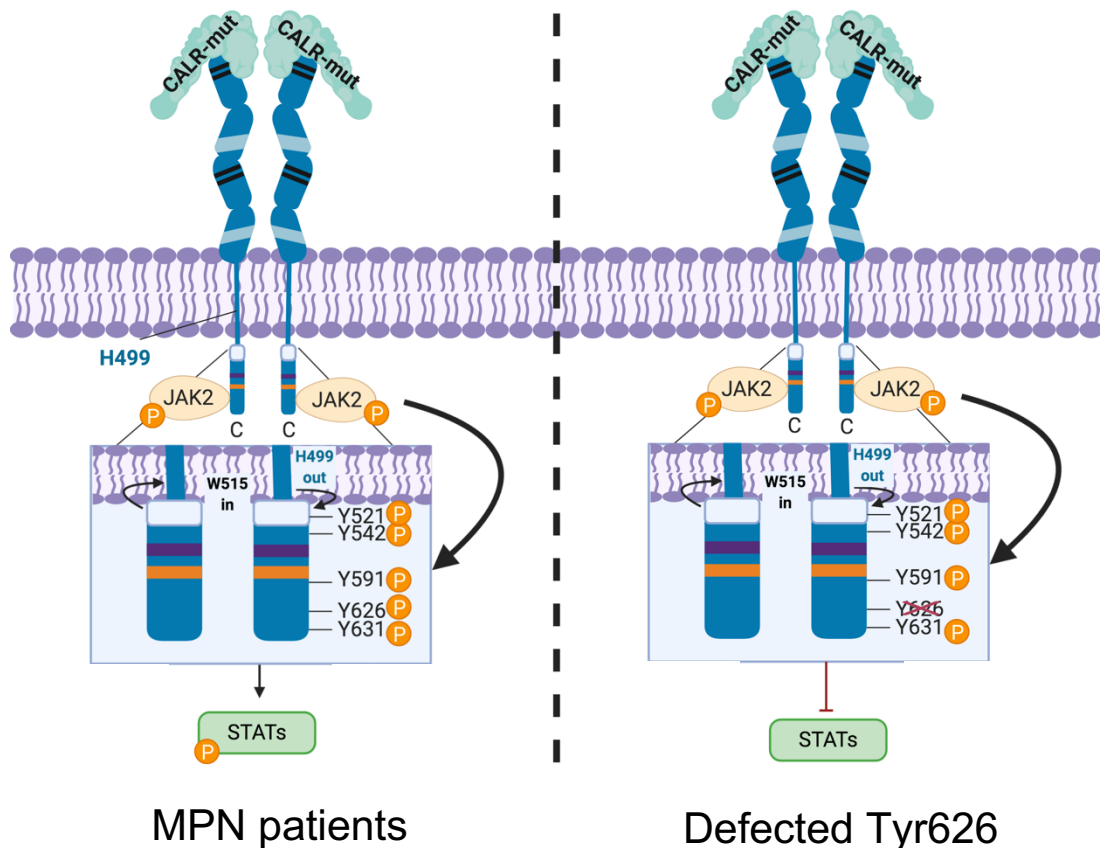


Figure 4.10 Schematic representation of CALR^{del52} binding to MPL on the cell surface. In MPN cells, CALR^{del52} stably associates with MPL to induce constitutive activation through the recruitment of JAK2 and subsequent tyrosine phosphorylation that result in the activation of STAT pathways. Upon Tyr626 disruption, binding of CALR remains intact, however, STAT signalling is attenuated.

Chapter 5

**Expression, purification and structural analysis of
wildtype CALR and CALR^{del52} purified from *E. coli***

Chapter 5

Expression, purification and structural analysis of wildtype CALR and CALR^{del52} purified from *E. coli*

5.1 Introduction

Until recently, structural data for CALR has been restricted to a crystal structure of the CALR N-domain and an NMR structure of the P-domain derived from rat CALR (L. Ellgaard et al., 2001; Chouquet et al., 2011; Kozlov et al., 2010). The N-domain crystal structure shows that human CALR, like its counterparts in calnexin (CANX) and mouse CALR, adopts a well-ordered globular shape characterised by a jelly-roll fold assembled into two anti-parallel beta sheets, one being convex and the other being concave (Chouquet et al., 2011). The NMR structure of the P-domain revealed a hairpin fold involving the entire span of the polypeptide chain with two chain ends that does not fold back on itself (Ellgaard et al., 2001). Recently, a structure of full length CALR was revealed using cryo-electron microscopy (cryo-EM) in complex with several other proteins within the human MHC-I peptide loading complex at a resolution of 5.8Å (Blees et al., 2017). The structure of the full-length CALR protein was found to resemble that of the luminal portions of CANX, in possessing a large, globular domain with an arm-like extension which reached around the MHC-I within the peptide loading complex with the tip of the arm interacting with the cochaperone ERp57.

MPN-associated *CALR* mutations create a mutant CALR protein (CALR^{del52}) that differs sequence-wise with wild-type CALR only within its C-terminus. The mutation causes a frameshift in the reading frame of the 3' end of the *CALR* transcript, and leads to replacement of the acidic residues of the wild-type C domain (mostly Glu and Asp) with basic residues in the mutant-specific C terminus (mostly Lys and Arg). To date, very little structural information is available for the wildtype C-domain, as it is predicted to be highly structurally disordered and is characterised by an isoelectric point (pI) of 3.98 (Shivarov et al., 2014). The full-length cryo-EM reconstruction, modelled the wild-type C-domain as a helical structure but with the caveat that this region was highly flexible (Blees et al., 2017). With regard to the CALR^{del52} C-domain, computational prediction tools suggest it would exhibit a pI in the range of 10.09-12 (depending on the type of mutation) and would be predicted to be similarly disordered (Shivarov et al., 2014). As with the wild-type C-terminus, little is known about the structure of the mutant-specific C-terminus nor about the effect it has on the rest of the CALR protein.

Resolving the atomic structure of proteins through NMR, electron microscopy and crystallography is crucial for our understanding of protein function and protein-protein interactions. In addition, resolving the structure of proteins could identify and elucidate particular domains that may be targetable as a therapeutic strategy in various diseases, including MPN. As *CALR* mutations are the second most common genetic lesion in MPN with no current targeted treatment regime, it is crucial to determine the structure of mutant CALR that

would enable the rational design of antibodies or affimers that can target CALR activity or induce an immune response against the CALR epitope.

5.2 Aims and Hypothesis

Elucidating the structure of CALR^{del52} will significantly further our understanding of its role in the pathogenesis of MPN. I hypothesise that the CALR^{del52} protein will display subtle structural differences to its wildtype counterpart. This investigation will be subdivided into three main aims:

- I. Optimise conditions for purification of wild-type and mutant calreticulin in bacterial expression systems;
- II. Test the functionality of these recombinant proteins by assessing its ability to bind to recombinant MPL;
- III. Use electron microscopy to identify potential differences in structure of mutant calreticulin relative to wildtype calreticulin.

5.3 Results

5.3.1 Cloning

To express calreticulin (WT and CALR^{del52}) in *E. coli*, the pOPIN vector system was used which demonstrates robust expression in both bacterial and eukaryotic systems. Wildtype and mutant CALR cDNAs were PCR amplified and cloned into a pOPINJ vector which introduces a dual GST-6xHis tag in frame to the CALR cDNA at the N-terminus. Successful cloning of CALR cDNAs was verified by diagnostic restriction digest and diagnostic PCR (**Figure 5.1**), and constructs were verified to contain the CALR cDNA in frame with the GST-6xHis tag by sequencing.

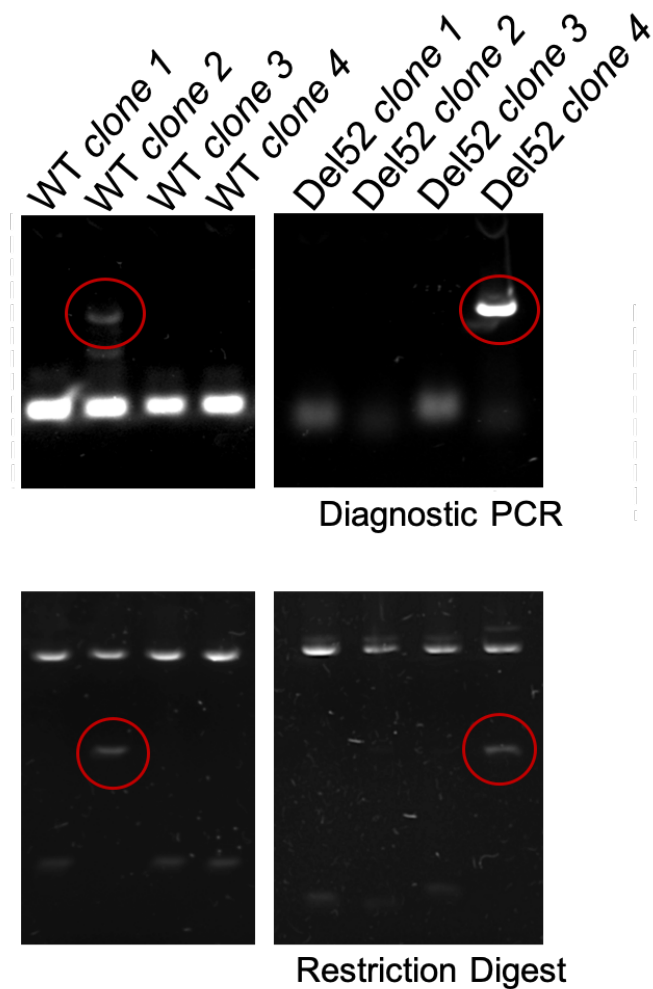


Figure 5.1 Successful cloning of CALR^{WT} and CALR^{del52} genes into pOPINJ vector. Diagnostic PCR electrophoresis image that confirmed successful cloning by PCR (upper panel) and restriction digest (lower panel). The successful clones were sent for DNA sequencing to confirm the gene of interest (indicated in red circle). Results are representative of 2 independent experiments.

5.3.2 Expression and small scale purification of CALR^{WT} and

CALR^{del52}

A small scale screening was first performed to identify bacterial strains and growth condition that could best support protein production of wild-type CALR and CALR^{del52}. The pOPINJ-CALR^{WT} and pOPINJ-CALR^{del52} plasmids were transformed into 9 different *E. coli* expression strains and expanded under 3 different temperatures. Automated purification on Ni-NTA columns to bind the His-tag was performed using a Hamilton robot as described in section 2.15 and purified proteins were analysed on SDS-PAGE and visualised by Coomassie blue staining. The screening demonstrated that robust purification of CALR^{WT} could be achieved using four different expression strains at 18°C (**Figure 5.2A, top panel**). In contrast, CALR^{del52} purification was significantly more challenging, and only Rosetta cells were able to stably express and allow purification of CALR^{del52} at both 18°C and 25°C (**Figure 5.2B, top panel**). Rosetta cells are BL21 derivative strains which express tRNAs for rare codons (AGG, AGA, AUA, CUA, CCC and GGA), which may suggest that these residues are important for synthesis of CALR^{del52}. Of note, AGG and AGA encode arginine, an amino acid that is over-represented in the mutant C-terminus of CALR^{del52}. These bands were confirmed to correspond to CALR by western blotting (**Figure 5.2A-B, bottom panels**). Therefore, from these expression and purification trials, it was determined that Rosetta cells provided an ideal expression strain for large scale purification of recombinant CALR^{del52}, and Rosetta-2 cells was an ideal strain for large scale purification of CALR^{WT}.

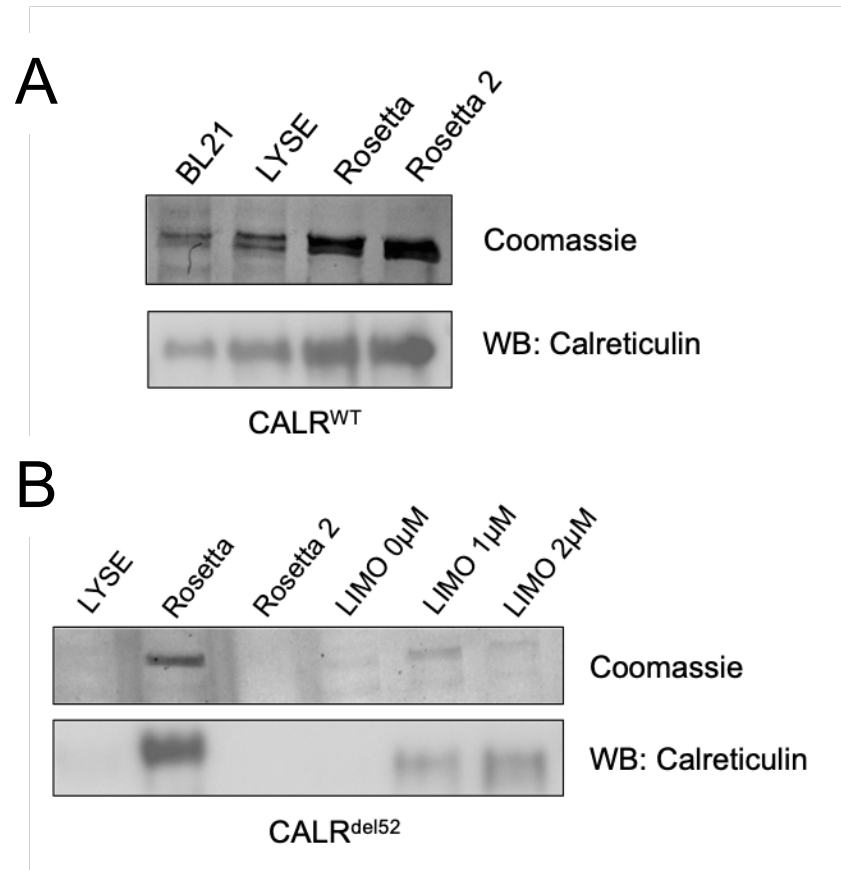


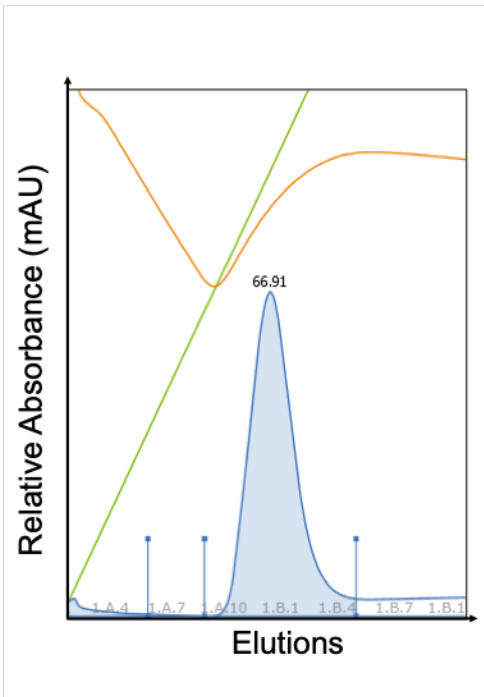
Figure 5.2 Small scale expression and purification of CALR^{WT} and CALR^{del52} in various *E. coli* strains. Purified CALR^{WT} (A) and CALR^{del52} (B) proteins were purified from various *E. coli* lines using Ni-affinity purification, and analysed by SDS-PAGE and western immunoblotting. Induction was performed at 18°C. Results are representative of 2 independent experiments.

5.3.3 Large scale purification of recombinant CALR^{WT} and CALR^{del52}

Next, large scale expression was performed. For purification of recombinant CALR^{WT}, 2L of pOPINJ-CALR^{WT}-expressing Rosetta-2 cells were grown at 18°C and bacterial lysates were prepared for standard AKTA His-affinity purification as described in section 2.16 (**Figure 5.3A**). Following affinity chromatography, elution fractions that contained traces of proteins were analysed by SDS-PAGE to determine if these proteins corresponded to CALR. Total lysate, flow through and wash fractions were also collected and analysed. A single elution peak was seen with 800mAU absorbance, and corresponded to a major protein species at ~75 kDa which corresponds to the molecular weight of CALR (48 kDa) combined with the GST and 6xHis tags (26 kDa) (**Figure 5.3B, upper panel**). western blotting was also performed and confirmed that the most dominant band seen through Coomassie staining corresponded to CALR^{WT} (**Figure 5.3B, lower panel**).

Next, since the elutions still contained protein contaminants, elution fractions were pooled and subjected to size exclusion chromatography. AKTA traces showed multiple high molecular weight peaks that suggest potential protein multimers (**Figure 5.4A**). These proteins were resolved on SDS-PAGE and stained with Coomassie blue, and revealed purified proteins corresponding to the molecular weight to GST-CALR^{WT} (**Figure 5.4B**).

A



B

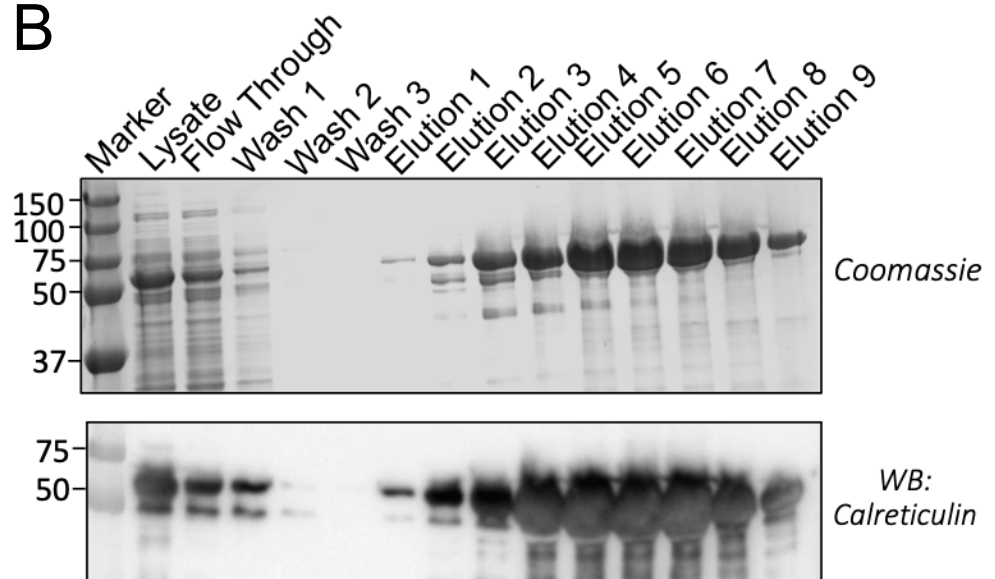
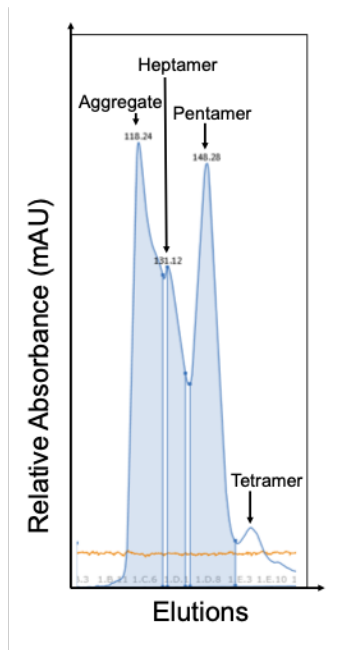


Figure 5.3 Large scale purification of CALR^{WT} (A) Representative AKTA trace demonstrating a single peak eluted out of the column. Blue lines represent UV wavelength, green represents concentration of elution buffer and orange represents conductivity. (B) Coomassie staining (upper panel) and western blots (lower panel) of representative elution fractions from Panel A. Strong bands at 75kDa corresponds to CALR^{WT}. These results are representative of three independent experiments. Results are representative of 3 independent experiments.

A



Next, the same protocol was used to express and purify recombinant CALR^{del52}. Given the reported instability of CALR^{del52}, I used a higher starting volume culture of 8 L of pOPINJ-CALR^{del52}-expressing to produce the CALR^{del52} protein. Rosetta cells was used given previous evidence that it was able to support production of CALR^{del52}. Following Ni-NTA affinity chromatography, the peaks were analysed prior to SDS-PAGE. In contrast to CALR^{WT}, two broad protein peaks (called Peak 1 and Peak 2) were observed on the AKTA traces corresponding to two potentially distinct protein species (**Figure 5.5**). The elution fractions corresponding to these 2 peaks were analysed SDS-PAGE, and analysed by Coomassie blue staining and western blotting. The Coomassie blue staining demonstrated that the quantity of proteins in the elution fractions were generally lower and far more non-specific than was seen for the purification of CALR^{WT} proteins. This was evidenced by significantly more non-specific bands, and the expected major protein species representing a smaller component of the total proteins in each elution fraction (**Figure 5.6A**). Western immunoblotting was performed on these fractions, and indicated that Peak 1 was likely a contaminant protein(s) whilst Peak 2 corresponded to CALR^{del52} (**Figure 5.6B**). As with the CALR^{WT} purification process, size exclusion chromatography was performed to further purify the sample, but this failed to improve the purity of CALR^{del52} proteins but rather led to dilution of the protein samples. Therefore, it was opted to proceed with the CALR^{del52} proteins that were purified following only the single Ni-NTA affinity purification step.

Finally, the identity of both CALR^{WT} and CALR^{del52} samples was confirmed to mass spectrometry (**Figure 5.7**). There was significantly better coverage for the CALR^{WT} protein sample, likely reflecting the greater abundance of protein that was achieved and the increased purity of the sample, compared to CALR^{del52}. Nevertheless, peptides were obtained for both proteins, including sequences derived from the wild-type-specific and mutant-specific C-termini.

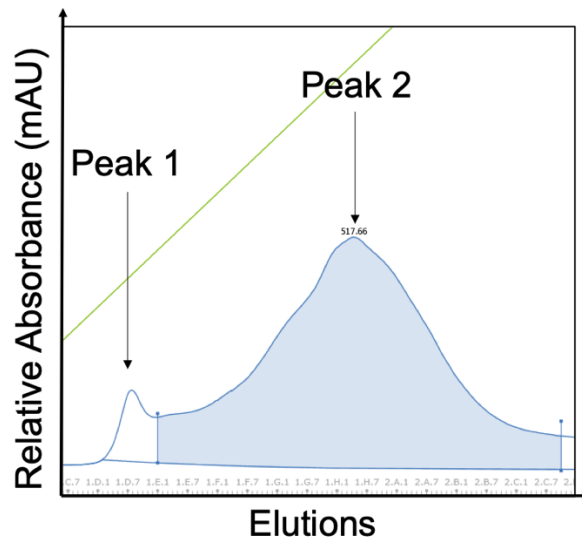


Figure 5.5 Large scale purification of CALR^{del52}. Representative AKTA demonstrating two broad peaks. Blue lines represent UV wavelength and green represents concentration of elution buffer. Results are representative of 5 independent experiments.

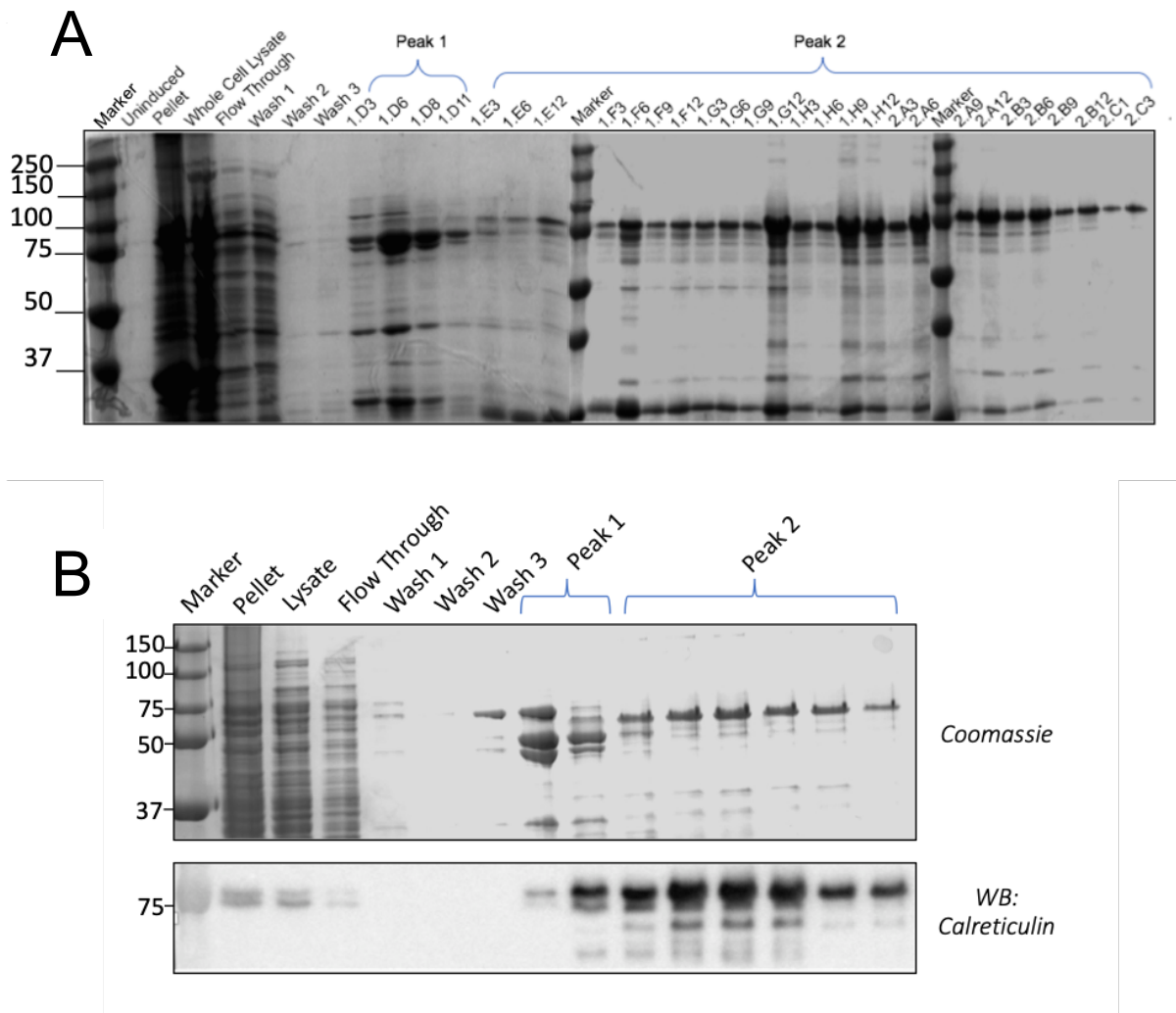


Figure 5.6 Confirmation of presence of CALR^{del52} in large scale purification. (A) Coomassie staining of pellet, flow through, washes and every other elution fractions from the AKTA Ni-NTA affinity chromatography. Peak 2 elutions was distributed over fractions Plate 1.E1- Plate 2.C9 in an elution volume of 40.5 mL and a concentration of 1.307 mg/mL and total mass of 52.9mg. (B) Representative Coomassie staining and western blotting of selected fractions from Panel A demonstrating that the Peak 2 corresponded to CALR^{del52}. Results are representative of 5 independent experiments.

A



B

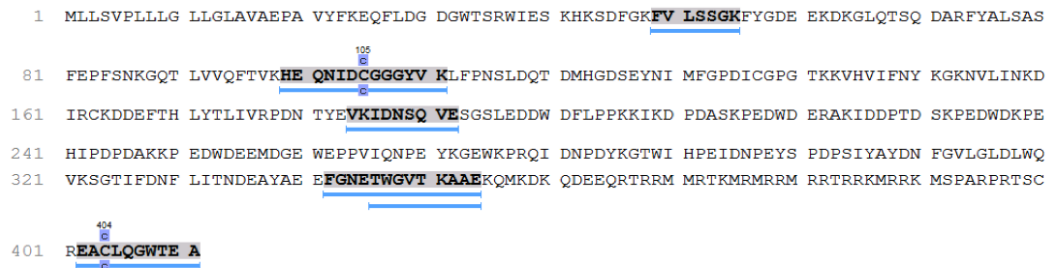


Figure 5.7 Mass spectrometry analysis confirms identify of the purified protein as CALR. Mass spectrometry analysis of recombinant CALR^{WT} demonstrate very good coverage and confirmed presence of peptides corresponding to wildtype CALR (including 2 peptides corresponding to the wild-type C-terminus). (B) Mass spectrometry analysis of recombinant CALR^{del52} demonstrate moderately lower coverage but confirmed presence of CALR^{del52} sequence (including 1 peptide corresponding to mutant-specific C-terminus). Blue line indicates individual peptide coverage. Results are representative of 2 independent experiments.

5.3.4 Cleavage of GST Tag from Purified CALR^{WT} and CALR^{del52}

The purified CALR^{WT} and CALR^{del52} contains a large ~26kDa GST-6xHis tag in its N-terminus which could impair its functional activity. To test this, GST-pulldowns was performed using recombinant CALR^{WT} or CALR^{del52} and commercially-available recombinant MPL. I observed that a recombinant GST-tagged CALR^{del52} was unable to bind to MPL and that the addition of a GST tag in the CALR^{del52} N-terminus significantly impaired this key oncogenic activity (**Figure 5.8A**). Moreover, 293T cells were transfected pOPINJ-CALR^{WT} and pOPINJ-CALR^{del52} in conjunction with MPL and subjected to GST-pulldown assays, and also demonstrated an inability to interact (**Figure 5.8B**). In contrast, CALR^{del52} fused with a FLAG epitope (which is a smaller tag) was still able to bind MPL in FLAG-pulldown assays (**Figure 5.8C**).

This implied that cleavage of the GST tags is required for the CALR^{del52} protein to be functional. Theoretically, the GST tag can be removed from the N-terminus of CALR by a 3C protease. The cleavage reaction was performed in a pair of linked columns, with the first column containing GST beads and the second containing nickel beads. GST-tagged CALR was bound to the first column, and exposed to a His-tagged 3C protease that can cleave the recombinant protein between the GST and the N-terminus of the CALR protein on-column and release the untagged CALR protein. The His-tagged 3C is trapped in the second nickel column, while the cleaved CALR protein released from the GST column would be predicted to flow through the nickel column.

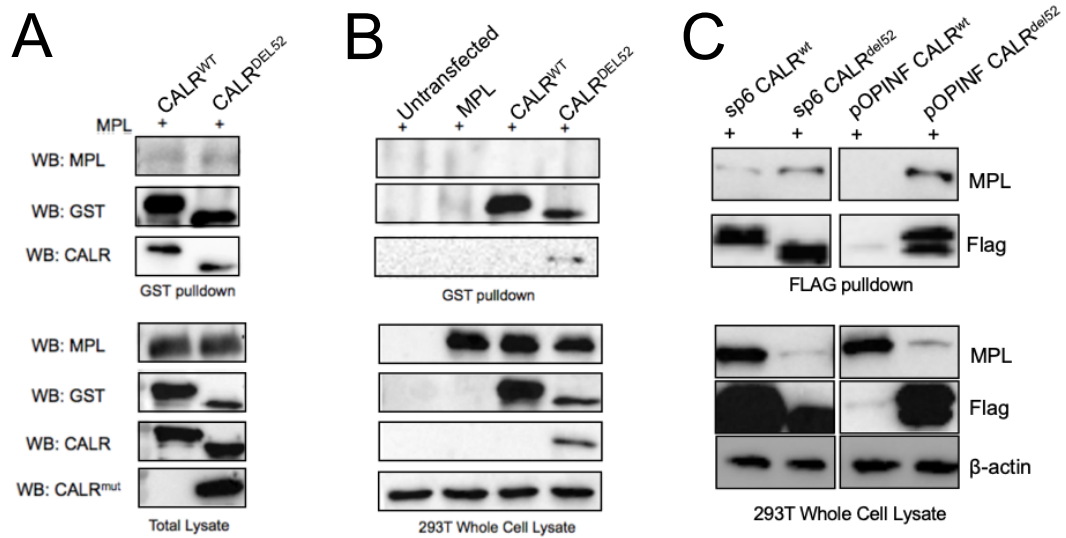


Figure 5.8 The GST tag disrupts binding capacity of CALR^{del52} to MPL.

(A) GST-pulldowns using recombinant CALR^{WT} or CALR^{del52}, and commercially-available recombinant MPL. (B) GST-pulldowns of 293T cell lysates transiently transfected with pOPINJ-CALR^{WT} and pOPINJ-CALR^{del52} and MPL-expression vector. (C) FLAG-pulldowns of 293T cell lysates transiently transfected with FLAG-tagged CALR^{WT} and CALR^{del52} and pOPINF FLAG-tagged CALR^{WT} and CALR^{del52}. Results are representative of 2 independent experiments.

Using this strategy, cleavage of the GST tag from CALR^{WT} was attempted. I observed that there was successful cleavage of GST-CALR^{WT}, and a protein species corresponding to untagged CALR^{WT} after treatment with His-3C protease (elutions 1-5) (**Figure 5.9A**). Subsequent elution using glutathione was able to elute uncleaved GST-CALR^{WT} and the GST tag left behind from previously successful cleavage events (elutions 6-12) (**Figure 5.9B**). This suggests that the cleavage conditions for CALR^{WT} is not fully optimal, as there still appeared to be uncleaved proteins remaining on the GST column. Nevertheless, the uncleaved CALR^{WT} proteins were successfully obtained in multiple fractions for future analysis.

Next, the same strategy was applied to GST-CALR^{del52} proteins to remove the GST tag. However, this cleavage process was significantly less efficient. I observed that very little cleaved CALR^{del52} was observed in the unbound eluates and was heavily contaminated with GST-tagged (uncleaved) CALR^{del52} (**Figure 5.10A, lane 6**). Examination of the protein remaining on the GST beads (**Figure 5.10A, lane 5**) revealed that the majority of CALR^{del52} protein remained bound to the beads and that this pool of CALR^{del52} protein contains both cleaved and uncleaved species. Attempts to elute the CALR^{del52} proteins off the beads were inefficient (**Figure 5.10A, lane 3**) and the eluted fractions were prone to precipitation (**Figure 5.10A, lane 4**). In all fractions examined, there was co-presence of both cleaved and uncleaved CALR^{del52} proteins, which was seen by Coomassie blue staining (**Figure**

5.10A) and confirmed by western immunoblotting to correspond to CALR protein species (**Figure 5.10B**).

I next attempted to separate the GST-tagged and untagged proteins from each other based on size using size exclusion chromatography (SEC). AKTA traces of the SEC analysis demonstrated the existence of three major peaks. Comparison with size standards revealed that Peak 1 was a protein complex with a molecular size of at least 600kDa, while the sizes of Peaks 2 and 3 were too small to be seen by SDS-PAGE and was assumed to be DNA and RNA contaminants (**Figure 5.11A**). SDS-PAGE of elution fractions representing these 3 peaks revealed the presence of proteins of ~45kDa and ~75kDa in Peak 1 and no proteins in Peaks 2 and 3 (**Figure 5.11B**), and western immunoblotting using a CALR-specific antibodies confirmed the protein species in Peak 1 to correspond to CALR and likely reflect both GST-tagged and -untagged forms CALR^{del52} (**Figure 5.11C**). Cumulatively, these data indicate that CALR^{del52} protein was susceptible to aggregation and/or multimerisation, which limited the ability to purify these proteins in isolation.

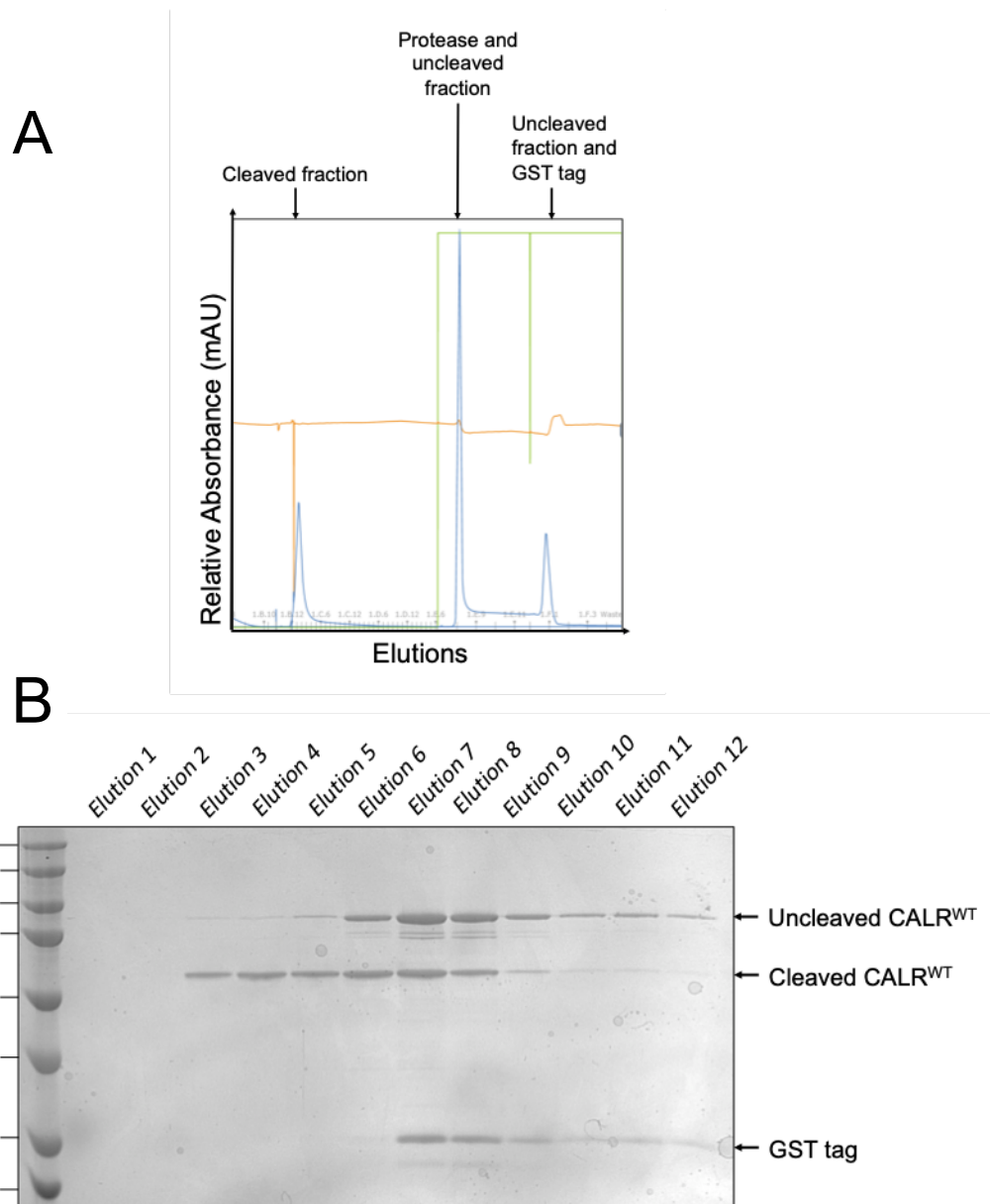


Figure 5.9 Tag cleavage was successful for CALR^{WT}. (A) AKTA trace image of GST Tag cleavage for CALR^{WT}. (B) Coomassie staining of eluted fractions. Results are representative of 2 independent experiments.

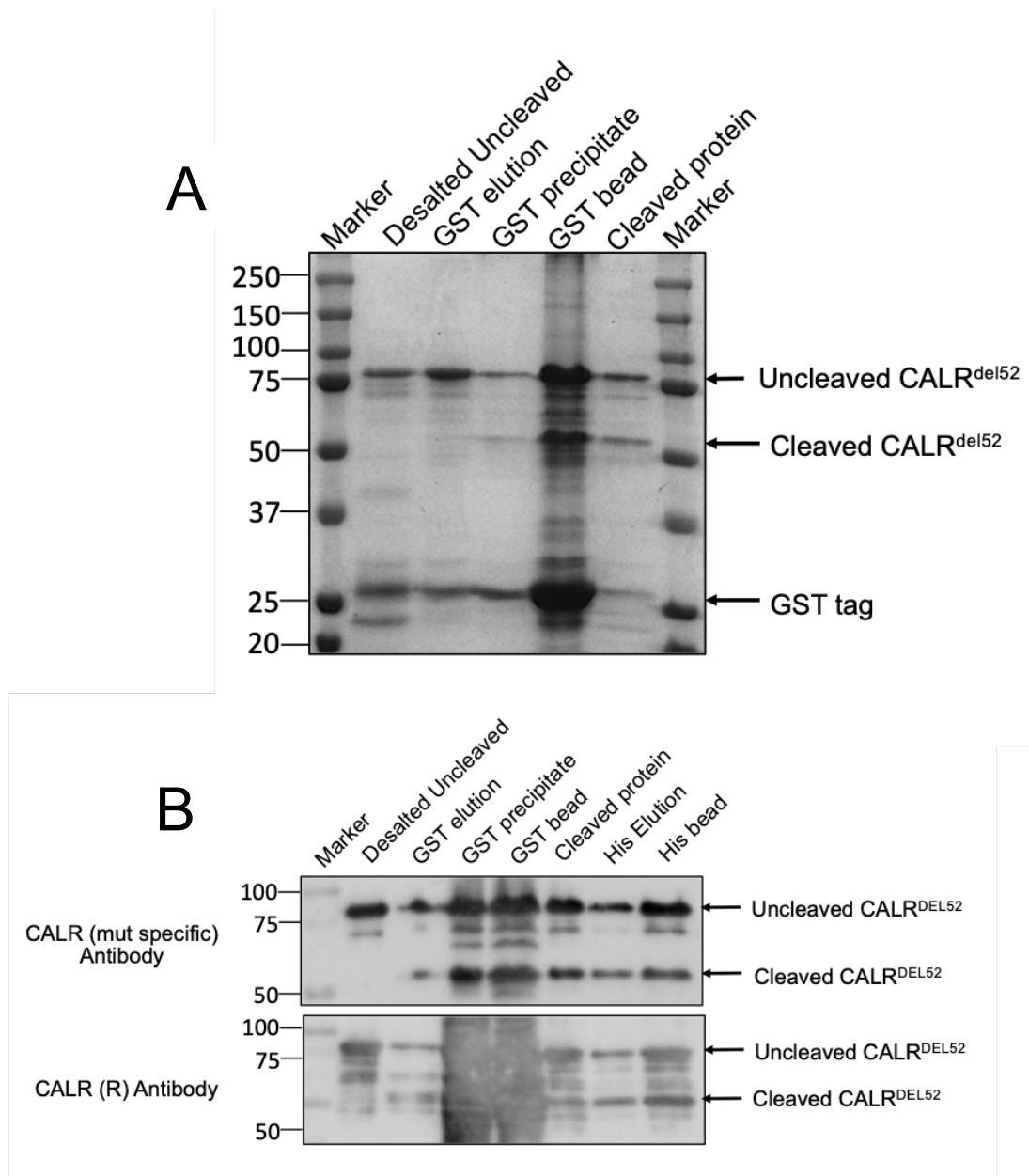


Figure 5.10 Successful cleavage of CALR^{del52} following manual overnight cleavage. (A) Coomassie staining and (B) Western blotting of manual GST tag cleavage removal of CALR^{del52} using 3C-His protease. Results are representative of 3 independent experiments.

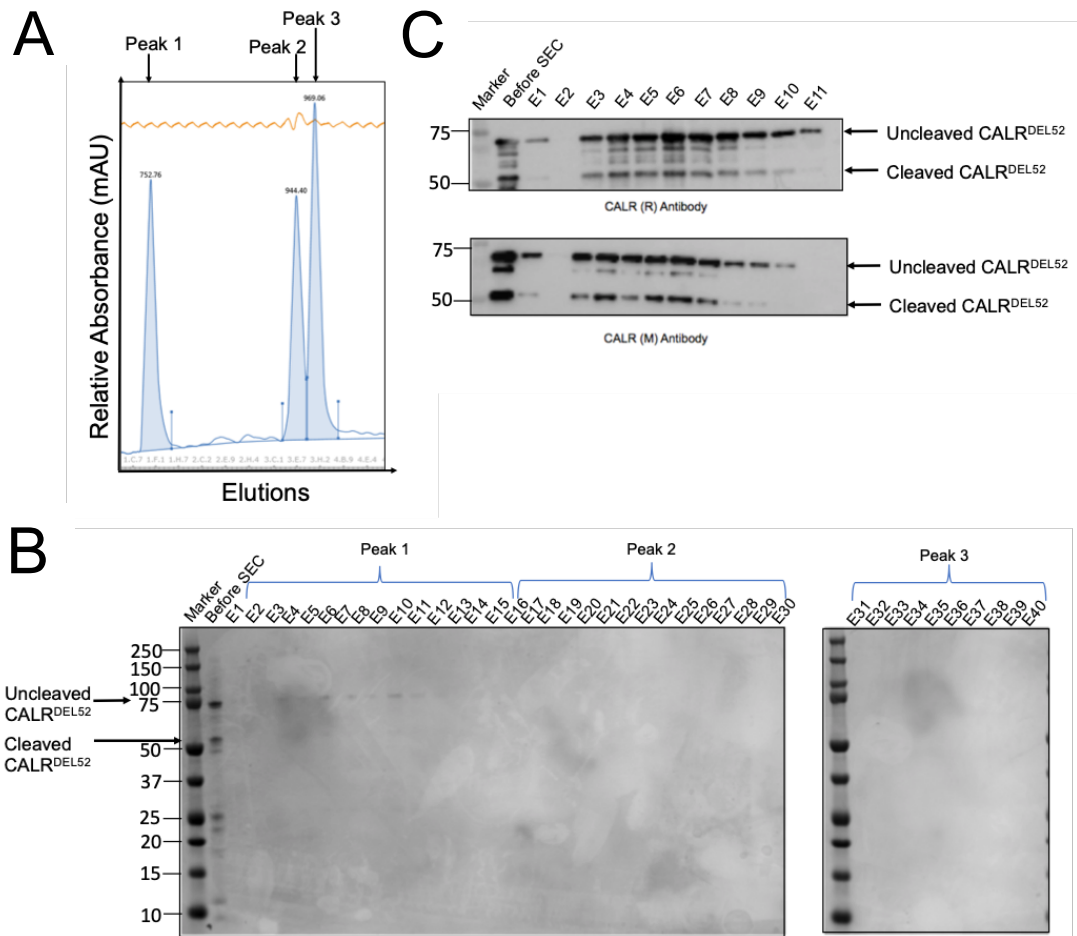


Figure 5.11 Size exclusion chromatography was unable to separate GST-tagged and untagged CALR^{del52}. (A) AKTA trace image of size exclusion chromatography showing three peaks that eluted at various fractions. Estimated sizes according to Superdex S200 columns indicative of aggregates, DNA and RNA. (B) Coomassie staining of eluted fractions from Panel A showed presence of ~45kDa and ~75kDa protein species in Peak 1. (C) Western blots of elution fractions from Peak 1 shows both protein species correspond to CALR proteins. Results are representative of 2 independent experiments.

Lastly, to test whether the purified CALR^{del52} was still functionally active, co-immunoprecipitation was performed. Western immunoblotting of preparations of cleaved and uncleaved CALR^{WT} and CALR^{del52} confirmed the identity of each protein preparation, and verified that the “cleaved CALR^{del52}” sample reflected a mixture of GST-tagged and GST-untagged CALR^{del52} (**Figure 5.12**). Previous results showed that a GST-tagged CALR^{del52} was incapable of binding to MPL (**Figure 5.8**). However, I hypothesised that it might be possible that GST-tagged CALR^{del52} would be able to coimmunoprecipitate with MPL indirectly in the presence of the non-tagged CALR^{del52} acting as a bridge. I therefore performed a GST pulldown using the “cleaved CALR^{del52}” sample spiked with recombinant MPL. As expected, “uncleaved CALR^{del52}” sample (reflecting GST-tagged CALR^{del52}) was incapable of binding to MPL (**Figure 5.13, lane 3**). Remarkably, the “cleaved CALR^{del52}” sample (reflecting a mixture of non-tagged and GST-tagged CALR^{del52}) was able to coimmunoprecipitate with MPL, presumably in an indirect manner (**Figure 5.13, lane 4**). These data suggest that the subpopulation of untagged CALR^{del52} protein in the sample was functionally active.

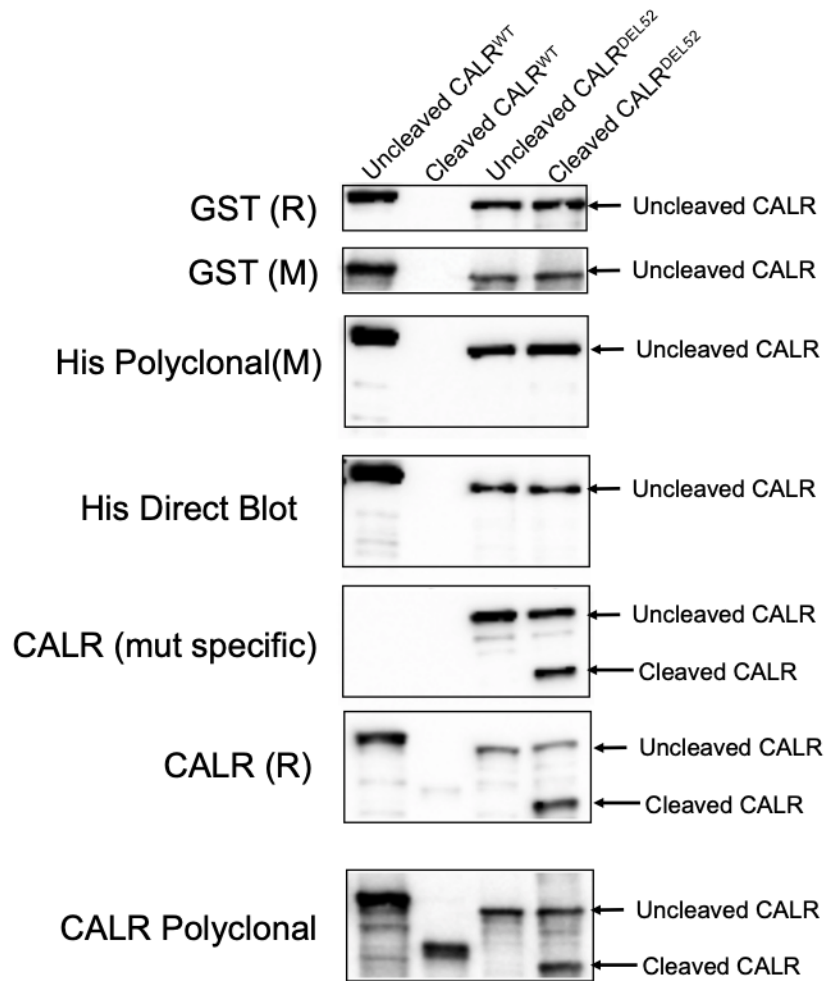


Figure 5.12 Western immunoblotting analysis of preparations of cleaved and uncleaved CALR^{WT} and CALR^{del52} samples. Western immunoblotting demonstrates that the “cleaved CALR^{del52}” sample represents a mixture of GST-tagged and untagged CALR^{del52}. Results are representative of 2 independent experiments.

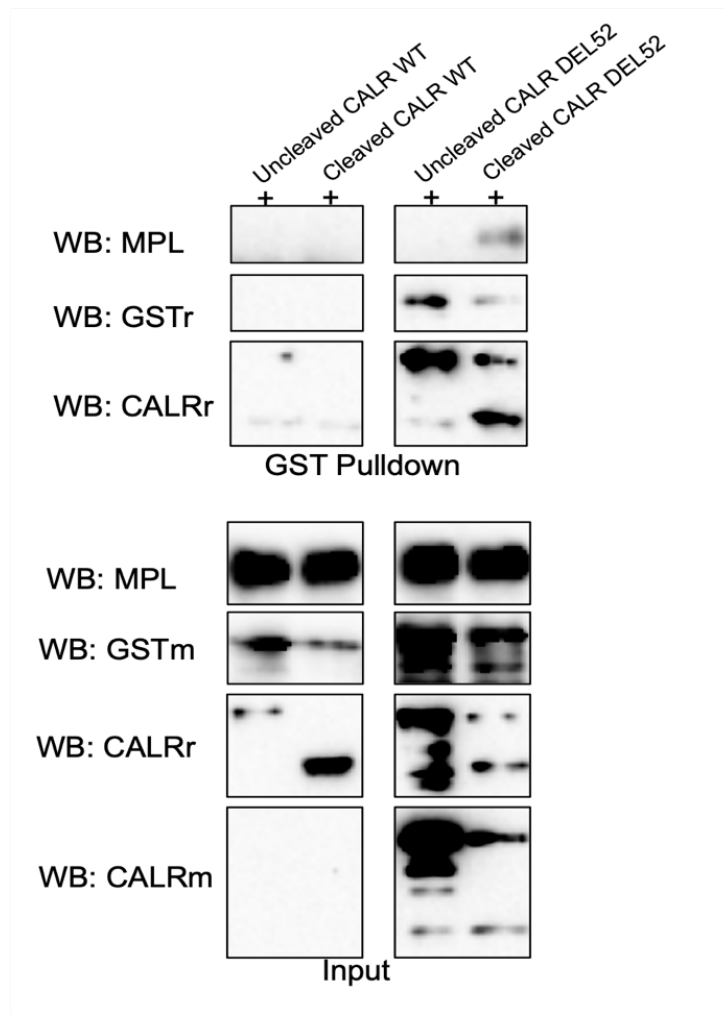


Figure 5.13 Cleaved CALR^{del52} proteins retain MPL binding capacity. GST pulldown of “cleaved CALR^{del52}” sample mixed with recombinant MPL demonstrate that GST-tagged CALR^{del52} was able to pull down MPL only in the presence of the untagged protein in the protein mixture. Results are representative of 2 independent experiments.

5.3.5 Structural and Functional Analysis

Given the sample heterogeneity in the CALR^{del52} sample (which reflects the presence of both GST-tagged and untagged protein species simultaneously) and the inability to separate these two pools by SEC, these samples were subjected to use electron microscopy (EM) to derive structural information and to potentially separate out distinct classes to distinguish between GST-tagged and untagged forms. Both purified GST-tagged and untagged CALR^{WT} and the post-cleavage CALR^{del52} protein sample (which includes GST-tagged and untagged species) were prepared onto the carbon grids and examined by electron microscopy (**Figure 5.14**).

A total of 40634 and 21499 particles were examined for GST-tagged and untagged CALR^{WT} proteins, respectively (**Figure 5.15A**) and used to construct a structure for both protein species. The models indicated that the presence of a GST tag on CALR^{WT} created a more compact “dumb-bell” structure (**Figure 5.15B, left**), whereas removal of the GST tag created a structure that comprised a prominent globular domain with an extended arm (**Figure 5.15B, right**) that is reminiscent to the CALR 3D model from previous published data (Blees et al., 2017) when overlaid (**Figure 5.15C**).

For CALR^{del52}, a total of 36476 particles were examined for the post-cleavage CALR^{del52} protein sample. Identification of different shapes were able to separate two major classes (13532 particles and 22944 particles) (**Figure 5.16A**). EM reconstructions identified that one class of particles exhibited a

compact shape that was similar to the GST-tagged CALR^{WT} protein above while the other class exhibited a protein with a prominent globular domain and an arm-like extension similar to the structure observed with untagged CALR^{WT} (**Figure 5.16B**) were overlaid with the existing previously published data (Blees et al., 2017) (**Figure 5.16C**). These data are consistent with the fact that the purified proteins likely correspond to GST-tagged and untagged versions of CALR^{del52}, and that cryo-EM is a valid technology to visualise structure differences in CALR^{del52}, but the purity of CALR^{del52} preparation need to be improved to allow for higher resolution deductions.

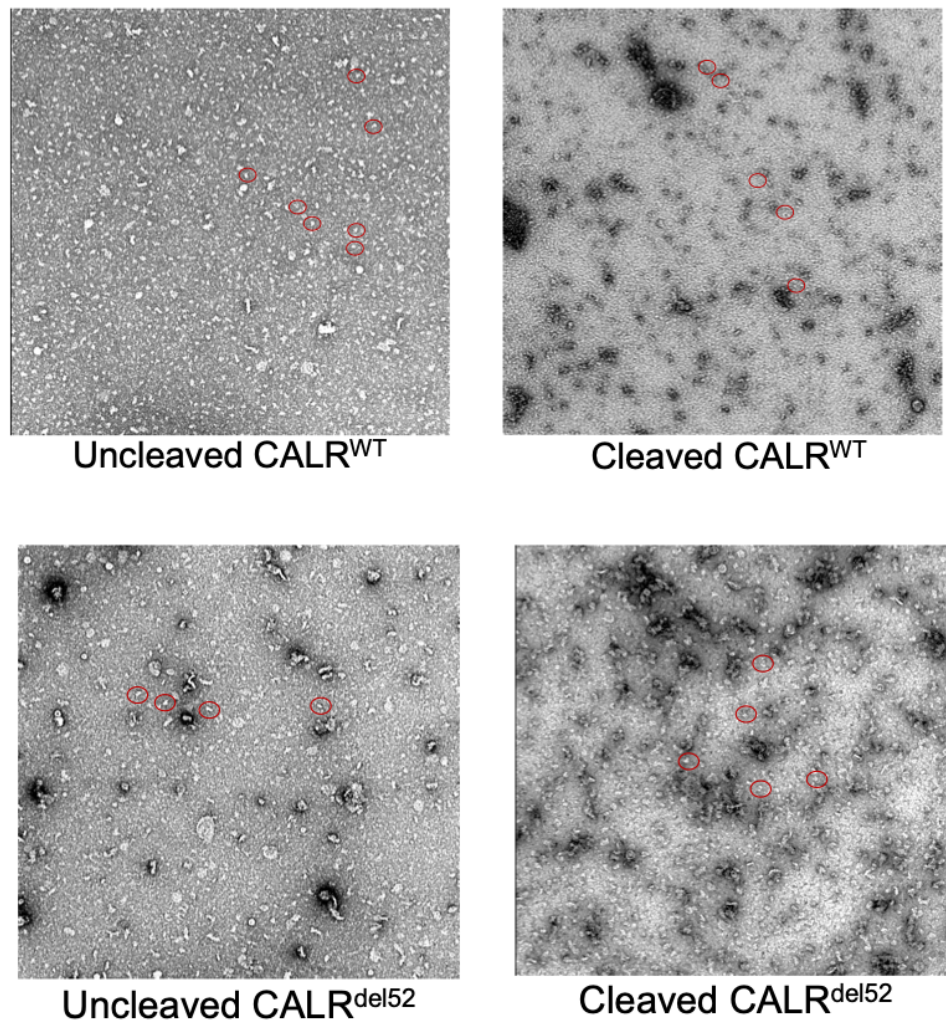


Figure 5.14 Negative staining EM staining images of recombinant CALR proteins. Representative images from negative EM staining of CALR species following CTF correction using RELION. Results are representative of 3 independent experiments.

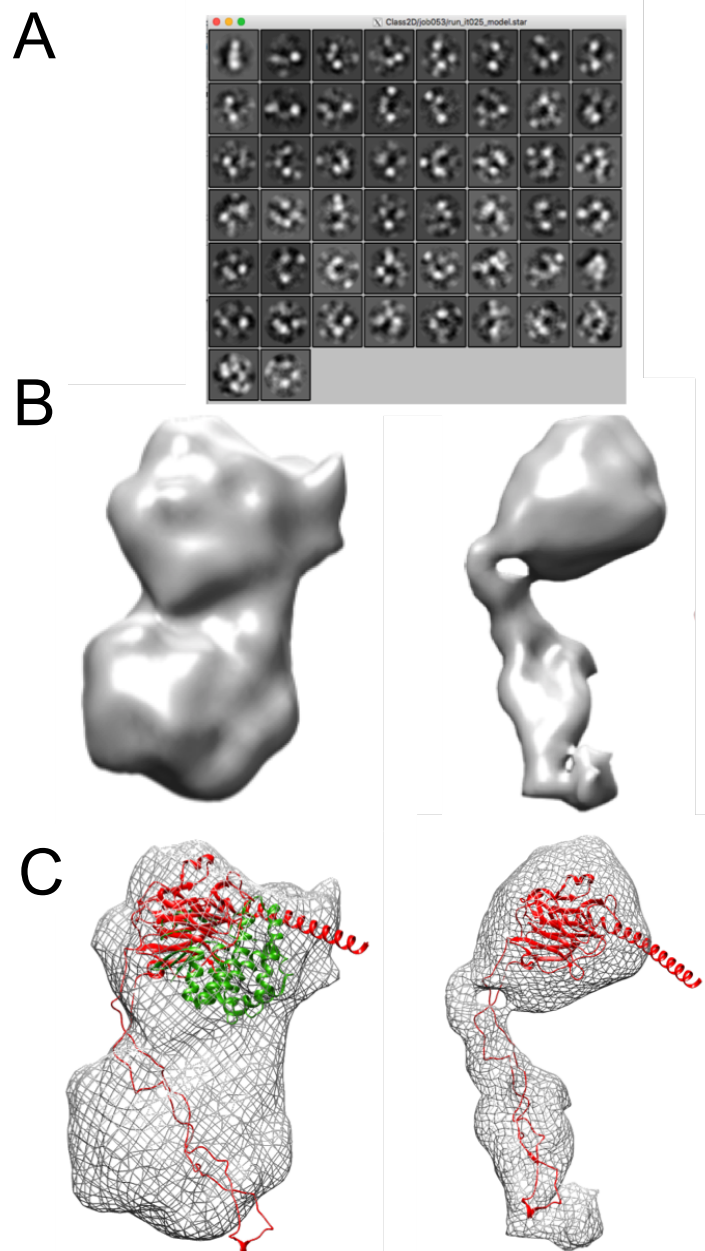


Figure 5.15 Structural analysis of CALR^{WT}. (A) 2D Classification of cleaved variants of CALR^{WT} by RELION. (B) 3D initial model of uncleaved (left panel) and (cleaved) CALR^{WT}. (C) 3D initial model overlaid with existing cryo-EM CALR^{WT} structure (Blees et al., 2017). Red structure denotes CALR; green structure denotes GST. Results are representative of 3 independent experiments.

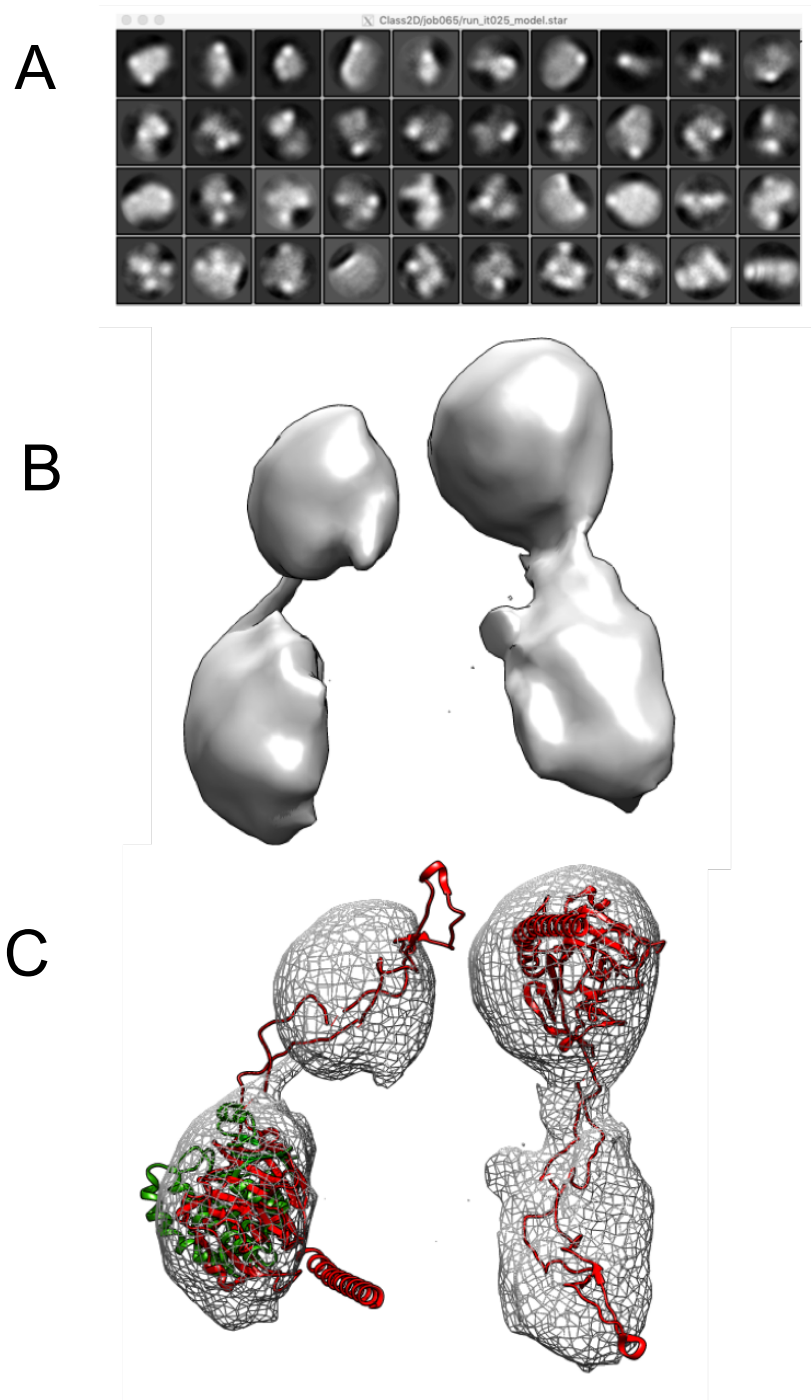


Figure 5.16 Structural analysis of CALR^{del52}. (A) 2D Classification of cleaved variants of CALR^{del52} by RELION. (B) 3D initial model of 2 classes of CALR^{del52} particles. (C) 3D initial model overlaid with existing cryoEM CALR^{del52} structure (Blees et al., 2017) suggests one class corresponds to GST-tagged (left panel) and one class of particles corresponds to GST-untagged (right panel). Red structure denotes CALR; green structure denotes GST.

5.4 Discussion

The aim of this investigation was to express and purify wildtype and mutant versions of CALR for downstream functional and structural analysis. Despite of the various barriers and challenges faced during expression and purification of the recombinant proteins, it was indeed possible to produce recombinant proteins at a sufficient yield for preliminary negative EM reconstruction.

Initial purification of CALR^{WT} showed a stable recombinant protein that was easily purified following one large scale growth. This was unsurprising since CALR^{WT} purification has been routinely performed in various biochemical assays (Andrin et al., 2000; Corbett et al., 2000). In contrast, it was significantly more challenging to purify CALR^{del52} proteins that were suitable for structural analysis. The challenges to this were due to two major issues: instability of CALR^{del52} in cells which has been reported by others (Marty et al., 2016; Han et al., 2016; Li et al., 2018), and the tendency of CALR^{del52} to aggregate.

The aggregation/oligomerisation of CALR^{del52} was an especially challenging technical problem. The size exclusion chromatography traces of CALR^{del52} displayed a single large peak of more than 600 kDa indicative of an aggregate. This supports recent reports that showed the ability of CALR^{del52} to form high molecular weight structures in comparison to its wildtype

counterpart (Araki et al., 2019). Furthermore, it was also shown that this homomultimerisation seems to be critical for MPL binding and activation, which is consistent with our findings that it was easier to purify a GST-tagged CALR^{del52} that was functionally inactive than a GST-untagged protein that was functionally active. These data also suggest that this oligomerisation was very stable. Previous studies have shown this can partially reversed upon addition of higher concentration of urea and SDS (Jørgensen et al., 2003), but this would make the resulting samples unsuitable for structural analysis. Given the tendency of CALR^{del52} to prefer to not exist in a monomeric state, future attempts to purify CALR^{del52} should perhaps be based on a strategy of co-purifying it in complex with a known partner, such as MPL.

Nevertheless, this present study generated preliminary negative EM staining data and derived preliminary reconstructions and models for CALR^{WT} and CALR^{del52}. These data suggest that GST-tagged and –untagged versions of CALR^{del52} appear different, which is consistent with the fact that they have different functionalities in terms of engendering MPN phenotypes. In contrast, the structures of CALR^{WT} and CALR^{del52} exhibit very similar structures, although the resolution achieved in these studies are likely too low to make significant interpretations regarding differences between CALR^{del52} and CALR^{WT}. Further studies are required to generate higher resolution structures to elucidate structural differences in CALR conformation associated with the mutant C-terminus.

Chapter 6

General Discussion

Chapter 6

General Discussion

MPN are clonal disorders characterised by proliferation of mature myeloid cells (Nangalia and Green, 2014). These disorders are associated with differentially expressed inflammatory cytokines, abnormal peripheral blood count and extramedullary haematopoiesis (Arber et al., 2016). The discovery of driver mutations in JAK2, MPL and CALR in MPN have significantly advanced our understanding of the mechanisms underlying the pathogenesis of these disorders (Levine et al., 2005; James et al., 2005; Kralovics et al., 2005; Baxter et al., 2005; Beer et al., 2008; Nangalia et al., 2013; Pikman et al., 2006; Klampfl et al., 2013). These driver mutations are usually mutually exclusive and have been demonstrated to share a common characteristic feature of constitutive activation of JAK-STAT pathway. However, the exact mechanisms of JAK-STAT constitutive activation and molecular pathology of these mutations are not clearly understood in some instances, and therefore there is a need for further investigation to improve treatment outcomes.

Indel mutations in the *CALR* gene represent the second most common mutation in MPN (Nangalia et al., 2013; Klampfl et al., 2013). Numerous studies have determined a strong association of MPL activation and mutant CALR (CALR^{del52}) in MPN pathophysiology (Chachoua et al., 2016; Elf et al., 2016). CALR^{del52} is thought to bind and activate MPL for its oncogenic activity. Furthermore, it was also determined that the positively charged novel C-

terminus of CALR is necessary to facilitate binding to MPL (Araki et al., 2016; Chachoua et al., 2016; Marty et al., 2016; Elf et al., 2016). However, despite the numerous research efforts in understanding the molecular pathology of CALR^{del52}, there are still gaps in our understanding of its mechanism of action including: other regions of CALR that contribute to its activity, the regions of MPL that are essential for transducing CALR^{del52} oncogenic activity and a detailed understanding of the structure of CALR^{del52}. This investigation aims to address these questions.

To determine regions of the globular N-domain of CALR^{del52} that are essential for its function, a thorough alanine mutagenesis screen was performed as described in [Chapter 3](#). Candidate residues identified in the alanine screen to be relevant for CALR^{del52} oncogenic activity are involved in two functional motifs: lectin activity and the zinc binding motifs. This study prompted downstream functional analysis of both functional groups that led to numerous interesting insights, including: i) the lectin motif is critical in MPL binding and activation of signalling cascade, ii) the zinc binding motif is important in the ability of CALR^{del52} to homomultimerise and bind MPL, iii) zinc chelation leads to loss of MPL binding and attenuation of STAT signalling specifically in cells expressing CALR^{del52}. These data have potential clinical implications and suggest that disrupting zinc homeostasis may be a possible therapeutic avenue for treatment of MPNs.

Despite the established dependency on MPL for CALR^{del52}-mediated oncogenic activity, the precise mechanism of how MPL is activated by

CALR^{del52} is not clearly understood. In Chapter 4, the role of tyrosine phosphorylation was tested to determine if CALR^{del52} activates MPL in a similar mechanism to that of the natural MPL ligand, thrombopoietin (TPO). I demonstrate that CALR^{del52} does indeed co-opt canonical MPL signalling and identified a specific residue, Tyr626, that is absolutely critical in STAT5 recruitment and activation. Furthermore, this present study also determined that other residues in MPL implicated in TPO binding and eltrombopag binding are dispensable for supporting CALR^{del52} activity. These data highlight that although CALR^{del52} can lead to activation of downstream canonical TPO signalling pathways, it does not activate MPL in the same manner as TPO extracellularly. Moreover, CALR^{del52} also does not act analogously to eltrombopag by binding to the H499 residue in the MPL transmembrane domain. The precise mechanism by which the CALR^{del52}-MPL binding event happens therefore warrants further investigation.

Given this and that the relationship between CALR^{del52} and MPL is absolutely critical in facilitating oncogenic transformation, it is therefore necessary to decipher the molecular structure of both proteins to further understand the structural relationship of these two proteins. Through NMR and X-ray crystallography, the globular N-domain and P-domain have been resolved (Chouquet et al., 2011; L Ellgaard et al., 2001). More recently, the full structure of wildtype CALR has been resolved following purification and cryo-EM structural analysis of MHC complex I (Blees et al., 2017). Chapter 5 described in detail the trying journey of attempting to purify CALR^{del52} in *E. coli*. Although purification of wild-type CALR was successful in my hands,

significant technical challenges arose when attempting to purify CALR^{del52}. These technical challenges included low protein yield in *E. coli*, instability of the CALR^{del52} in cells and *in vitro*, and the tendency of CALR^{del52} to oligomerise/aggregate as evidenced by high molecular forms. These multimers however are consistent with recent reports that CALR^{del52} can homomultimerise (Araki et al., 2019). Future work should focus on co-expressing both proteins in mammalian cells to ensure that correct MPL posttranslational modifications are made and to co-purify the entire complex which may ameliorate the issues of protein stability and aggregation.

Collectively, the results in this thesis provides numerous insights into CALR^{del52} activity, including elucidating novel biochemical properties and signalling pathways that are required for it to exert its oncogenic effects.

Bibliography

Bibliography

- Adamson, J.W. 1968. The erythropoietin-hematocrit relationship in normal and polycythemic man: implications of marrow regulation. *Blood*. **32**(4),pp.597–609.
- Adamson, J.W., Fialkow, P.J., Murphy, S., Prchal, J.F. and Steinmann, L. 1976. Polycythemia Vera: Stem-Cell and Probable Clonal Origin of the Disease. *New England Journal of Medicine*. **295**(17),pp.913–916.
- Akada, H., Yan, D., Zou, H., Fiering, S., Hutchison, R.E. and Mohi, M.G. 2010. Conditional expression of heterozygous or homozygous Jak2V617F from its endogenous promoter induces a polycythemia vera-like disease. *Blood*. **115**(17),pp.3589–97.
- Alexander, W.S., Metcalf, D. and Dunn, A.R. 1995. Point mutations within a dimer interface homology domain of c-Mpl induce constitutive receptor activity and tumorigenicity. *The EMBO Journal*. **14**(22),pp.5569–5578.
- Andrin, C., Corbett, E.F., Johnson, S., Dabrowska, M., Campbell, I.D., Eggleton, P., Opas, M. and Michalak, M. 2000. Expression and purification of mammalian calreticulin in *Pichia pastoris*. *Protein expression and purification*. **20**(2),pp.207–15.
- Araki, M., Yang, Y., Imai, M., Mizukami, Y., Kihara, Y., Sunami, Y., Masubuchi, N., Edahiro, Y., Hironaka, Y., Osaga, S., Ohsaka, A. and Komatsu, N. 2019. Homomultimerization of mutant calreticulin is a prerequisite for MPL binding and activation. *Leukemia*. **33**(1),pp.122–131.
- Araki, M., Yang, Y., Masubuchi, N., Hironaka, Y., Takei, H., Morishita, S., Mizukami, Y., Kan, S., Shirane, S., Edahiro, Y., Sunami, Y., Ohsaka, A. and Komatsu, N. 2016. Activation of the thrombopoietin receptor by mutant calreticulin in CALR-mutant myeloproliferative neoplasms. *Blood*. **127**(10),pp.1307–1316.
- Arber, D.A., Orazi, A., Hasserjian, R., Thiele, J., Borowitz, M.J., Le Beau, M.M., Bloomfield, C.D., Cazzola, M. and Vardiman, J.W. 2016. The 2016 revision to the World Health Organization classification of myeloid neoplasms and acute leukemia. *Blood*. **127**(20),pp.2391–2405.

- Bainton, D.F. 2004. The development of neutrophilic polymorphonuclear leukocytes in human bone marrow: origin and content of azurophilic and specific granules. *Journal of Experimental Medicine*.
- Baksh, S., Spamer, C., Heilmann, C. and Michalak, M. 1995. Identification of the Zn²⁺ binding region in calreticulin. *FEBS letters*. **376**(1–2),pp.53–7.
- Ballmaier, M., Germeshausen, M., Schulze, H., Cherkaoui, K., Lang, S., Gaudig, A., Krukemeier, S., Eilers, M., Strauß, G. and Welte, K. 2001. c-mpl mutations are the cause of congenital amegakaryocytic thrombocytopenia. *Blood*. **97**(1),pp.139–146.
- Bandaranayake, R.M., Ungureanu, D., Shan, Y., Shaw, D.E., Silvennoinen, O. and Hubbard, S.R. 2012. Crystal structures of the JAK2 pseudokinase domain and the pathogenic mutant V617F. *Nature Structural & Molecular Biology*. **19**(8),pp.754–759.
- Bao, H., Jacobs-Helber, S.M., Lawson, A.E., Penta, K., Wickrema, A. and Sawyer, S.T. 1999. Protein kinase B (c-Akt), phosphatidylinositol 3-kinase, and STAT5 are activated by erythropoietin (EPO) in HCD57 erythroid cells but are constitutively active in an EPO-independent, apoptosis-resistant subclone (HCD57-SREI cells). *Blood*. **93**(11),pp.3757–73.
- Bass, J., Chiu, G., Argon, Y. and Steiner, D.F. 1998. Folding of insulin receptor monomers is facilitated by the molecular chaperones calnexin and calreticulin and impaired by rapid dimerization. *The Journal of cell biology*. **141**(3),pp.637–46.
- Baxter, E.J., Scott, L.M., Campbell, P.J., East, C., Fourouclas, N., Swanton, S., Vassiliou, G.S., Bench, A.J., Boyd, E.M., Curtin, N., Scott, M.A., Erber, W.N. and Green, A.R. 2005. Acquired mutation of the tyrosine kinase JAK2 in human myeloproliferative disorders. *The Lancet*. **365**(9464),pp.1054–1061.
- Beer, P.A., Campbell, P.J., Scott, L.M., Bench, A.J., Erber, W.N., Bareford, D., Wilkins, B.S., Reilly, J.T., Hasselbalch, H.C., Bowman, R., Wheatley, K., Buck, G., Harrison, C.N. and Green, A.R. 2008. MPL mutations in myeloproliferative disorders: analysis of the PT-1 cohort. *Blood*.

112(1),pp.141–9.

- Benekli, M., Baer, M.R., Baumann, H. and Wetzler, M. 2003. Signal transducer and activator of transcription proteins in leukemias. *Blood*. **101(8)**,pp.2940–54.
- Bennett, J.H. 1845. Case of hypertrophy of the spleen and liver, which death took place from suppuration of the blood. *Edinburgh Medical and Surgical Journal*. **64(165)**,pp.413–423.
- Bergeron, J.J., Brenner, M.B., Thomas, D.Y. and Williams, D.B. 1994. Calnexin: a membrane-bound chaperone of the endoplasmic reticulum. *Trends in biochemical sciences*. **19(3)**,pp.124–8.
- Bersenev, A., Wu, C., Balcerek, J. and Tong, W. 2008. Lnk controls mouse hematopoietic stem cell self-renewal and quiescence through direct interactions with JAK2. *The Journal of clinical investigation*. **118(8)**,pp.2832–44.
- Bianchi, E., Norfo, R., Pennucci, V., Zini, R. and Manfredini, R. 2016. Genomic landscape of megakaryopoiesis and platelet function defects. *Blood*. **127(10)**,pp.1249–1259.
- Bibi, A., Agarwal, N.K., Dihazi, G.H., Eltoweissy, M., Van Nguyen, P., Mueller, G.A. and Dihazi, H. 2011. Calreticulin is crucial for calcium homeostasis mediated adaptation and survival of thick ascending limb of Henle's loop cells under osmotic stress. *The international journal of biochemistry & cell biology*. **43(8)**,pp.1187–97.
- Blees, A., Janulienė, D., Hofmann, T., Koller, N., Schmidt, C., Trowitzsch, S., Moeller, A. and Tampé, R. 2017. Structure of the human MHC-I peptide-loading complex. *Nature*. **551(7681)**,pp.525–528.
- Bouscary, D., Lecoq-Lafon, C., Chrétien, S., Zompi, S., Fichelson, S., Muller, O., Porteu, F., Dusanter-Fourt, I., Gisselbrecht, S., Mayeux, P. and Lacombe, C. 2001. Role of Gab proteins in phosphatidylinositol 3-kinase activation by thrombopoietin (Tpo). *Oncogene*. **20(18)**,pp.2197–2204.
- Brewer, D.B. 2006. Max Schultze (1865), G. Bizzozzero (1882) and the discovery of the platelet. *British Journal of Haematology*.

133(3),pp.251–258.

Brown, G. and Ceredig, R. 2019. Modeling the hematopoietic landscape.

Frontiers in Cell and Developmental Biology. **7**(JUN).

Burns, K., Duggan, B., Atkinson, E.A., Famulski, K.S., Nemer, M., Bleackley, R.C. and Michalak, M. 1994. Modulation of gene expression by

calreticulin binding to the glucocorticoid receptor. *Nature.*

367(6462),pp.476–80.

Butcher, C.M., Hahn, U., To, L.B., Gecz, J., Wilkins, E.J., Scott, H.S., Bardy, P.G. and D'Andrea, R.J. 2008. Two novel JAK2 exon 12 mutations in

JAK2V617F-negative polycythaemia vera patients. *Leukemia.*

22(4),pp.870–3.

Cerquozzi, S. and Tefferi, A. 2015. Blast transformation and fibrotic

progression in polycythemia vera and essential thrombocythemia: a

literature review of incidence and risk factors. *Blood Cancer Journal.*

5(11),pp.e366–e366.

Chachoua, I., Pecquet, C., El-Khoury, M., Nivarthi, H., Albu, R.-I., Marty, C.,

Gryshkova, V., Defour, J.-P., Vertenoil, G., Ngo, A., Koay, A., Raslova,

H., Courtoy, P.J., Choong, M.L., Plo, I., Vainchenker, W., Kralovics, R.

and Constantinescu, S.N. 2016. Thrombopoietin receptor activation by

myeloproliferative neoplasm associated calreticulin mutants. *Blood.*

127(10),pp.1325–1335.

Chaligné, R., Tonetti, C., Besancenot, R., Roy, L., Marty, C., Mossuz, P.,

Kiladjian, J.-J., Socié, G., Bordessoule, D., Le Bousse-Kerdilès, M.-C.,

Vainchenker, W. and Giraudier, S. 2008. New mutations of MPL in

primitive myelofibrosis: only the MPL W515 mutations promote a G1/S-

phase transition. *Leukemia.* **22**(8),pp.1557–1566.

Chateauvieux, S., Grigorakaki, C., Morceau, F., Dicato, M. and Diederich, M.

2011. Erythropoietin, erythropoiesis and beyond. *Biochemical*

Pharmacology. **82**(10),pp.1291–1303.

Chen, E., Beer, P.A., Godfrey, A.L., Ortmann, C.A., Li, J., Costa-Pereira,

A.P., Ingle, C.E., Dermitzakis, E.T., Campbell, P.J. and Green, A.R.

2010. Distinct clinical phenotypes associated with JAK2V617F reflect

- differential STAT1 signaling. *Cancer cell*. **18**(5),pp.524–35.
- Chen, G.L. and Prchal, J.T. 2007. X-linked clonality testing: interpretation and limitations. *Blood*. **110**(5),p.1411.
- Chouquet, A., Païdassi, H., Ling, W.L., Frachet, P., Houen, G., Arlaud, G.J. and Gaboriaud, C. 2011. X-Ray Structure of the Human Calreticulin Globular Domain Reveals a Peptide-Binding Area and Suggests a Multi-Molecular Mechanism B. Kobe, ed. *PLoS ONE*. **6**(3),p.e17886.
- Christie, R.V. 1987. Galen on Erasistratus. *muse.jhu.edu*.
- Del Cid, N., Jeffery, E., Rizvi, S.M., Stamper, E., Peters, L.R., Brown, W.C., Provoda, C. and Raghavan, M. 2010. Modes of calreticulin recruitment to the major histocompatibility complex class I assembly pathway. *Journal of Biological Chemistry*. **285**(7),pp.4520–4535.
- Cobb, M. 2000. Reading and writing The Book of Nature: Jan Swammerdam (1637–1680). *Endeavour*. **24**(3),pp.122–128.
- Coe, H. and Michalak, M. 2009. Calcium binding chaperones of the endoplasmic reticulum. *General physiology and biophysics*. **28 Spec No Focus**,pp.F96–F103.
- Colaizzo, D., Amitrano, L., Tiscia, G.L., Grandone, E., Guardascione, M.A. and Margaglione, M. 2007. A new JAK2 gene mutation in patients with polycythemia vera and splanchnic vein thrombosis. *Blood*. **110**(7),pp.2768–9.
- Cooper, B. 2011. The origins of bone marrow as the seedbed of our blood: from antiquity to the time of Osler. *Proceedings (Baylor University Medical Center)*. **24**(2),pp.115–8.
- Coppolino, M.G., Woodside, M.J., Demarex, N., Grinstein, S., St-Arnaud, R. and Dedhar, S. 1997. Calreticulin is essential for integrin-mediated calcium signalling and cell adhesion. *Nature*. **386**(6627),pp.843–847.
- Corbett, E.F., Michalak, K.M., Oikawa, K., Johnson, S., Campbell, I.D., Eggleton, P., Kay, C. and Michalak, M. 2000. The conformation of calreticulin is influenced by the endoplasmic reticulum luminal environment. *The Journal of biological chemistry*. **275**(35),pp.27177–85.

- Correa, P.N., Eskinazi, D. and Axelrad, A.A. 1994. Circulating erythroid progenitors in polycythemia vera are hypersensitive to insulin-like growth factor-1 in vitro: studies in an improved serum-free medium. *Blood*. **83**(1),pp.99–112.
- Le Couedic, J.P., Mitjavila, M.T., Villeval, J.L., Feger, F., Gobert, S., Mayeux, P., Casadevall, N. and Vainchenker, W. 1996. Missense mutation of the erythropoietin receptor is a rare event in human erythroid malignancies. *Blood*. **87**(4),pp.1502–11.
- Craigie, D.J. 1845. Cases of disease and enlargement of the spleen in which death took place from the presence of purulent matter in the blood. *Edinburgh Med. Surg.*
- Cruse, J.M. 1999. History of medicine: the metamorphosis of scientific medicine in the ever-present past. *The American journal of the medical sciences*. **318**(3),pp.171–80.
- Dai, C., Chung, I.-J. and Krantz, S.B. 2005. Increased erythropoiesis in polycythemia vera is associated with increased erythroid progenitor proliferation and increased phosphorylation of Akt/PKB. *Experimental Hematology*. **33**(2),pp.152–158.
- Dai, C.H., Krantz, S.B., Dessypris, E.N., Means, R.T., Horn, S.T. and Gilbert, H.S. 1992. Polycythemia vera. II. Hypersensitivity of bone marrow erythroid, granulocyte-macrophage, and megakaryocyte progenitor cells to interleukin-3 and granulocyte-macrophage colony-stimulating factor. *Blood*. **80**(4),pp.891–9.
- Dai, W.J., Bartens, W., Kohler, G., Hufnagel, M., Kopf, M. and Brombacher, F. 1997. Impaired macrophage listericidal and cytokine activities are responsible for the rapid death of listeria monocytogenes infected IFN- γ receptor deficient mice. *Immunobiology*. **197**(2–4),pp.315–316.
- Dameshek, W. 1951. Some speculations on the myeloproliferative syndromes. *Blood*. **6**(4),pp.372–5.
- David, V., Hochstenbach, F., Rajagopalan, S. and Brenner, M.B. 1993. Interaction with newly synthesized and retained proteins in the endoplasmic reticulum suggests a chaperone function for human

- integral membrane protein IP90 (calnexin). *The Journal of biological chemistry*. **268**(13),pp.9585–92.
- Deane, C.M., Kroemer, R.T. and Richards, W.G. 1997. A structural model of the human thrombopoietin receptor complex. *Journal of molecular graphics & modelling*. **15**(3),pp.170–8, 185–8.
- Decker, T. and Kovarik, P. 2000. Serine phosphorylation of STATs. *Oncogene*. **19**(21),pp.2628–2637.
- Dedhar, S., Rennie, P.S., Shago, M., Hagesteijn, C.Y., Yang, H., Filmus, J., Hawley, R.G., Bruchofsky, N., Cheng, H. and Matusik, R.J. 1994. Inhibition of nuclear hormone receptor activity by calreticulin. *Nature*. **367**(6462),pp.480–3.
- Defour, J.-P., Itaya, M., Gryshkova, V., Brett, I.C., Pecquet, C., Sato, T., Smith, S.O. and Constantinescu, S.N. 2013. Tryptophan at the transmembrane-cytosolic junction modulates thrombopoietin receptor dimerization and activation. *Proceedings of the National Academy of Sciences*. **110**(7),pp.2540–2545.
- Degen, E., Cohen-Doyle, M.F. and Williams, D.B. 1992. Efficient dissociation of the p88 chaperone from major histocompatibility complex class I molecules requires both beta 2-microglobulin and peptide. *The Journal of experimental medicine*. **175**(6),pp.1653–61.
- DePaolis, A.M., Advani, J. V. and Sharma, B.G. 1995. Characterization of Erythropoietin Dimerization. *Journal of Pharmaceutical Sciences*. **84**(11),pp.1280–1284.
- Dijkers, P.F., van Dijk, T.B., de Groot, R.P., Raaijmakers, J.A., Lammers, J.W., Koenderman, L. and Coffey, P.J. 1999. Regulation and function of protein kinase B and MAP kinase activation by the IL-5/GM-CSF/IL-3 receptor. *Oncogene*. **18**(22),pp.3334–42.
- Dobeikovski, A., Uzan, G., Dobeikovski, Z., Prandini, M.H., Porteu, F., Gisselbrecht, S. and Dusanter-Fourt, I. 1997. Thrombopoietin-induced expression of the glycoprotein IIb gene involves the transcription factor PU.1/Spi-1 in UT7-Mpl cells. *The Journal of biological chemistry*. **272**(39),pp.24300–7.

- Drachman, J.G., Griffin, J.D. and Kaushansky, K. 1995. The c-Mpl ligand (thrombopoietin) stimulates tyrosine phosphorylation of Jak2, Shc, and c-Mpl. *The Journal of biological chemistry*. **270**(10),pp.4979–82.
- Drews, J. 2004. Paul Ehrlich: Magister Mundi. *Nature Reviews Drug Discovery*. **3**(9),pp.797–801.
- DuBridg, R.B., Tang, P., Hsia, H.C., Leong, P.M., Miller, J.H. and Calos, M.P. 1987. Analysis of mutation in human cells by using an Epstein-Barr virus shuttle system. *Molecular and cellular biology*. **7**(1),pp.379–87.
- Dupont, S., Massé, A., James, C., Teyssandier, I., Lécluse, Y., Larbret, F., Ugo, V., Saulnier, P., Koscielny, S., Le Couédic, J.P., Casadevall, N., Vainchenker, W. and Delhommeau, F. 2007. The JAK2 617V>F mutation triggers erythropoietin hypersensitivity and terminal erythroid amplification in primary cells from patients with polycythemia vera. *Blood*. **110**(3),pp.1013–1021.
- Van Duyn Graham, L., Sweetwyne, M.T., Pallero, M.A. and Murphy-Ullrich, J.E. 2010. Intracellular calreticulin regulates multiple steps in fibrillar collagen expression, trafficking, and processing into the extracellular matrix. *Journal of Biological Chemistry*. **285**(10),pp.7067–7078.
- Eaton, D.L. and de Sauvage, F.J. 1997. Thrombopoietin: the primary regulator of megakaryocytopoiesis and thrombopoiesis. *Experimental hematology*. **25**(1),pp.1–7.
- Ehrlich, P. 1877. Beiträge zur Kenntniss der Anilinfärbungen und ihrer Verwendung in der mikroskopischen Technik. *Archiv für Mikroskopische Anatomie*. **13**(1),pp.263–277.
- El-Harith, E.-H.A., Roesl, C., Ballmaier, M., Germeshausen, M., Frye-Boukhriss, H., von Neuhoff, N., Becker, C., Nürnberg, G., Nürnberg, P., Ahmed, M.A.M., Hübener, J., Schmidtke, J., Welte, K. and Stuhmann, M. 2009. Familial thrombocytosis caused by the novel germ-line mutation p.Pro106Leu in the MPL gene. *British journal of haematology*. **144**(2),pp.185–94.
- Elf, S., Abdelfattah, N.S., Baral, A.J., Beeson, D., Rivera, J.F., Ko, A., Florescu, N., Birrane, G., Chen, E. and Mullally, A. 2018. Defining the

- requirements for the pathogenic interaction between mutant calreticulin and MPL in MPN. *Blood*. **131**(7),pp.782–786.
- Elf, S., Abdelfattah, N.S., Chen, E., Perales-Paton, J., Rosen, E.A., Ko, A., Peisker, F., Florescu, N., Giannini, S., Wolach, O., Morgan, E.A., Tothova, Z., Losman, J.-A., Schneider, R.K., Al-Shahrour, F. and Mullally, A. 2016. Mutant Calreticulin Requires Both Its Mutant C-terminus and the Thrombopoietin Receptor for Oncogenic Transformation. *Cancer Discovery*. **6**(4),pp.368–381.
- Ellgaard, L., Riek, R., Braun, D., Herrmann, T., Helenius, A. and Wüthrich, K. 2001. Three-dimensional structure topology of the calreticulin P-domain based on NMR assignment. *FEBS letters*. **488**(1–2),pp.69–73.
- Ellgaard, L., Riek, R., Herrmann, T., Güntert, P., Braun, D., Helenius, A. and Wüthrich, K. 2001. NMR structure of the calreticulin P-domain. *Proceedings of the National Academy of Sciences of the United States of America*. **98**(6),pp.3133–8.
- Epstein, E. and Goedel, A. 1934. Hamorrhagische thrombozythämie bei vascularer schrumpfmilz (Hemorrhagic thrombocytopenia with a vascular, sclerotic spleen). *Virchows Archiv A Pathol Anat Histopathol*. **293**,pp.233–248.
- Fahreus, R. 1921. The suspension-stability of the blood. *Acta Med Scand*. **55**,pp.1–228.
- Falagas, M.E., Zarkadoulia, E.A., Bliziotis, I.A. and Samonis, G. 2006. Science in Greece: from the age of Hippocrates to the age of the genome. *The FASEB Journal*. **20**(12),pp.1946–1950.
- Fialkow, P.J., Faguet, G.B., Jacobson, R.J., Vaidya, K. and Murphy, S. 1981. *Evidence That Essential Thrombocytopenia is a Clonal Disorder With Origin in a Multipotent Stem Cell*.
- Fialkow, P.J., Gartler, S.M. and Yoshida, A. 1967. Clonal origin of chronic myelocytic leukemia in man. *Proc Natl Acad Sci*. **58**,pp.1468–1471.
- Fishley, B. and Alexander, W.S. 2004. Thrombopoietin signalling in physiology and disease. *Growth factors (Chur, Switzerland)*. **22**(3),pp.151–5.

- Fox, N.E., Lim, J., Chen, R. and Geddis, A.E. 2010. F104S c-Mpl responds to a transmembrane domain-binding thrombopoietin receptor agonist: proof of concept that selected receptor mutations in congenital amegakaryocytic thrombocytopenia can be stimulated with alternative thrombopoietic agents. *Experimental hematology*. **38**(5),pp.384–91.
- Frank, S.J. 2002. Receptor dimerization in GH and erythropoietin action--it takes two to tango, but how? *Endocrinology*. **143**(1),pp.2–10.
- French, D.L. and Seligsohn, U. 2000. Platelet glycoprotein IIb/IIIa receptors and Glanzmann's thrombasthenia. *Arteriosclerosis, Thrombosis, and Vascular Biology*.
- Funakoshi-Tago, M., Pelletier, S., Matsuda, T., Parganas, E. and Ihle, J.N. 2006. Receptor specific downregulation of cytokine signaling by autophosphorylation in the FERM domain of Jak2. *The EMBO journal*. **25**(20),pp.4763–72.
- Gadina, M., Hilton, D., Johnston, J.A., Morinobu, A., Lighvani, A., Zhou, Y.-J., Visconti, R. and O'Shea, J.J. 2001. Signaling by Type I and II cytokine receptors: ten years after. *Current Opinion in Immunology*. **13**(3),pp.363–373.
- Gao, B., Adhikari, R., Howarth, M., Nakamura, K., Gold, M.C., Hill, A.B., Knee, R., Michalak, M. and Elliott, T. 2002. Assembly and antigen-presenting function of MHC class I molecules in cells lacking the ER chaperone calreticulin. *Immunity*. **16**(1),pp.99–109.
- Geddis, A.E., Linden, H.M. and Kaushansky, K. 2002. Thrombopoietin: a pan-hematopoietic cytokine. *Cytokine & growth factor reviews*. **13**(1),pp.61–73.
- Gery, S. and Koeffler, H.P. 2013. Role of the adaptor protein LNK in normal and malignant hematopoiesis. *Oncogene*. **32**(26),pp.3111–3118.
- Gewirtz, A., Bruno, E., Elwell, J. and Hoffman, R. 1983. In vitro studies of megakaryocytopoiesis in thrombocytotic disorders of man. *Blood*. **61**(2).
- Godfrey, A., Chen, E., Massie, C., ... Y.S.- and 2016, U. 2016. STAT1 activation in association with JAK2 exon 12 mutations. *ncbi.nlm.nih.gov*. **101**(1),pp.e15–e19.

- Gold, L.I., Eggleton, P., Sweetwyne, M.T., Van Duyn, L.B., Greives, M.R., Naylor, S.-M., Michalak, M. and Murphy-Ullrich, J.E. 2010. Calreticulin: non-endoplasmic reticulum functions in physiology and disease. *The FASEB Journal*. **24**(3),pp.665–683.
- de Graaf, C.A. and Metcalf, D. 2011. Thrombopoietin and hematopoietic stem cells. *Cell cycle (Georgetown, Tex.)*. **10**(10),pp.1582–9.
- Griesshammer, M., Hornkohl, A., Nichol, J.L., Hecht, T., Raghavachar, A., Heimpel, H. and Schrezenmeier, H. 1998. High levels of thrombopoietin in sera of patients with essential thrombocythemia: cause or consequence of abnormal platelet production? *Annals of hematology*. **77**(5),pp.211–5.
- Grisouard, J., Li, S., Kubovcakova, L., Rao, T.N., Meyer, S.C., Lundberg, P., Hao-Shen, H., Romanet, V., Murakami, M., Radimerski, T., Dirnhofer, S. and Skoda, R.C. 2016. JAK2 exon 12 mutant mice display isolated erythrocytosis and changes in iron metabolism favoring increased erythropoiesis. *Blood*. **128**(6),pp.839–51.
- Grisouard, J., Shimizu, T., Duek, A., Kubovcakova, L., Hao-Shen, H., Dirnhofer, S. and Skoda, R.C. 2015. Deletion of Stat3 in hematopoietic cells enhances thrombocytosis and shortens survival in a JAK2-V617F mouse model of MPN. *Blood*. **125**(13),pp.2131–40.
- Guo, L., Groenendyk, J., Papp, S., Dabrowska, M., Knoblach, B., Kay, C., Parker, J M Robert, Opas, M. and Michalak, M. 2003. Identification of an N-domain histidine essential for chaperone function in calreticulin. *The Journal of biological chemistry*. **278**(50),pp.50645–53.
- Guo, L., Groenendyk, J., Papp, S., Dabrowska, M., Knoblach, B., Kay, C., Parker, J. M.Robert, Opas, M. and Michalak, M. 2003. Identification of an N-domain Histidine Essential for Chaperone Function in Calreticulin. *Journal of Biological Chemistry*. **278**(50),pp.50645–50653.
- Hammarén, H.M., Virtanen, A.T., Raivola, J. and Silvennoinen, O. 2019. The regulation of JAKs in cytokine signaling and its breakdown in disease. *Cytokine*. **118**,pp.48–63.
- Han, L., Schubert, C., Köhler, J., Schemionek, M., Isfort, S., Brümmendorf,

- T.H., Koschmieder, S. and Chatain, N. 2016. Calreticulin-mutant proteins induce megakaryocytic signaling to transform hematopoietic cells and undergo accelerated degradation and Golgi-mediated secretion. *Journal of Hematology & Oncology*. **9**(1),p.45.
- Hedley, B.D., Allan, A.L. and Xenocostas, A. 2011. The Role of Erythropoietin and Erythropoiesis-Stimulating Agents in Tumor Progression. *Clinical Cancer Research*. **17**(20),pp.6373–6380.
- Helenius, A. and Aebi, M. 2004. Roles of N-Linked Glycans in the Endoplasmic Reticulum. *Annual Review of Biochemistry*. **73**(1),pp.1019–1049.
- Hess, G., Rose, P., Gamm, H., Papadileris, S., Huber, C. and Seliger, B. 1994. Molecular analysis of the erythropoietin receptor system in patients with polycythaemia vera. *British journal of haematology*. **88**(4),pp.794–802.
- Heuek, G. and Assistenzarzt, K. 1879. Zwei Falle von Leukamie mit eigenthumlichem Blut- resp. Knochenmarksbefund (Two cases of leukemia with peculiar blood and bone marrow findings, respectively). *Arch Pathol Anat Physiol Virchows*. **78**,pp.475–496.
- Hirsch, R. 1935. Generalised osteosclorosis with chronic polycythemia vera. *Arch Pathol*. **19**,pp.91–97.
- Hitchcock, I.S., Chen, M.M., King, J.R. and Kaushansky, K. 2008. YRRL motifs in the cytoplasmic domain of the thrombopoietin receptor regulate receptor internalization and degradation. *Blood*. **112**(6),pp.2222–31.
- Hitchcock, I.S. and Kaushansky, K. 2014. Thrombopoietin from beginning to end. *British Journal of Haematology*. **165**(2),pp.259–268.
- Hofmann, I. 2015. Myeloproliferative neoplasms in children. *Journal of Hematopathology*. **8**(3),pp.143–157.
- Holaska, J.M., Black, B.E., Rastinejad, F. and Paschal, B.M. 2002. Ca²⁺-dependent nuclear export mediated by calreticulin. *Molecular and cellular biology*. **22**(17),pp.6286–97.
- Hooke, R. and Allestry, J. 1665. *Micrographia Some Physiological*

- Descriptions of Minute Bodies Made by Magnifying Glasses with Observations and Inquiries* 1st editio. London: J Martyn and J Allestry: London.
- Hubbard, S.R. 2018. Mechanistic insights into regulation of JAK2 tyrosine kinase. *Frontiers in Endocrinology*. **8**(JAN).
- Ihara, K., Ishii, E., Eguchi, M., Takada, H., Suminoe, A., Good, R.A. and Hara, T. 1999. Identification of mutations in the c-mpl gene in congenital amegakaryocytic thrombocytopenia. *Proceedings of the National Academy of Sciences of the United States of America*. **96**(6),pp.3132–6.
- Ihle, J.N. 1995. Cytokine receptor signalling. *Nature*. **377**(6550),pp.591–594.
- Ihle, J.N. and Gilliland, D.G. 2007. Jak2: normal function and role in hematopoietic disorders. *Current opinion in genetics & development*. **17**(1),pp.8–14.
- Ishida, S., Akiyama, H., Umezawa, Y., Okada, K., Nogami, A., Oshikawa, G., Nagao, T. and Miura, O. 2018. Mechanisms for mTORC1 activation and synergistic induction of apoptosis by ruxolitinib and BH3 mimetics or autophagy inhibitors in JAK2-V617F-expressing leukemic cells including newly established PVTL-2. *Oncotarget*. **9**(42),pp.26834–26851.
- Ivanovs, A., Rybtsov, S., Ng, E.S., Stanley, E.G., Elefanty, A.G. and Medvinsky, A. 2017. Human haematopoietic stem cell development: From the embryo to the dish. *Development (Cambridge)*. **144**(13),pp.2323–2337.
- Jacobson, R.J., Salo, A. and Fialkow, P.J. 1978. Agnogenic myeloid metaplasia: a clonal proliferation of hematopoietic stem cells with secondary myelofibrosis. *Blood*. **51**(2),pp.189–94.
- Jagannathan-Bogdan, M. and Zon, L.I. 2013. Hematopoiesis. *Development (Cambridge)*. **140**(12),pp.2463–2467.
- James, C., Ugo, V., Le Couédic, J.-P., Staerk, J., Delhommeau, F., Lacout, C., Garçon, L., Raslova, H., Berger, R., Bennaceur-Griscelli, A., Villeval, J.L., Constantinescu, S.N., Casadevall, N. and Vainchenker, W. 2005. A unique clonal JAK2 mutation leading to constitutive signalling causes polycythaemia vera. *Nature*. **434**(7037),pp.1144–1148.

- Jenkins, B.J., Blake, T.J. and Gonda, T.J. 1998. Saturation mutagenesis of the beta subunit of the human granulocyte-macrophage colony-stimulating factor receptor shows clustering of constitutive mutations, activation of ERK MAP kinase and STAT pathways, and differential beta subunit tyrosine phosphorylation. *Blood*. **92**(6),pp.1989–2002.
- Johnson, S., Michalak, M., Opas, M. and Eggleton, P. 2001. The ins and outs of calreticulin: from the ER lumen to the extracellular space. *Trends in cell biology*. **11**(3),pp.122–9.
- Jørgensen, C.S., Ryder, L.R., Steinø, A., Højrup, P., Hansen, J., Beyer, N.H., Heegaard, N.H.H. and Houen, G. 2003. Dimerization and oligomerization of the chaperone calreticulin. *European Journal of Biochemistry*. **270**(20),pp.4140–4148.
- Juvonen, E., Ikkala, E., Oksanen, K. and Ruutu, T. 1993. Megakaryocyte and erythroid colony formation in essential thrombocythaemia and reactive thrombocytosis: diagnostic value and correlation to complications. *British Journal of Haematology*. **83**(2),pp.192–197.
- Kapoor, M., Ellgaard, L., Gopalakrishnapai, J., Schirra, C., Gemma, E., Oscarson, S., Helenius, A. and Surolia, A. 2004. Mutational analysis provides molecular insight into the carbohydrate-binding region of calreticulin: pivotal roles of tyrosine-109 and aspartate-135 in carbohydrate recognition. *Biochemistry*. **43**(1),pp.97–106.
- Kaushansky, K. 1997. Thrombopoietin the primary regulator of platelet production. *Trends in endocrinology and metabolism: TEM*. **8**(2),pp.45–50.
- Kaushansky, K., Broudy, V.C., Grossmann, A., Humes, J., Lin, N., Ren, H.P., Bailey, M.C., Papayannopoulou, T., Forstrom, J.W. and Sprugel, K.H. 1995. Thrombopoietin expands erythroid progenitors, increases red cell production, and enhances erythroid recovery after myelosuppressive therapy. *The Journal of clinical investigation*. **96**(3),pp.1683–7.
- Kaushansky, K., Lin, N., Grossmann, A., Humes, J., Sprugel, K.H. and Broudy, V.C. 1996. Thrombopoietin expands erythroid, granulocyte-

macrophage, and megakaryocytic progenitor cells in normal and myelosuppressed mice. *Experimental hematology*. **24**(2),pp.265–9.

Kawahara, R. 2011. Leukopoiesis *In: xPharm: The Comprehensive Pharmacology Reference*.

Kawasaki, H., Nakano, T., Kohdera, U. and Kobayashi, Y. 2001. Hypersensitivity of megakaryocyte progenitors to thrombopoietin in essential thrombocythemia. *American journal of hematology*. **68**(3),pp.194–7.

Kennedy, A.D. and Deleo, F.R. 2009. Neutrophil apoptosis and the resolution of infection. *Immunologic Research*.

Kiu, H. and Nicholson, S.E. 2012. Biology and significance of the JAK/STAT signalling pathways. *Growth Factors*. **30**(2),pp.88–106.

Klampfl, T., Gisslinger, H., Harutyunyan, A.S., Nivarthi, H., Rumi, E., Milosevic, J.D., Them, N.C.C., Berg, T., Gisslinger, B., Pietra, D., Chen, D., Vladimer, G.I., Bagienski, K., Milanese, C., Casetti, I.C., Sant'Antonio, E., Ferretti, V., Elena, C., Schischlik, F., Cleary, C., Six, M., Schalling, M., Schönegger, A., Bock, C., Malcovati, L., Pascutto, C., Superti-Furga, G., Cazzola, M. and Kralovics, R. 2013. Somatic Mutations of Calreticulin in Myeloproliferative Neoplasms. *New England Journal of Medicine*. **369**(25),pp.2379–2390.

Kobayashi, M., Laver, J.H., Kato, T., Miyazaki, H. and Ogawa, M. 1995. Recombinant human thrombopoietin (Mpl ligand) enhances proliferation of erythroid progenitors. *Blood*. **86**(7),pp.2494–9.

Kozlov, G., Pocanschi, C.L., Rosenauer, A., Bastos-Aristizabal, S., Gorelik, A., Williams, D.B. and Gehring, K. 2010. Structural Basis of Carbohydrate Recognition by Calreticulin. *Journal of Biological Chemistry*. **285**(49),pp.38612–38620.

Kralovics, R., Passamonti, F., Buser, A.S., Teo, S.-S., Tiedt, R., Passweg, J.R., Tichelli, A., Cazzola, M. and Skoda, R.C. 2005. A Gain-of-Function Mutation of *JAK2* in Myeloproliferative Disorders. *New England Journal of Medicine*. **352**(17),pp.1779–1790.

Kuhr, D. and Wojchowski, D.M. 2015. Emerging EPO and EPO receptor

- regulators and signal transducers. *Blood*. **125**(23),pp.3536–3541.
- Kuraishi, T., Manaka, J., Kono, M., Ishii, H., Yamamoto, N., Koizumi, K., Shiratsuchi, A., Lee, B.L., Higashida, H. and Nakanishi, Y. 2007. Identification of calreticulin as a marker for phagocytosis of apoptotic cells in *Drosophila*. *Experimental cell research*. **313**(3),pp.500–10.
- Lacombe, C. and Mayeux, P. 1999. Plenary lecture. The molecular biology erythropoietin. *Nephrology Dialysis Transplantation*. **14**(90002),pp.22–28.
- Lawrence, S.M., Corriden, R. and Nizet, V. 2018. The Ontogeny of a Neutrophil: Mechanisms of Granulopoiesis and Homeostasis. *Microbiology and Molecular Biology Reviews*.
- Leach, M.R., Cohen-Doyle, M.F., Thomas, D.Y. and Williams, D.B. 2002. Localization of the lectin, ERp57 binding, and polypeptide binding sites of calnexin and calreticulin. *The Journal of biological chemistry*. **277**(33),pp.29686–29697.
- van Leeuwenhoek, A. 1674. A Philosophical transactions of the Royal Society. *London*. **9**,pp.121–128.
- Leroy, E., Defour, J.-P., Sato, T., Dass, S., Gryshkova, V., Shwe, M.M., Staerk, J., Constantinescu, S.N. and Smith, S.O. 2016. His499 Regulates Dimerization and Prevents Oncogenic Activation by Asparagine Mutations of the Human Thrombopoietin Receptor. *The Journal of biological chemistry*. **291**(6),pp.2974–87.
- Levine, R.L. 2012. JAK-mutant myeloproliferative neoplasms. *Current Topics in Microbiology and Immunology*. **355**,pp.119–133.
- Levine, R.L., Wadleigh, M., Cools, J., Ebert, B.L., Wernig, G., Huntly, B.J.P., Boggon, T.J., Wlodarska, I., Clark, J.J., Moore, S., Adelsperger, J., Koo, S., Lee, J.C., Gabriel, S., Mercher, T., D'Andrea, A., Fröhling, S., Döhner, K., Marynen, P., Vandenberghe, P., Mesa, R.A., Tefferi, A., Griffin, J.D., Eck, M.J., Sellers, W.R., Meyerson, M., Golub, T.R., Lee, S.J. and Gilliland, D.G. 2005. Activating mutation in the tyrosine kinase JAK2 in polycythemia vera, essential thrombocythemia, and myeloid metaplasia with myelofibrosis. *Cancer Cell*. **7**(4),pp.387–397.

- Li, J., Kent, D.G., Chen, E. and Green, A.R. 2011. Mouse models of myeloproliferative neoplasms: JAK of all grades. *Disease models & mechanisms*. **4**(3),pp.311–7.
- Li, J., Prins, D., Park, H.J., Grinfeld, J., Gonzalez-Arias, C., Loughran, S., Dovey, O.M., Klampfl, T., Bennett, C., Hamilton, T.L., Pask, D.C., Sneade, R., Williams, M., Aungier, J., Ghevaert, C., Vassiliou, G.S., Kent, D.G. and Green, A.R. 2018. Mutant calreticulin knockin mice develop thrombocytosis and myelofibrosis without a stem cell self-renewal advantage. *Blood*. **131**(6),pp.649–661.
- Li, J., Spensberger, D., Ahn, J.S., Anand, S., Beer, P.A., Ghevaert, C., Chen, E., Forrai, A., Scott, L.M., Ferreira, R., Campbell, P.J., Watson, S.P., Liu, P., Erber, W.N., Huntly, B.J.P., Ottersbach, K. and Green, A.R. 2010. JAK2 V617F impairs hematopoietic stem cell function in a conditional knock-in mouse model of JAK2 V617F-positive essential thrombocythemia. *Blood*. **116**(9),pp.1528–38.
- Lieschke, G.J., Grail, D., Hodgson, G., Metcalf, D., Stanley, E., Cheers, C., Fowler, K.J., Basu, S., Zhan, Y.F. and Dunn, A.R. 1994. Mice lacking granulocyte colony-stimulating factor have chronic neutropenia, granulocyte and macrophage progenitor cell deficiency, and impaired neutrophil mobilization. *Blood*.
- Lieutaud, J. 1749. *Elementa physiologiae: juxta solertiora...*
- Lin, P., Yao, Y., Hofmeister, R., Tsiens, R.Y. and Farquhar, M.G. 1999. Overexpression of CALNUP (Nucleobindin) Increases Agonist and Thapsigargin Releasable Ca²⁺ Storage in the Golgi. *The Journal of Cell Biology*. **145**(2),pp.279–289.
- Lorenz, E., Uphoff, D., Reid, T.R. and Shelton, E. 1951. Modification of Irradiation Injury in Mice and Guinea Pigs by Bone Marrow Injections. *JNCI: Journal of the National Cancer Institute*. **12**(1),pp.197–201.
- Lu, X., Levine, R., Tong, W., Wernig, G., Pikman, Y., Zarnegar, S., Gilliland, D.G. and Lodish, H. 2005. Expression of a homodimeric type I cytokine receptor is required for JAK2V617F-mediated transformation. *Proceedings of the National Academy of Sciences*. **102**(52),pp.18962–

18967.

Mao, X., Ren, Z., Parker, G.N., Sondermann, H., Pastorello, M.A., Wang, W., McMurray, J.S., Demeler, B., Darnell, J.E. and Chen, X. 2005. Structural bases of unphosphorylated STAT1 association and receptor binding. *Molecular Cell*.

Marianayagam, N.J., Sunde, M. and Matthews, J.M. 2004. The power of two: protein dimerization in biology. *Trends in Biochemical Sciences*. **29**(11),pp.618–625.

Marino, V.J. and Roguin, L.P. 2008. The granulocyte colony stimulating factor (G-CSF) activates Jak/STAT and MAPK pathways in a trophoblastic cell line. *Journal of Cellular Biochemistry*.

Martínez-Avilés, L., Besses, C., Alvarez-Larrán, A., Cervantes, F., Hernández-Boluda, J.C. and Bellosillo, B. 2007. JAK2 exon 12 mutations in polycythemia vera or idiopathic erythrocytosis. *Haematologica*. **92**(12),pp.1717–8.

Martins, I., Kepp, O., Galluzzi, L., Senovilla, L., Schlemmer, F., Adjemian, S., Menger, L., Michaud, M., Zitvogel, L. and Kroemer, G. 2010. Surface-exposed calreticulin in the interaction between dying cells and phagocytes. *Annals of the New York Academy of Sciences*. **1209**(1),pp.77–82.

Marty, C., Lacout, C., Martin, A., Hasan, S., Jacquot, S., Birling, M.C., Vainchenker, W. and Villeval, J.L. 2010. Myeloproliferative neoplasm induced by constitutive expression of JAK2 V617F in knock-in mice. *Blood*. **116**(5),pp.783–787.

Marty, C., Pecquet, C., Nivarthi, H., El-Khoury, M., Chachoua, I., Tulliez, M., Villeval, J.-L., Raslova, H., Kralovics, R., Constantinescu, S.N., Plo, I. and Vainchenker, W. 2016. Calreticulin mutants in mice induce an MPL-dependent thrombocytosis with frequent progression to myelofibrosis. *Blood*. **127**(10),pp.1317–24.

Mehta, H.M., Malandra, M. and Corey, S.J. 2015. G-CSF and GM-CSF in Neutropenia. *The Journal of Immunology*.

Metcalf, D. 2008. Hematopoietic cytokines. *Blood*. **111**(2),pp.485–91.

- Michalak, M., Burns, K., Andrin, C., Mesaeli, N., Jass, G.H., Busaan, J.L. and Opas, M. 1996. Endoplasmic reticulum form of calreticulin modulates glucocorticoid-sensitive gene expression. *The Journal of biological chemistry*. **271**(46),pp.29436–45.
- Michalak, M., Corbett, E.F., Mesaeli, N., Nakamura, K. and Opas, M. 1999. *Calreticulin : one protein, one gene, many functions*.
- Michalak, M., Groenendyk, J., Szabo, E., Gold, L.I. and Opas, M. 2009. Calreticulin, a multi-process calcium-buffering chaperone of the endoplasmic reticulum. *Biochemical Journal*. **417**(3),pp.651–666.
- Mittelman, M., Gardyn, J., Carmel, M., Malovani, H., Barak, Y. and Nir, U. 1996. Analysis of the erythropoietin receptor gene in patients with myeloproliferative and myelodysplastic syndromes. *Leukemia research*. **20**(6),pp.459–66.
- Moliterno, A.R., Williams, D.M., Gutierrez-Alamillo, L.I., Salvatori, R., Ingersoll, R.G. and Spivak, J.L. 2004. Mpl Baltimore: a thrombopoietin receptor polymorphism associated with thrombocytosis. *Proceedings of the National Academy of Sciences of the United States of America*. **101**(31),pp.11444–7.
- Montagna, C., Massaro, P., Morali, F., Foa, P., Maiolo, A.T. and Eridani, S. 1994. In vitro sensitivity of human erythroid progenitors to hemopoietic growth factors: studies on primary and secondary polycythemia. *Haematologica*. **79**(4),pp.311–8.
- Mullally, A., Lane, S.W., Ball, B., Megerdichian, C., Okabe, R., Al-Shahrour, F., Paktinat, M., Haydu, J.E., Housman, E., Lord, A.M., Wernig, G., Kharas, M.G., Mercher, T., Kutok, J.L., Gilliland, D.G. and Ebert, B.L. 2010. Physiological Jak2V617F Expression Causes a Lethal Myeloproliferative Neoplasm with Differential Effects on Hematopoietic Stem and Progenitor Cells. *Cancer Cell*. **17**(6),pp.584–596.
- Muraoka, K., Ishii, E., Tsuji, K., Yamamoto, S., Yamaguchi, H., Hara, T., Koga, H., Nakahata, T. and Miyazaki, S. 1997. Defective response to thrombopoietin and impaired expression of c-mpl mRNA of bone marrow cells in congenital amegakaryocytic thrombocytopenia. *British*

journal of haematology. **96**(2),pp.287–92.

Murphy, J.M., Tannahill, G.M., Hilton, D.J. and Greenhalgh, C.J. 2010. The negative regulation of jak/stat signaling *In: Handbook of Cell Signaling*, 2/e.

Naka, T., Narazaki, M., Hirata, M., Matsumoto, T., Minamoto, S., Aono, A., Nishimoto, N., Kajita, T., Taga, T., Yoshizaki, K., Akira, S. and Kishimoto, T. 1997. Structure and function of a new STAT-induced STAT inhibitor. *Nature*.

Nakamura-Ishizu, A. and Suda, T. 2019. Multifaceted roles of thrombopoietin in hematopoietic stem cell regulation. *Annals of the New York Academy of Sciences*.

Nakamura-Ishizu, A., Takizawa, H. and Suda, T. 2014. The analysis, roles and regulation of quiescence in hematopoietic stem cells. *Development (Cambridge)*. **141**(24),pp.4656–4666.

Nangalia, J. and Green, T.R. 2014. The evolving genomic landscape of myeloproliferative neoplasms. *Hematology. American Society of Hematology. Education Program*. **2014**(1),pp.287–96.

Nangalia, J., Grinfeld, J. and Green, A.R. 2016. Pathogenesis of Myeloproliferative Disorders. *Annual Review of Pathology: Mechanisms of Disease*. **11**(1),pp.101–126.

Nangalia, J., Massie, C.E., Baxter, E.J., Nice, F.L., Gundem, G., Wedge, D.C., Avezov, E., Li, J., Kollmann, K., Kent, D.G., Aziz, A., Godfrey, A.L., Hinton, J., Martincorena, I., Van Loo, P., Jones, A.V., Guglielmelli, P., Tarpey, P., Harding, H.P., Fitzpatrick, J.D., Goudie, C.T., Ortmann, C.A., Loughran, S.J., Raine, K., Jones, D.R., Butler, A.P., Teague, J.W., O’Meara, S., McLaren, S., Bianchi, M., Silber, Y., Dimitropoulou, D., Bloxham, D., Mudie, L., Maddison, M., Robinson, B., Keohane, C., Maclean, C., Hill, K., Orchard, K., Tauro, S., Du, M.-Q., Greaves, M., Bowen, D., Huntly, B.J.P., Harrison, C.N., Cross, N.C.P., Ron, D., Vannucchi, A.M., Papaemmanuil, E., Campbell, P.J. and Green, A.R. 2013. Somatic *CALR* Mutations in Myeloproliferative Neoplasms with Nonmutated *JAK2*. *New England Journal of Medicine*.

369(25),pp.2391–2405.

Neumann, E. 1869. Ueber die Bedeutung des Knochenmarkes für die Blutbildung. Ein Beitrag zur Entwicklungsgeschichte der Blutkörperchen. *Archives Heilkunde*. **10**,pp.68–102.

Ng, A.P. and Alexander, W.S. 2017. Haematopoietic stem cells: Past, present and future. *Cell Death Discovery*. **3**.

Ng, A.P., Kauppi, M., Metcalf, D., Hyland, C.D., Josefsson, E.C., Lebois, M., Zhang, J.-G., Baldwin, T.M., Di Rago, L., Hilton, D.J. and Alexander, W.S. 2014. Mpl expression on megakaryocytes and platelets is dispensable for thrombopoiesis but essential to prevent myeloproliferation. *Proceedings of the National Academy of Sciences of the United States of America*. **111**(16),pp.5884–9.

Nishigaki, K., Thompson, D., Ruscetti, S., Hanson, C., Muszynski, K. and Ohashi, T. 2000. Erythroid cells rendered erythropoietin independent by infection with friend spleen focus-forming virus show constitutive activation of phosphatidylinositol 3-kinase and Akt kinase: Involvement of insulin receptor substrate-related adapter proteins. *Journal of Virology*.

Nowell, P.C. 2002. Progress with Chronic Myelogenous Leukemia: A Personal Perspective over Four Decades. *Annual Review of Medicine*. **53**(1),pp.1–13.

Ogden, C.A., DeCathelineau, A., Hoffmann, P.R., Bratton, D., Fadok, B., Ghebrehiwet, V.A. and Henson, P.M. 2001. C1q and mannose binding lectin engagement of cell surface calreticulin and CD91 initiates macropinocytosis and uptake of apoptotic cells. *Journal of Experimental Medicine*. **194**(6),pp.781–795.

Ohyashiki, J.H., Hisatomi, H., Shimizu, S., Sugaya, M. and Ohyashiki, K. 2009. Detection of low allele burden of JAK2 exon 12 mutations using TA-cloning in patients with erythrocytosis. *Japanese journal of clinical oncology*. **39**(8),pp.509–13.

Orkin, S.H. 2000. Diversification of haematopoietic stem cells to specific lineages. *Nature Reviews Genetics*. **1**(1),pp.57–64.

- Orkin, S.H. and Zon, L.I. 2008. Hematopoiesis: An Evolving Paradigm for Stem Cell Biology. *Cell*. **132**(4),pp.631–644.
- Osler, S. 1908. A Clinical Lecture on Erythraemia (polycythaemia with Cyanosis, *Maladie de Vaquez*).
- Osler, W. 1903. Chronic cyanosis with polycythemia and enlarged spleen: a new clinical entity. *Trans. Ass. Amer.*
- Ostwald, T.J. and MacLennan, D.H. 1974. Isolation of a high affinity calcium-binding protein from sarcoplasmic reticulum. *The Journal of biological chemistry*. **249**(3),pp.974–9.
- Pardanani, A., Lasho, T.L., Finke, C., Hanson, C.A. and Tefferi, A. 2007. Prevalence and clinicopathologic correlates of JAK2 exon 12 mutations in JAK2V617F-negative polycythemia vera. *Leukemia*. **21**(9),pp.1960–3.
- Pardanani, A.D., Levine, R.L., Lasho, T., Pikman, Y., Mesa, R.A., Wadleigh, M., Steensma, D.P., Elliott, M.A., Wolanskyj, A.P., Hogan, W.J., McClure, R.F., Litzow, M.R., Gilliland, D.G. and Tefferi, A. 2006. MPL515 mutations in myeloproliferative and other myeloid disorders: a study of 1182 patients. *Blood*. **108**(10),pp.3472–3476.
- Parodi, A.J. 2000. Protein Glucosylation and Its Role in Protein Folding. *Annual Review of Biochemistry*. **69**(1),pp.69–93.
- Pear, W.S., Nolan, G.P., Scott, M.L. and Baltimore, D. 1993. Production of high-titer helper-free retroviruses by transient transfection. *Proceedings of the National Academy of Sciences*. **90**(18),pp.8392–8396.
- Pecquet, C., Staerk, J., Chaligné, R., Goss, V., Lee, K.A., Zhang, X., Rush, J., Van Hees, J., Poirel, H.A., Scheiff, J.-M., Vainchenker, W., Giraudier, S., Polakiewicz, R.D. and Constantinescu, S.N. 2010. Induction of myeloproliferative disorder and myelofibrosis by thrombopoietin receptor W515 mutants is mediated by cytosolic tyrosine 112 of the receptor. *Blood*. **115**(5),pp.1037–48.
- Peterson, J.R., Ora, A., Van, P.N. and Helenius, A. 1995. Transient, lectin-like association of calreticulin with folding intermediates of cellular and viral glycoproteins. *Molecular Biology of the Cell*. **6**(9),pp.1173–1184.

- Pikman, Y., Lee, B.H., Mercher, T., McDowell, E., Ebert, B.L., Gozo, M., Cuker, A., Wernig, G., Moore, S., Galinsky, I., DeAngelo, D.J., Clark, J.J., Lee, S.J., Golub, T.R., Wadleigh, M., Gilliland, D.G. and Levine, R.L. 2006. MPLW515L Is a Novel Somatic Activating Mutation in Myelofibrosis with Myeloid Metaplasia C. Sawyers, ed. *PLoS Medicine*. **3**(7),p.e270.
- Pocanschi, C.L., Kozlov, G., Brockmeier, U., Brockmeier, A., Williams, D.B. and Gehring, K. 2011. Structural and Functional Relationships between the Lectin and Arm Domains of Calreticulin. *Journal of Biological Chemistry*. **286**(31),pp.27266–27277.
- Pozzan, T., Rizzuto, R., Volpe, P. and Meldolesi, J. 1994. *Molecular and Cellular Physiology of Intracellular Calcium Stores*.
- Prchal, J.F. and Axelrad, A.A. 1974. Bone-Marrow Responses in Polycythemia Vera. *New England Journal of Medicine*. **290**(24),p.1382.
- Prigge, J.R., Hoyt, T.R., Dobrinen, E., Capecchi, M.R., Schmidt, E.E. and Meissner, N. 2015. Type I IFNs Act upon Hematopoietic Progenitors To Protect and Maintain Hematopoiesis during Pneumocystis Lung Infection in Mice. *The Journal of Immunology*. **195**(11),pp.5347–5357.
- Promega Corporation 2019. Automated MagneHis™ Protein Purification System Automated Protocol #EP011. [Accessed 17 December 2019]. Available from: <https://www.promega.com/-/media/files/resources/protocols/automated-protocols/0/automated-magnehis-protein-purification-system.pdf>.
- Radosevic, N., Winterstein, D., Keller, J.R., Neubauer, H., Pfeffer, K. and Linnekin, D. 2004. JAK2 contributes to the intrinsic capacity of primary hematopoietic cells to respond to stem cell factor. *Experimental Hematology*. **32**(2),pp.149–156.
- Raghavan, M., Wijeyesakere, S.J., Peters, L.R. and Del Cid, N. 2013. Calreticulin in the immune system: Ins and outs. *Trends in Immunology*. **34**(1),pp.13–21.
- Randi, M.L., Putti, M.C., Pacquola, E., Luzzatto, G., Zanesco, L. and Fabris, F. 2005. Normal thrombopoietin and its receptor (c-mpl) genes in

- children with essential thrombocythemia. *Pediatric blood & cancer*. **44**(1),pp.47–50.
- Rawlings, J.S., Rosler, K.M. and Harrison, D.A. 2004. The JAK/STAT signaling pathway. *Journal of Cell Science*. **117**(8),pp.1281–1283.
- Riecken, K. 2015. Lentiviral Gene Ontology Vectors. [Accessed 17 December 2019]. Available from: <http://www.lentigo-vectors.de/vectors.htm>.
- Robb, L. 2007. Cytokine receptors and hematopoietic differentiation. *Oncogene*. **26**(47),pp.6715–6723.
- Röder, S., Steimle, C., Meinhardt, G. and Pahl, H.L. 2001. STAT3 is constitutively active in some patients with Polycythemia rubra vera. *Experimental hematology*. **29**(6),pp.694–702.
- Rojnuckarin, P., Drachman, J.G. and Kaushansky, K. 1999. Thrombopoietin-induced activation of the mitogen-activated protein kinase (MAPK) pathway in normal megakaryocytes: role in endomitosis. *Blood*. **94**(4),pp.1273–82.
- Rossi, D.J., Seita, J., Czechowicz, A., Bhattacharya, D., Bryder, D. and Weissman, I.L. 2007. Hematopoietic Stem Cell Quiescence Attenuates DNA Damage Response and Permits DNA Damage Accumulation During Aging. *Cell Cycle*. **6**(19),pp.2371–2376.
- Sabath, D.F., Kaushansky, K. and Broudy, V.C. 1999. Deletion of the extracellular membrane-distal cytokine receptor homology module of Mpl results in constitutive cell growth and loss of thrombopoietin binding. *Blood*. **94**(1),pp.365–7.
- Saharinen, P. and Silvennoinen, O. 2002. The Pseudokinase Domain Is Required for Suppression of Basal Activity of Jak2 and Jak3 Tyrosine Kinases and for Cytokine-inducible Activation of Signal Transduction. *Journal of Biological Chemistry*. **277**(49),pp.47954–47963.
- Saito, Y., Ihara, Y., Leach, M.R., Cohen-Doyle, M.F. and Williams, D.B. 1999. Calreticulin functions in vitro as a molecular chaperone for both glycosylated and non-glycosylated proteins. *The EMBO journal*. **18**(23),pp.6718–29.

- Sangkhae, V., Etheridge, S.L., Kaushansky, K. and Hitchcock, I.S. 2014. The thrombopoietin receptor, MPL, is critical for development of a JAK2V617F-induced myeloproliferative neoplasm. *Blood*. **124**(26),pp.3956–3963.
- Sattler, M., Durstin, M.A., Frank, D.A., Okuda, K., Kaushansky, K., Salgia, R. and Griffin, J.D. 1995. The thrombopoietin receptor c-MPL activates JAK2 and TYK2 tyrosine kinases. *Experimental hematology*. **23**(9),pp.1040–8.
- Schrag, J.D., Bergeron, J.J.M., Li, Y., Borisova, S., Hahn, M., Thomas, D.Y. and Cygler, M. 2001. The Structure of Calnexin, an ER Chaperone Involved in Quality Control of Protein Folding. *Molecular Cell*. **8**(3),pp.633–644.
- Schuettpelz, L.G., Borgerding, J.N., Christopher, M.J., Gopalan, P.K., Romine, M.P., Herman, A.C., Woloszynek, J.R., Greenbaum, A.M. and Link, D.C. 2014. G-CSF regulates hematopoietic stem cell activity, in part, through activation of Toll-like receptor signaling. *Leukemia*. **28**(9),pp.1851–1860.
- Scott, Linda M, Tong, W., Levine, R.L., Scott, M. a, Beer, P. a, Stratton, M.R., Futreal, P.A., Erber, W.N., McMullin, M.F., Harrison, C.N., Warren, A.J., Gilliland, D.G., Lodish, H.F., Green, A.R., Ph, D., Path, F.R.C., Path, M.R.C. and Sci, F.M. 2007. Exon 12 Mutations in Polycythemia Vera and Idiopathic Erythrocytosis. *The New England journal of medicine*.
- Scott, Linda M., Tong, W., Levine, R.L., Scott, M.A., Beer, P.A., Stratton, M.R., Futreal, P.A., Erber, W.N., McMullin, M.F., Harrison, C.N., Warren, A.J., Gilliland, D.G., Lodish, H.F. and Green, A.R. 2007. JAK2 Exon 12 Mutations in Polycythemia Vera and Idiopathic Erythrocytosis. *New England Journal of Medicine*. **356**(5),pp.459–468.
- Seif, F., Khoshmirsafa, M., Aazami, H., Mohsenzadegan, M., Sedighi, G. and Bahar, M. 2017. The role of JAK-STAT signaling pathway and its regulators in the fate of T helper cells. *Cell Communication and Signaling*. **15**(1).

- Shi, Y., Liu, C.H., Roberts, A.I., Das, J., Xu, G., Ren, G., Zhang, Y., Zhang, L., Zeng, R.Y., Tan, H.S.W., Das, G. and Devadas, S. 2006. Granulocyte-macrophage colony-stimulating factor (GM-CSF) and T-cell responses: What we do and don't know *In: Cell Research*.
- Shimoda, K., Iwasaki, H., Okamura, S., Ohno, Y., Kubota, A., Arima, F., Otsuka, T. and Niho, Y. 1994. G-CSF induces tyrosine phosphorylation of the JAK2 protein in the human myeloid G-CSF responsive and proliferative cells, but not in mature neutrophils. *Biochemical and Biophysical Research Communications*.
- Shivarov, V., Ivanova, M. and Tiu, R. V. 2014. Mutated calreticulin retains structurally disordered C terminus that cannot bind Ca²⁺: Some mechanistic and therapeutic implications. *Blood Cancer Journal*. **4**(2).
- Shlush, L.I. 2018. Age-related clonal hematopoiesis. *Blood*. **131**(5),pp.496–504.
- Silva, M., Benito, A., Sanz, C., Prosper, F., Ekhterae, D., Nuñez, G. and Fernandez-Luna, J.L. 1999. Erythropoietin can induce the expression of Bcl-x(L) through Stat5 in erythropoietin-dependent progenitor cell lines. *Journal of Biological Chemistry*.
- Silvennoinen, O. and Hubbard, S.R. 2015. Molecular insights into regulation of JAK2 in myeloproliferative neoplasms. *Blood*. **125**(22),pp.3388–3392.
- Solar, G.P., Kerr, W.G., Zeigler, F.C., Hess, D., Donahue, C., de Sauvage, F.J. and Eaton, D.L. 1998. Role of c-mpl in early hematopoiesis. *Blood*. **92**(1),pp.4–10.
- Spivak, J.L. 2005. The anaemia of cancer: death by a thousand cuts. *Nature Reviews Cancer*. **5**(7),pp.543–555.
- Staerk, J. and Constantinescu, Stefan N 2012. The JAK-STAT pathway and hematopoietic stem cells from the JAK2 V617F perspective. *JAK-STAT*. **1**(3),pp.184–90.
- Staerk, J. and Constantinescu, Stefan N. 2012. The JAK-STAT pathway and hematopoietic stem cells from the JAK2 V617F perspective. *JAK-STAT*. **1**(3),pp.184–190.

- Staerk, J., Lacout, C., Sato, T., Smith, S.O., Vainchenker, W. and Constantinescu, S.N. 2006. An amphipathic motif at the transmembrane-cytoplasmic junction prevents autonomous activation of the thrombopoietin receptor. *Blood*. **107**(5),pp.1864–1871.
- Starr, R. and Hilton, D.J. 1999. Negative regulation of the JAK/STAT pathway. *BioEssays*.
- Starr, R., Willson, T.A., Viney, E.M., Murray, L.J.L., Rayner, J.R., Jenkins, B.J., Gonda, T.J., Alexander, W.S., Metcalf, D., Nicola, N.A. and Hilton, D.J. 1997. A family of cytokine-inducible inhibitors of signalling. *Nature*.
- Sytkowski, A.J., Lunn, E.D., Davis, K.L., Feldman, L. and Siekman, S. 1998. Human erythropoietin dimers with markedly enhanced in vivo activity. *Proceedings of the National Academy of Sciences of the United States of America*. **95**(3),pp.1184–8.
- Tefferi, Ayalew 2008. Mutant Molecules of Interest in Myeloproliferative Neoplasms: Introduction. *Acta Haematologica*. **119**(4),pp.192–193.
- Tefferi, A. 2008. The history of myeloproliferative disorders: Before and after Dameshek. *Leukemia*.
- Tefferi, A. and Pardanani, A. 2015. Myeloproliferative Neoplasms. *JAMA Oncology*. **1**(1),p.97.
- Teofili, L., Giona, F., Martini, M., Cenci, T., Guidi, F., Torti, L., Palumbo, G., Amendola, A., Foà, R. and Larocca, L.M. 2007. Markers of Myeloproliferative Diseases in Childhood Polycythemia Vera and Essential Thrombocythemia. *Journal of Clinical Oncology*. **25**(9),pp.1048–1053.
- Thomson, S.P. and Williams, D.B. 2005. Delineation of the lectin site of the molecular chaperone calreticulin. *Cell stress & chaperones*. **10**(3),pp.242–51.
- Traver, D. and Akashi, K. 2004. Lineage Commitment and Developmental Plasticity in Early Lymphoid Progenitor Subsets. *Advances in Immunology*. **83**,pp.1–54.
- Ungureanu, D., Vanhatupa, S., Kotaja, N., Yang, J., Aittomäki, S., Jänne,

- O.A., Palvimo, J.J. and Silvennoinen, O. 2003. PIAS proteins promote SUMO-1 conjugation to STAT1. *Blood*.
- Vaquez, H. 1895. Sur une forme speciale de cyanose s'accompagnant d'hyperglobulie excessive et persistente (On a special form of cyanosis accompanied by excessive and persistent erythrocytosis). *Compt rend Soc de biol and suppl note, Bull et mem Soc med d'hop de Paris*. **12**(60).
- Varghese, L.N., Defour, J.P., Pecquet, C. and Constantinescu, S.N. 2017. The thrombopoietin receptor: Structural basis of traffic and activation by ligand, mutations, agonists, and mutated calreticulin. *Frontiers in Endocrinology*. **8**(MAR).
- Vaughan, J.M. and Harrison, C. V. 1939. Leuco-erythroblastic anæmia and myelosclerosis. *The Journal of Pathology and Bacteriology*. **48**(2),pp.339–352.
- Vigon, I., Mornon, J.P., Cocault, L., Mitjavila, M.T., Tambourin, P., Gisselbrecht, S. and Souyri, M. 1992. Molecular cloning and characterization of MPL, the human homolog of the v-mpl oncogene: identification of a member of the hematopoietic growth factor receptor superfamily. *Proceedings of the National Academy of Sciences*. **89**(12),pp.5640–5644.
- Virchow, R. 1845. Weisses blut. *Froiep Notizen*. **36**,pp.151–156.
- Walz, C., Ahmed, W., Lazarides, K., Betancur, M., Patel, N., Hennighausen, L., Zaleskas, V.M. and Van Etten, R.A. 2012. Essential role for Stat5a/b in myeloproliferative neoplasms induced by BCR-ABL1 and JAK2(V617F) in mice. *Blood*. **119**(15),pp.3550–60.
- Wang, J.C. and Hashmi, G. 2003. Elevated thrombopoietin levels in patients with myelofibrosis may not be due to enhanced production of thrombopoietin by bone marrow. *Leukemia research*. **27**(1),pp.13–7.
- Ware, F.E., Vassilakos, A., Peterson, P.A., Jackson, M.R., Lehrman, M.A. and Williams, D.B. 1995. The molecular chaperone calnexin binds Glc1Man9GlcNAc2 oligosaccharide as an initial step in recognizing unfolded glycoproteins. *The Journal of biological chemistry*.

270(9),pp.4697–704.

- Warr, M.R., Pietras, E.M. and Passegué, E. 2011. Mechanisms controlling hematopoietic stem cell functions during normal hematopoiesis and hematological malignancies. *Wiley Interdisciplinary Reviews: Systems Biology and Medicine*. **3**(6),pp.681–701.
- Wearsch, P., Zhang, W. and Cresswell, P. 2011. Essential glycan-dependent interactions optimize MHC class I peptide loading (100.51). *The Journal of Immunology*. **186**(1 Supplement).
- Wearsch, P.A. and Cresswell, P. 2008. The quality control of MHC class I peptide loading. *Current Opinion in Cell Biology*. **20**(6),pp.624–631.
- Wernig, G., Mercher, T., Okabe, R., Levine, R.L., Lee, B.H. and Gilliland, D.G. 2006. Expression of Jak2V617F causes a polycythemia vera-like disease with associated myelofibrosis in a murine bone marrow transplant model. *Blood*. **107**(11),pp.4274–4281.
- Wijeyesakere, S.J., Gagnon, J.K., Arora, K., Brooks, C.L. and Raghavan, M. 2015. Regulation of calreticulin-major histocompatibility complex (MHC) class I interactions by ATP. *Proceedings of the National Academy of Sciences of the United States of America*. **112**(41),pp.E5608–E5617.
- Williams, D.M., Kim, A.H., Rogers, O., Spivak, J.L. and Moliterno, A.R. 2007. Phenotypic variations and new mutations in JAK2 V617F-negative polycythemia vera, erythrocytosis, and idiopathic myelofibrosis. *Experimental hematology*. **35**(11),pp.1641–6.
- Wilson, A., Laurenti, E., Oser, G., van der Wath, R.C., Blanco-Bose, W., Jaworski, M., Offner, S., Dunant, C.F., Eshkind, L., Bockamp, E., Lió, P., MacDonald, H.R. and Trumpp, A. 2008. Hematopoietic Stem Cells Reversibly Switch from Dormancy to Self-Renewal during Homeostasis and Repair. *Cell*. **135**(6),pp.1118–1129.
- Witthuhn, B.A., Quelle, F.W., Silvennoinen, O., Yi, T., Tang, B., Miura, O. and Ihle, J.N. 1993. JAK2 associates with the erythropoietin receptor and is tyrosine phosphorylated and activated following stimulation with erythropoietin. *Cell*. **74**(2),pp.227–36.
- de Wolf, J.T., Beentjes, J.A., Esselink, M.T., Smit, J.W., Halie, R.M., Clark,

- S.C. and Vellenga, E. 1989. In polycythemia vera human interleukin 3 and granulocyte-macrophage colony-stimulating factor enhance erythroid colony growth in the absence of erythropoietin. *Experimental hematology*. **17**(9),pp.981–3.
- Yamaoka, K., Saharinen, P., Pesu, M., Holt, V.E.T., Silvennoinen, O., O'Shea, J.J. and O'Shea, J.J. 2004. The Janus kinases (Jaks). *Genome biology*. **5**(12),p.253.
- Yan, D., Hutchison, R.E. and Mohi, G. 2012. Critical requirement for Stat5 in a mouse model of polycythemia vera. *Blood*. **119**(15),pp.3539–49.
- Yan, D., Jobe, F., Hutchison, R.E. and Mohi, G. 2015. Deletion of Stat3 enhances myeloid cell expansion and increases the severity of myeloproliferative neoplasms in Jak2V617F knock-in mice. *Leukemia*. **29**(10),pp.2050–2061.
- Yan, D. and Mohi, G. 2013. Stat3 Negatively Regulates Myeloproliferative Neoplasm Induced By Jak2V617F. *Blood*. **122**(21),pp.111–111.
- Yogarajah, M. and Tefferi, A. 2017. Leukemic Transformation in Myeloproliferative Neoplasms: A Literature Review on Risk, Characteristics, and Outcome. *Mayo Clinic Proceedings*. **92**,pp.1118–1128.
- Yoshihara, H., Arai, F., Hosokawa, K., Hagiwara, T., Takubo, K., Nakamura, Y., Gomei, Y., Iwasaki, H., Matsuoka, S., Miyamoto, K., Miyazaki, H., Takahashi, T. and Suda, T. 2007. Thrombopoietin/MPL Signaling Regulates Hematopoietic Stem Cell Quiescence and Interaction with the Osteoblastic Niche. *Cell Stem Cell*. **1**(6),pp.685–697.
- Yu, C., Yang, Q., Chen, Y., Wang, D., Levine, R., Crispino, J., Wen, Q. and Huang, Z. 2016. Tyrosine 625 plays a key role and cooperates with tyrosine 630 in MPL W515L-induced signaling and myeloproliferative neoplasms. *Cell & bioscience*. **6**,p.34.
- Zanjani, E.D., Lutton, J.D., Hoffman, R. and Wasserman, L.R. 1977. Erythroid colony formation by polycythemia vera bone marrow in vitro. Dependence on erythropoietin. *Journal of Clinical Investigation*. **59**(5),p.841.

Bibliography

Zapun, A., Darby, N.J., Tessier, D.C., Michalak, M., Bergeron, J.J. and Thomas, D.Y. 1998. Enhanced catalysis of ribonuclease B folding by the interaction of calnexin or calreticulin with ERp57. *The Journal of biological chemistry*. **273**(11),pp.6009–12.

Zimmerman, K.A., Graham, L. V, Pallero, M.A. and Murphy-Ullrich, J.E. 2013. Calreticulin regulates transforming growth factor- β -stimulated extracellular matrix production. *The Journal of biological chemistry*. **288**(20),pp.14584–98.

Zivot, A., Lipton, J.M., Narla, A. and Blanc, L. 2018. Erythropoiesis: insights into pathophysiology and treatments in 2017. *Molecular Medicine*. **24**(1),p.11.

Zou, H., Yan, D. and Mohi, G. 2011. Differential biological activity of disease-associated JAK2 mutants. *FEBS Letters*. **585**(7),pp.1007–1013.